VTT WORKING PAPERS 112

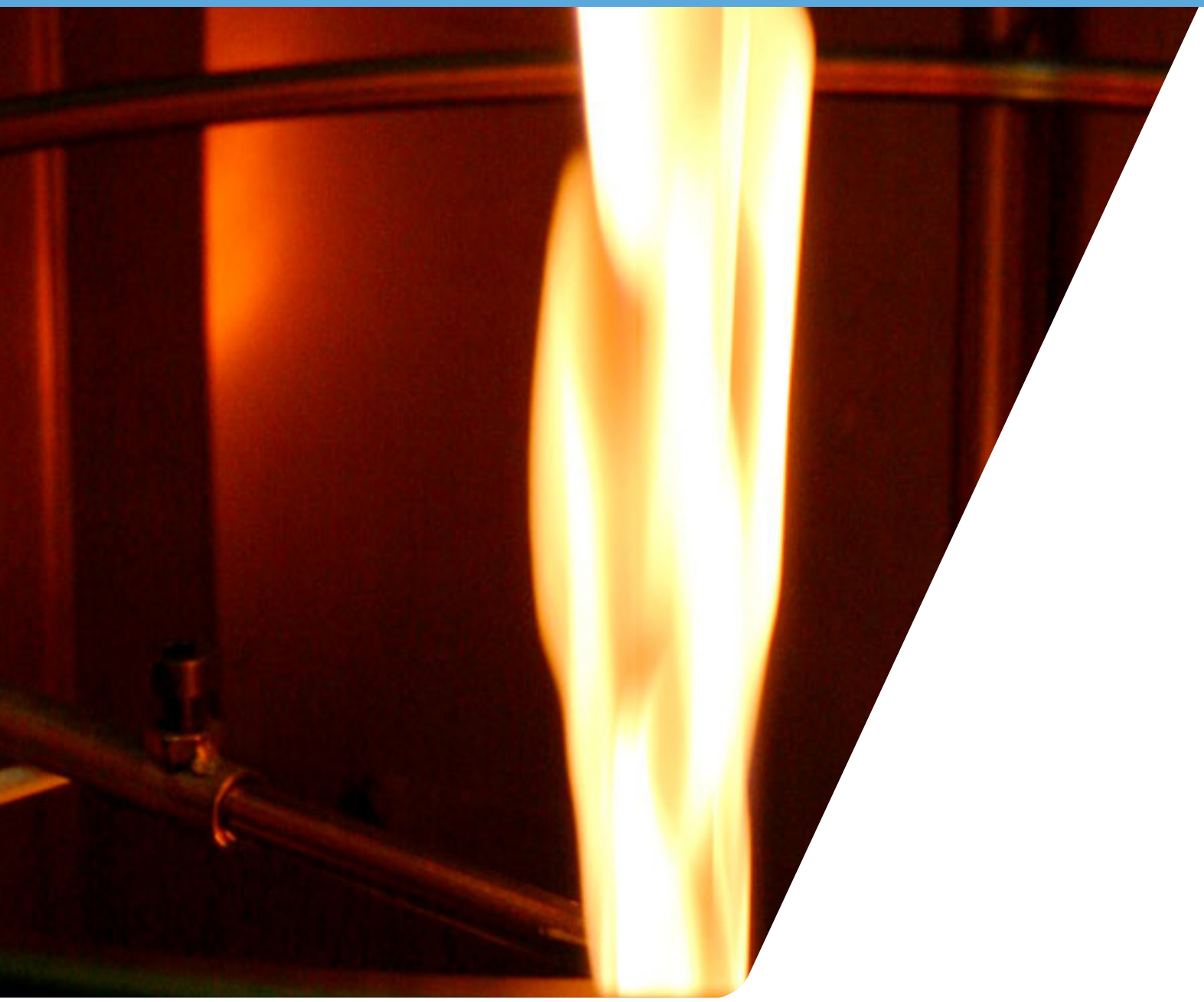

Johan Mangs

A new apparatus for flame spread experiments

ISBN 978-951-38-7173-4 (URL: http://www.vtt.fi/publications/index.jsp)
ISSN 1459-7683 (URL: http://www.vtt.fi/publications/index.jsp)

JULKAISIJA – UTGIVARE – PUBLISHER

VTT, Vuorimiehentie 3, PL 1000, 02044 VTT
puh. vaihde 020 722 111, faksi 020 722 7001

VTT, Bergsmansvägen 3, PB 1000, 02044 VTT
tel. växel 020 722 111, fax 020 722 7001

VTT Technical Research Centre of Finland, Vuorimiehentie 5, P.O. Box 1000, FI-02044 VTT, Finland
phone internat. +358 20 722 111, fax +358 20 722 7001

Series title, number and report code of publication

VTT Working Papers
VTT–WORK–112

Author(s)
Johan Mangs

Title
A new apparatus for flame spread experiments

Abstract

In fire-PSAs of nuclear power plants, flame spread on solids, especially cables, is a significant scenario. In previous projects at VTT on fire safety in nuclear power plants, a new instrument for measuring flame spread at different ambient temperatures was proposed. This report presents the realization of the new apparatus for flame spread measurements on 2 m long samples, as well as start-up tests on the instrument describing its functionality, and flame spread experiments.

Air flow and heating tests were carried out to examine the features of the new instrument. Two series of flame spread experiments were carried out, on cylindrical birch wood samples and PVC cable samples. Flame spread velocities in the range 6 ... 62 mm/s were determined in a temperature at ignition range 22...271 ^{o}C for wood samples and velocities 3...8 mm/s in a temperature at ignition range 22...187 ^{o}C for PVC cable samples.

The new apparatus seems to be appropriate for determining vertical flame spread as a function of temperature.

ISBN
978-951-38-7173-4 (URL: http://www.vtt.fi/publications/index.jsp)

Series title and ISSN		Project number
VTT Working Papers 1459-7683 (URL: http://www.vtt.fi/publications/index.jsp)		32599 FIRAS 2009
Date 2009	Language	Pages 51 p. + App. 28 p.
Name of project Implementation of Quantitative Fire Risk Assessment in PSA	Commissioned by State Nuclear Waste Management Fund (VYR), VTT	
Keywords Flame spread, fire experiments, flame front velocity, temperature measurements, fire safety	Publisher VTT Technical Research Centre of Finland P.O. Box 1000, FI-02044 VTT, Finland Phone internat. +358 20 722 4520 Fax +358 20 722 4374	

Preface

This study was carried out as a part of the Implementation of Quantitative Fire Risk Assessment in PSA project (FIRAS) which is one of the projects in the Finnish Research Programme on Nuclear Power Plant Safety 2007–2010 (SAFIR2010). The study has partially been financed by Finnish Nuclear Waste Management Fund (VYR). Construction of and start-up tests on the new 2 m test rig were financed by VTT outside FIRAS project.

Protoshop Oy is acknowledged for detail design and construction of the 2 m test rig.

Contents

1. Introduction

In fire-PSAs[1] of nuclear power plants, flame spread on solids, especially cables, is a significant scenario. Studies on flame spread, the biggest unsolved problem of fire science, was a central issue in POTFIS (Potential of fire spread) project, which preceded the present FIRAS project. The approach in POTFIS was to carry out interactively modelling, numerical simulation and experimental work on the relevant, most promising simple solid fuel scenarios for qualification and validation of specific models (Hostikka & Keski-Rahkonen 2007, Keski-Rahkonen & Mangs 2005a, 2005b, 2006, and Mangs et al. 2006).

One of the results was a proposal for a new flame spread measuring instrument: a 2 m vertical sample test rig for the measurement of flame spread velocity as a function of initial temperature. It had been observed in flame spread experiments, that at some distance above the point of ignition, flame spread was approaching constant velocity. Sample length 2 m was estimated to be enough to reach this state.

Operating principles, structure and materials for the new instrument were presented to fine-mechanical workshop Protoshop Oy, where detail design and construction was carried out in close co-operation with VTT. The 2 m test rig was completed in summer 2007, and start-up tests were initiated at VTT. This report describes features and function of the test rig as results from start-up tests, and two series of vertical flame spread experiments, on cylindrical birch wood samples and on PVC cable samples.

[1] PSA = Probabilistic Safety Assessment

2. Realization of the test rig

The basis for the design of the test rig is described in Mangs et al. (2006), Keski-Rahkonen & Mangs (2005a) and is not repeated here. The purpose is to obtain a continuous preheated air supply throughout the experiment to be able to measure flame spread velocity at different initial temperatures, starting from ordinary room temperatures up to temperatures near auto-ignition level. Basic requirements are: sample length 2 m, diameter at maximum less than 100 mm, and initial temperature at maximum 400 ^{o}C. Thermocouples close to the sample surface indicate flame front propagation along the sample.

2.1 Test rig

The structure of the test rig is shown in Figure 1. The device consists of a heating channel and a test channel (width 300 mm, depth 330 mm), separated from each other by a thin stainless steel sheet and connected to each other at the upper and lower parts of the channels. The device is insulated with 100 mm thick Kaowool insulation between 0.5 mm stainless steel plates. There is a door on the front side to the channels, an air inlet in the upper part of the heating channel and a smoke outlet at top of the test channel. The device is pivoted to a massive steel support at its lower end, and can be used in either vertical or horizontal position. This report considers operation in vertical position only.

Air is heated with a 7.0 kW heating resistor and is circulated with a fan located in the upper part of the heating channel. In the heating phase the air inlet and roof hatch are closed and air is circulated within the cabinet (Figure 2a), heating the sample. During the flame spread experiment the fan draws in fresh air through the intake in the upper part of the heating channel, onwards through the heater to the test channel, and fire effluents exit through the outlet (Figure 2b), with the upper opening connecting the channels closed.

Air flow is controlled with a Commander SK frequency transformer regulating the fan speed. The temperature in the system is regulated with a Drews R 1140 controller. All control functions are located in a control unit on the outside of the cabinet.

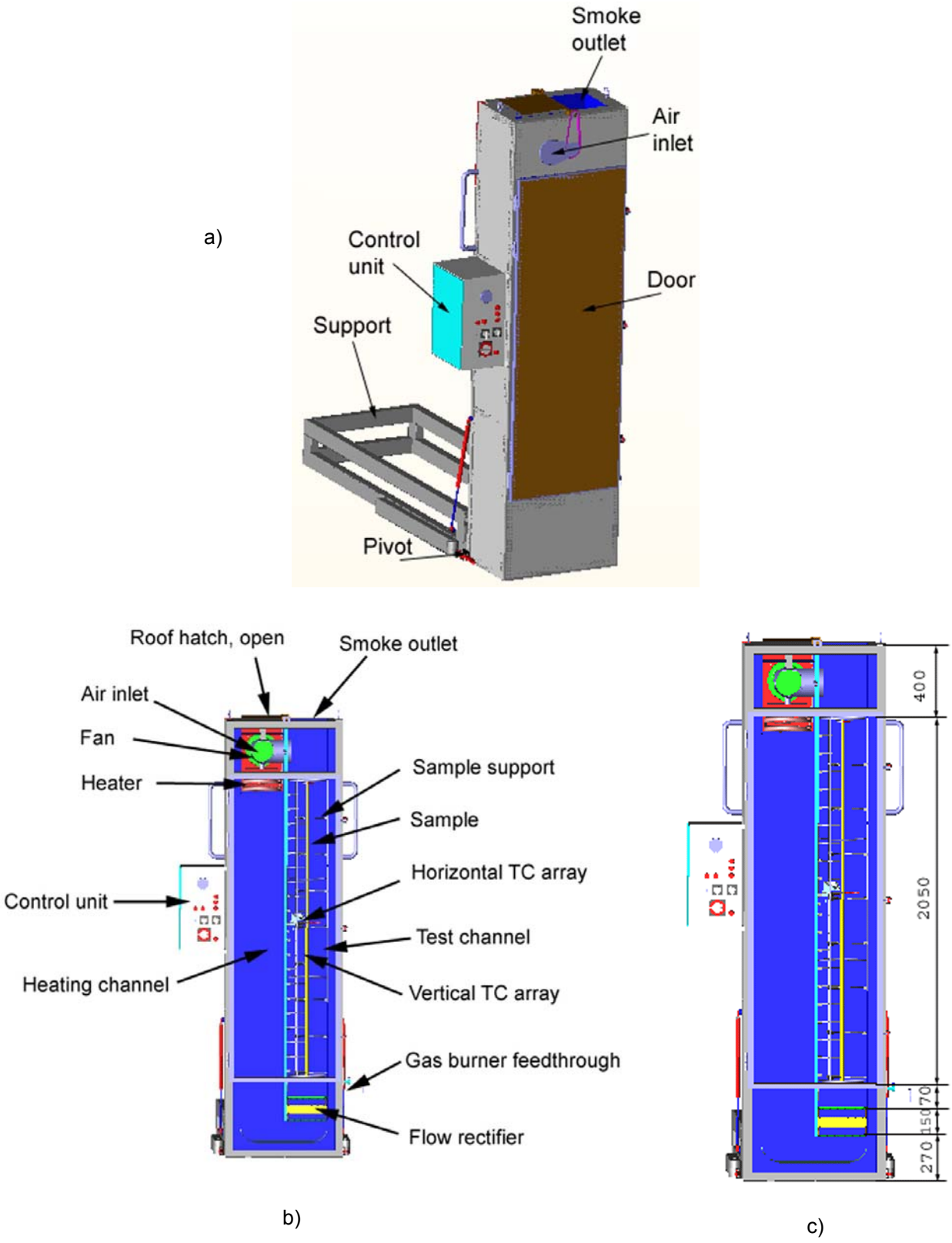

Figure 1. 2 m test rig in vertical position. a) general view, b) cross-section with essential features, c) vertical dimensions. Original drawings by Protoshop.

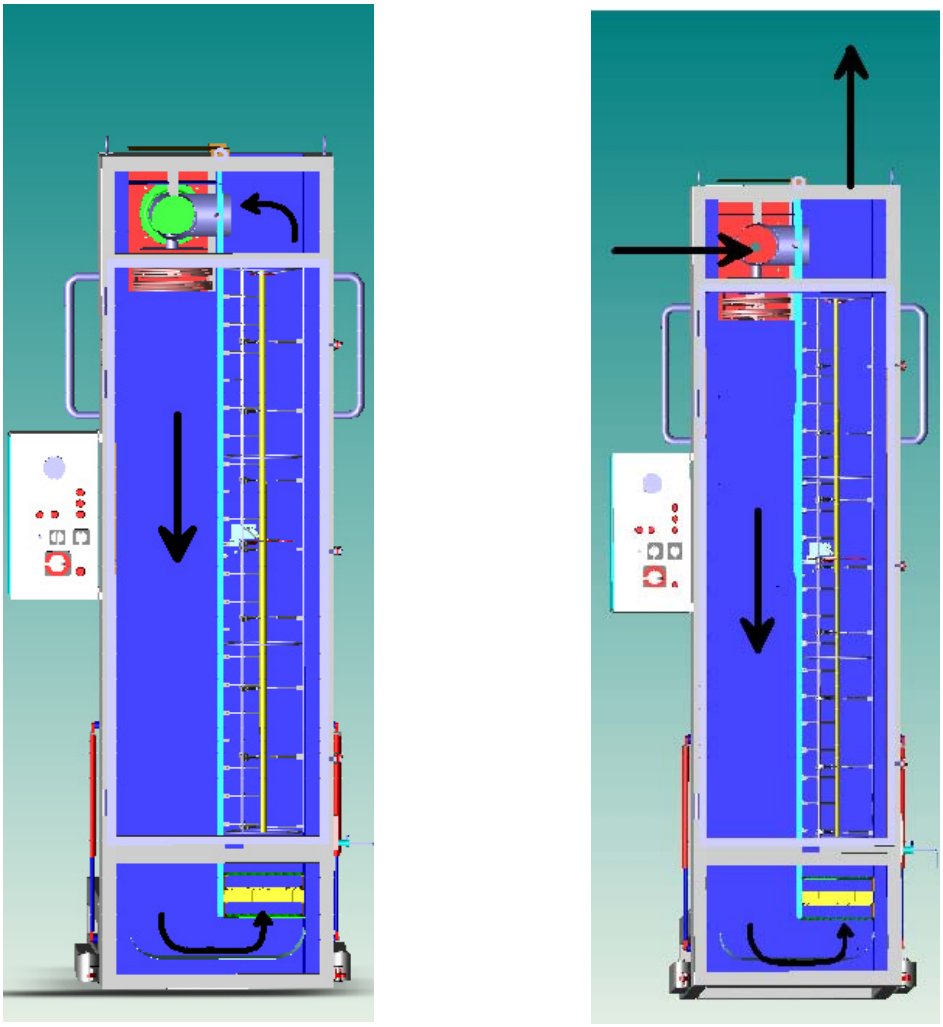

a) b)

Figure 2. a) circulation of air during the heating phase, b) fresh air intake from upper part of the heating channel and fire effluent outlet from top of test channel during experiment, upper opening connecting the channels closed. Original drawings by Protoshop.

The maximum rate of heat release from samples in the cabinet can be estimated, starting from the heat release density of solids (100 … 200 kW/m^2) and oxygen consumption calorimetry (2.94 MJ/kg of dry air), to remain below 100 kW (mostly below 20 kW), which would mean average vertical air flow velocities smaller than 0.3 m/s (mostly below 50 mm/s).

Air should circulate to some extent during heating to avoid damage to the resistors. A minimum flow rate of 0.3 m/s (frequency transformer setting 5 Hz) was suggested. This air flow should provide sufficient oxygen for burning during the experiment. Flow rate 0.3 m/s corresponds to volumetric flow rate 30 dm^3/s in the 0.3 m x 0.33 m channel.

The air flow into the test channel is straightened with a flow rectifier consisting of two 1 mm steel wire screens above and below a honeycomb, with cell length 50 mm and diameter 5 mm. The structure of the flow rectifier is presented in Figure 3.

Air flow velocity is monitored with a bidirectional probe connected to a Setra model 264 pressure transducer. The probe is located centrally in the flow rectifier unit, between the lower steel wire screen and the honeycomb.

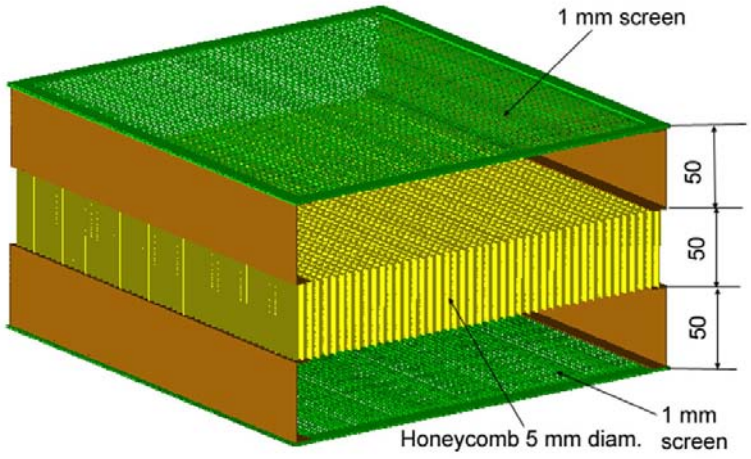

Figure 3. Structure of flow rectifier located in the lower part of the test channel. Original drawing by Protoshop.

2.2 Sample support and thermocouples

The 2 m long sample is suspended from its upper end in a support (Figure 4, Figure 24). The sample is kept in place with pins as shown in Figure 4 at 250 mm vertical intervals. Vertical gas temperatures are measured with 0.25 mm K-type thermocouples T1...T19 supported by ceramic insulator tubes shielded with steel tubes. Vertical co-ordinates for T1…T19 and first thermocouple R1 in horizontal array, with lowest thermocouple T1 as origin, are given in Figure 4. The thermocouples are set to be in contact with the sample surface.

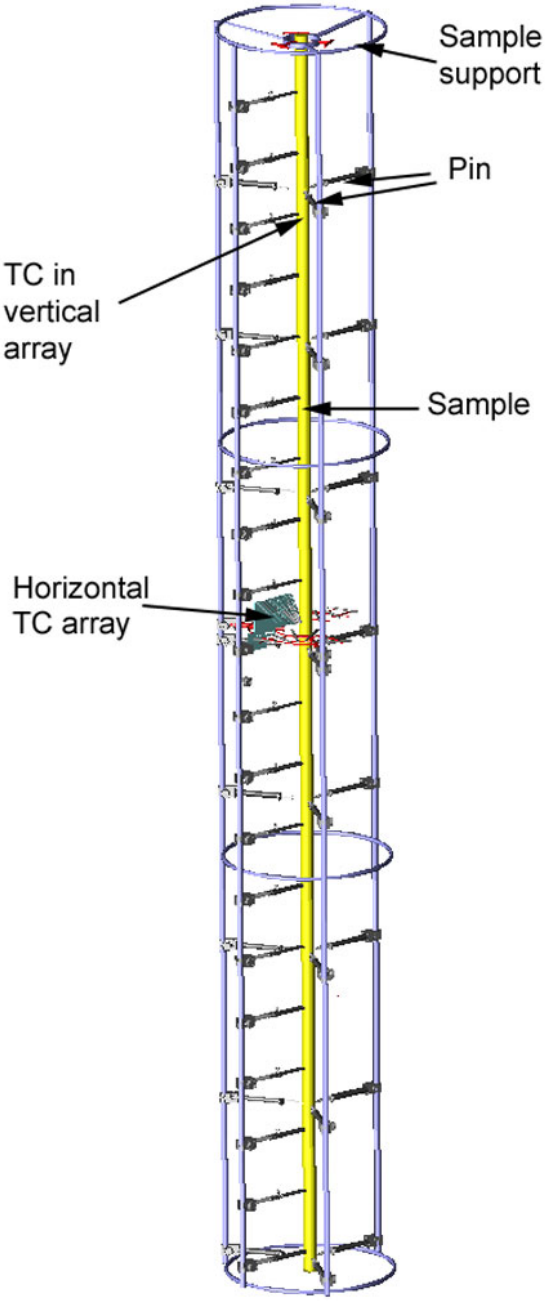

a)

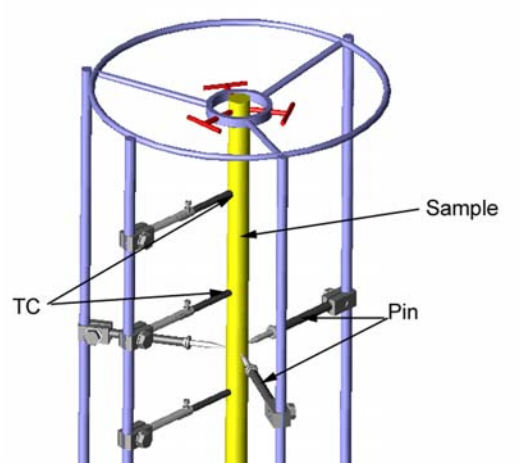

b)

Thermocouple	Vertical coordinate (mm)
T1 (lowest)	0
T2	99
T3	198
T4	300
T5	397
T6	500
T7	597
T8	698
T9	796
T10	896
T11	1099
T12	1202
T13	1300
T14	1400
T15	1502
T16	1600
T17	1700
T18	1801
T19 (highest)	1901
R1	1009

Figure 4. a) Sample support for 2 m long sample. The sample is supported from its upper end and kept in place with pins at 250 mm vertical intervals. Thermocouples TC are in vertical and horizontal arrays, b) close-up of the upper part. Original drawings by Protoshop.

In addition to the principal subject of vertical flame spread, an attempt was made to measure the horizontal temperature distribution in a direction perpendicular to the sample surface. A row of 0.25 mm K-type thermocouples R1...R12 in ceramic insulator tubes was attached to a 3 mm thick steel plate (Figure 4a, Figure 5), with R1 set to be in contact with the sample surface. Experience from the flame spread experiments showed, however, the construction to be prone to short-cuts and disturbances. Horizontal temperatures were measured only in the beginning of the wood sample series.

Thermo-couple	Horizontal coordinate (mm)
R1	0.0
R2	2.1
R3	3.2
R4	4.6
R5	6.0
R6	8.9
R7	9.0
R8	9.8
R9	12.2
R10	16.2
R11	19.0
R12	32.0
R13	41.2

Figure 5. Close-up of horizontal thermocouples R1...R13 in ceramic insulator tubes attached to a 3 mm thick steel plate and horizontal co-ordinates for R1…R13 with R1 as origin.

2.3 Ignition source

The sample is ignited from below with a propane burner and a glow wire. The burner is constructed of stainless steel tubing, 6 mm outer and 4 mm inner diameter, and one end welded closed. The tube is bent into helical shape with holes, 1.5 mm diameter, drilled with 10 mm intervals through one side of the tubing. The glow wire is twisted into a helical coil 30 mm in length and 10 mm in diameter, with shortest distance to thermocouple T1 about 20 mm. Propane gas flow is monitored with a rotameter. The system with burner diameter restricted to 30 mm is presented in Figure 6.

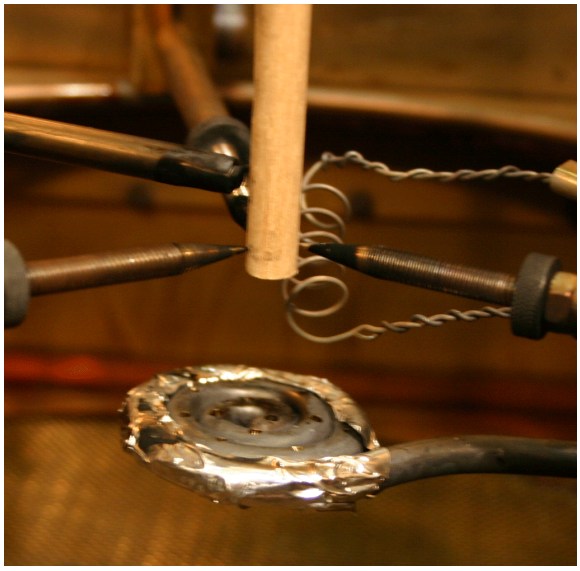

a)

b)

c)

Figure 6. a) Propane burner and glow wire beneath a cylindrical birch wood sample, b) and c) flame shape with rotameter setting 17 mm, without sample.

The influence of burner flame on the thermocouples was checked at different propane gas flow rates (Figure 7) at ordinary room temperature and frequency transformer setting 5 Hz (air flow rate 0.3 m/s) without sample. From these results and from visual observations of the flame shape a 15 mm rotameter setting was chosen for wood sample experiments (Figure 7a). The flame at this flow rate is about 40 mm high and symmetrical (cf. Figure 6b and c), ensuring that the lower end of a sample smaller than burner diameter is ignited symmetrically. Burner power output at this level is estimated to 200…250 W.

Flame retarded cable samples do not ignite as easily as wood samples, and a more powerful propane flame was used for a longer time. Rotameter setting range 25...45 mm was used for burner flow rates in experiments with PVC cable type MMJ. This corresponds to 0.4...0.6 kW power output and burner flame height 100...200 mm without sample. Figure 7b shows temperature response at higher propane flow rates. The rapid rise of temperature T1 is a good indicator for ignition of the burner as shown in Figure 7b. Only thermocouples T1...T3 show notable response to a burner power output of 0.4...0.6 kW (rotameter settings 25...45 mm).

a)

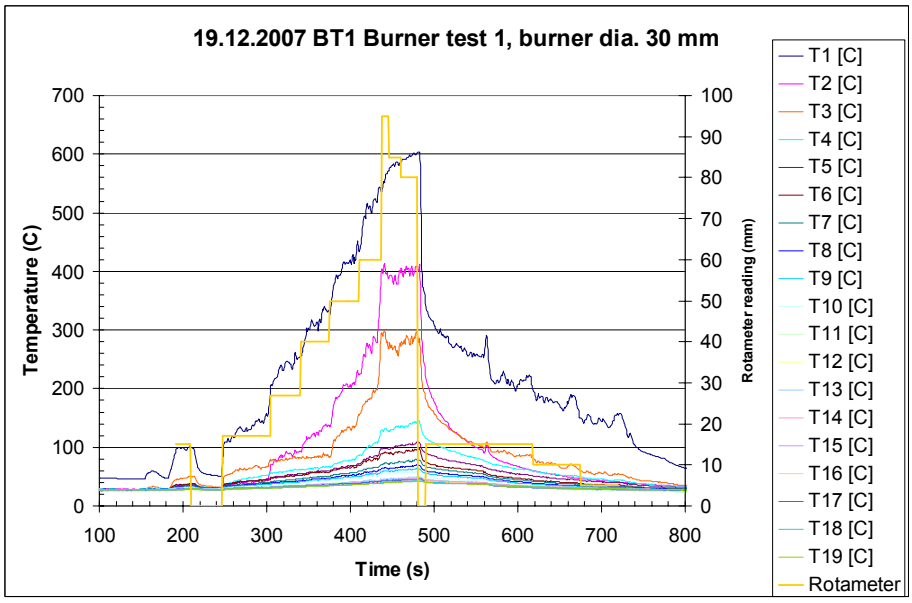

b)

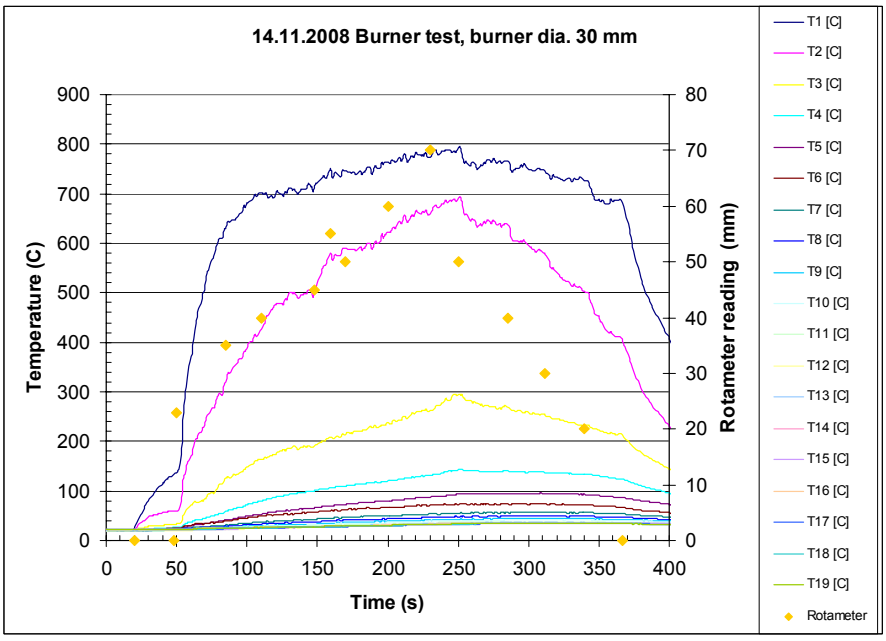

Figure 7. Influence of burner propane flow rate on temperatures. Influence of glow wire alone without propane flame is seen in the lower figure at time interval 20...50 s.

An example of the influence of glow wire at ordinary room temperature and frequency transformer setting 5 Hz (air flow rate 0.3 m/s) without sample is given as temperature curves in Figure 8. Main influence is on thermocouple T1 only, with a final temperature rise of about 25 °C. Other thermocouples indicate temperature rise 2…5 °C.

Glow wire influence is also seen in Figure 7b, time interval 20...50 s. Here the glow wire has been closer to T1, increasing the temperature near the lowest thermocouple.

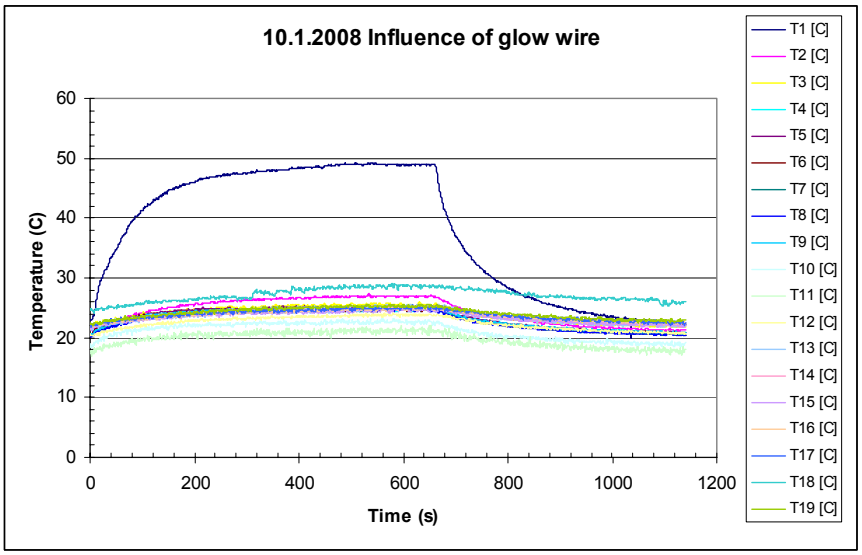

Figure 8. Influence of glow wire on temperatures in test channel. Glow turned on at 0 s and off at 660 s.

3. Start-up tests with the 2 m rig

Start-up tests were carried out to examine, and if necessary improve the performance of the rig. Two series were carried out, one considering air flow in the test channel and one considering heating of the test channel.

3.1 Flow tests

In the flow tests the following issues were studied:

- flow velocity at different settings of the frequency transformer controlling fan speed
- comparison between flow velocity measured with a hot-wire anemometer and a bi-directional probe
- flow velocity profile across the test channel at different heights and effect of gas burner
- generation of eddies near the walls.

A summary of the flow tests is presented in Table 1. All tests were carried out at room temperature.

The bidirectional probe in the flow rectifier was in place during the flow tests. Flow velocity in the test channel above the flow rectifier was measured with an additional bidirectional probe connected to a Setra model 264 pressure transducer and a TSI VelociCalc model 8345 hot-wire anemometer. A plywood sheet with holes for the velocity probe was used as a temporary door. The position of the moving probe was monitored with a Hottinger-Baldwin WA 500 displacement transducer. All tests except # 19 were carried out with the roof hatch open as in flame spread experiment circumstances. Tests 1 to 16 were carried out without gas burner, and tests 17 to 21 with a gas burner 50 mm in diameter in place, but unlit.

3.1.1 Flow velocities at different fan speed

Flow velocities in the centre of the test channel 120 mm above the top of the flow rectifier were studied at different fan speeds in three tests using a bidirectional probe. The results are presented in Figure 9.

Table 1. Air flow start-up tests with 2 m apparatus. FR Flow rectifier, BP bidirectional probe, FT frequency transformer.

Test no	Purpose	FT setting (Hz)	Flow velocity before honey-comb rectifier (m/s)	Flow velocity probe	Note
1	BP check	70.0	2.7	BP	
2	BP check	70.0	2.7	BP	
3	Flow profile 120 mm above FR	70.0	2.7	BP	BP stuck 50…70 mm from plywood sheet
4	As # 3	70.0	2.7	BP	
5	As # 3	70.0	2.6	BP	Larger holes in plywood sheet to get BP close, end of test bad displacement data
6	As # 3	70.0	2.6…2.7	BP	
7	As # 3	70.0	2.6…2.7	BP	Test 6 repeated
8	As # 3	70.0	2.6…2.7	hot-wire anemometer	Test 6 repeated with hot wire anemometer in channel
9	Channel flow 120 mm above FR	10…70, 10 Hz increments	0.8…3.2	BP	Burner module was not in place
10	As # 9	10…90, 10 Hz increments	0.8…3.2	BP	Burner module in place Without burner
11	Comparison between BP and hot-wire anemometer	10, 20, 30 ,40, 50	0.8…3.3	BP and hot-wire anemometer	Without plywood sheet Without burner
12	Whirls in back and rear wall corner in channel	50	3.3	BP	Without plywood sheet Without burner

13	As #12	50	3.2	BP	Without plywood sheet Without burner
14	As #12	50	3.2	BP	Without plywood sheet Without burner
15	As #12	50	3.2	BP	Without plywood sheet Without burner
16	Flow profile 120 mm above FR	5, 10, 30, 50	0.3…3.2	BP	Without burner
17	Flow profile 120 mm above FR	10	0.8	BP	50 mm burner in place
18	Flow profile 370 mm above FR	10	0.8	BP	50 mm burner in place
19	Flow profile 370 mm above FR	10	0.8	BP	Roof hatch closed 50 mm burner in place
20	Flow profile 620 mm above FR	10	0.8	BP	50 mm burner in place
21	Flow profile 370 mm above FR	10	0.8	BP	50 mm burner in place

Repeatability for flow velocity before the honeycomb rectifier is good. Small scattering appears for velocities in the channel. In test 9, the gas burner module was not in place in the right wall, leaving a 100 mm x 100 mm opening in the wall, which might explain the slightly slower flow in the test channel. Flow velocities in the range 0.3…2.8 m/s were achieved in the test channel. Figure 10 presents velocities before and after the flow rectifier showing its effect on flow velocity. Larger losses are noted at higher velocities.

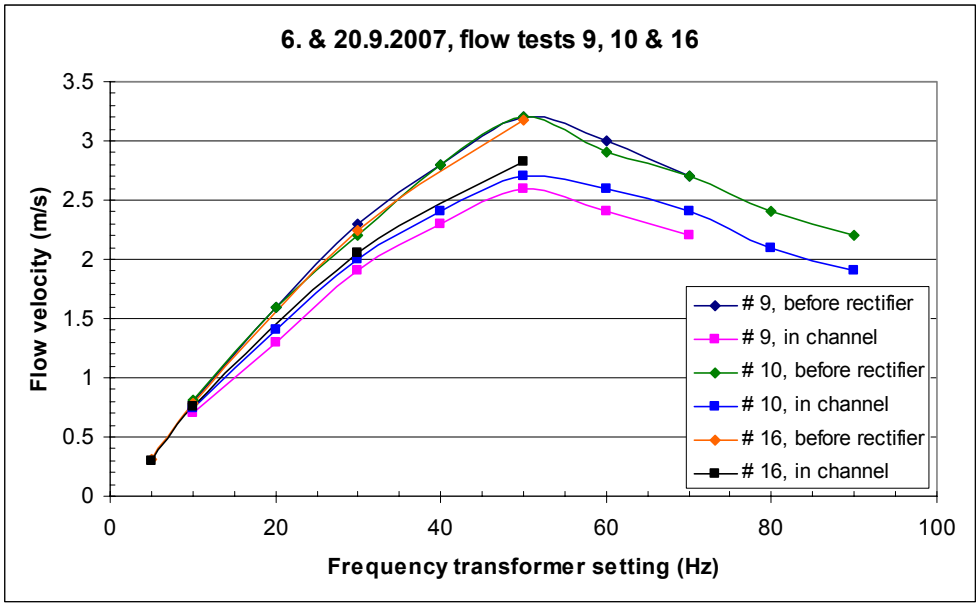

Figure 9. Flow velocities in test channel, before honeycomb rectifier and 120 mm above flow rectifier unit at different frequency transformer settings.

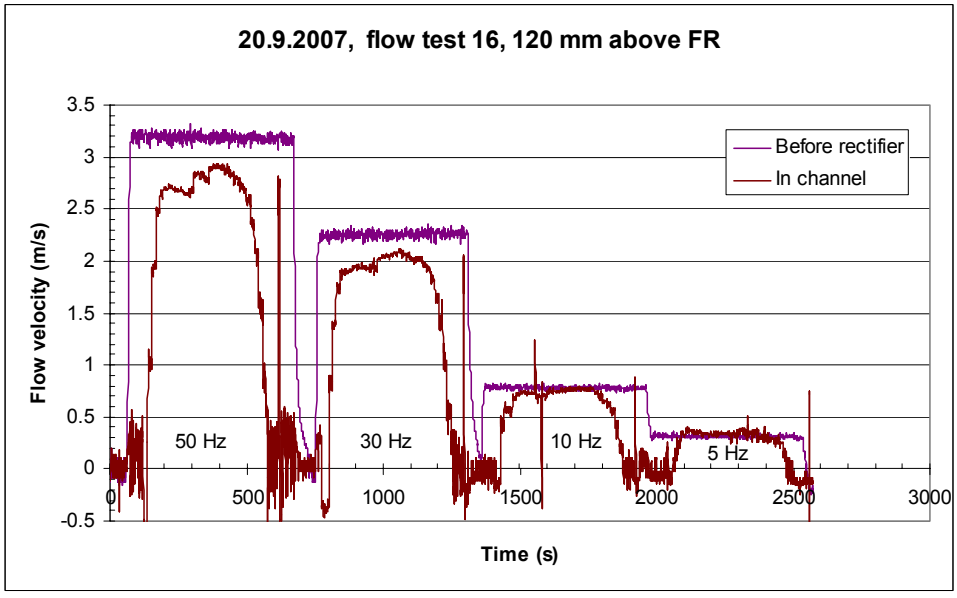

Figure 10. Flow velocities in test channel, before honeycomb rectifier and 120 mm above flow rectifier unit at different frequency transformer settings.

3.1.2 Air flow velocity profiles with bidirectional probe and hot-wire anemometer

Flow velocity profiles were carried out varying

- flow velocity
- height above top of flow rectifier
- bidirectional probe/hot-wire anemometer
- burner/no burner present
- roof hatch open/closed.

A hot-wire anemometer was tried because the outer diameter of the bidirectional probe was 16 mm and could possible have too low resolution for small eddies near the walls.

The two probes were checked against each other at different flow rates in the channel 120 mm above the top of the flow rectifier, 100 mm from the rear wall and 105 mm from the right wall, with no obstacles beneath (Figure 11a). Results are presented in Figure 11b. The bidirectional probe indicated 7…10 % higher flow velocities than the hot-wire anemometer, which had been calibrated 18.6.2007.

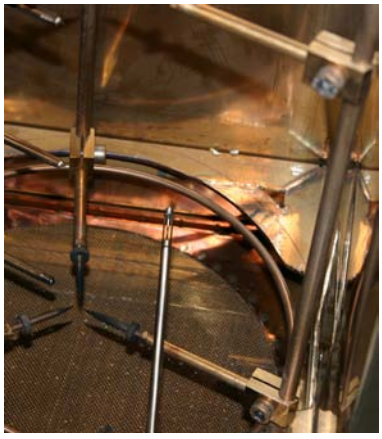

a)

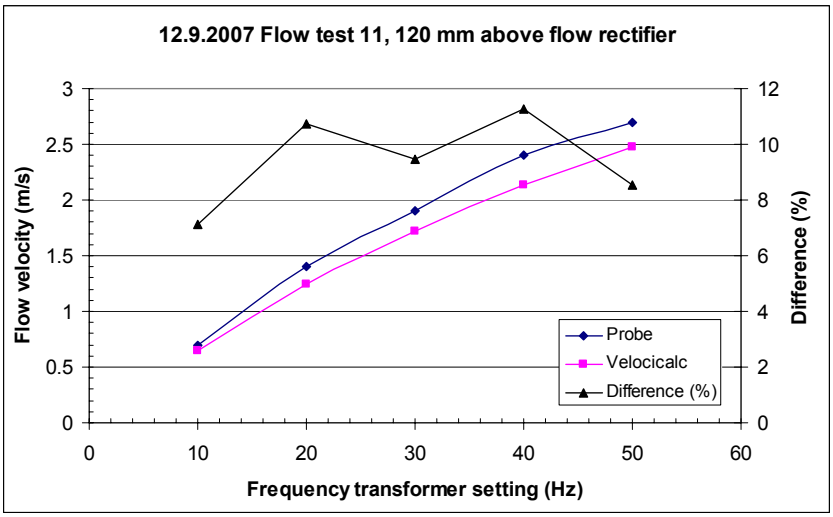

b)

Figure 11. Comparison between bidirectional probe and hot-wire anemometer VelociCalc at different flow rates in the channel. a) hot-wire anemometer in place, b) results.

The velocity profile tests were carried out as shown in Figure 12, starting from the centre of the rear wall of the test channel and moving the probe manually 10 mm step by step horizontally towards the plywood sheet, which temporarily replaced the door. After each step the probe was held in place for 15…30 s, with data acquisition at 1 Hz. The hot-wire anemometer was read manually from the display. Figure 12b shows the position of the bidirectional probe in test 21 with the 50 mm burner in place. The probes were controlled outside the plywood sheet, and no visual observations could be made.

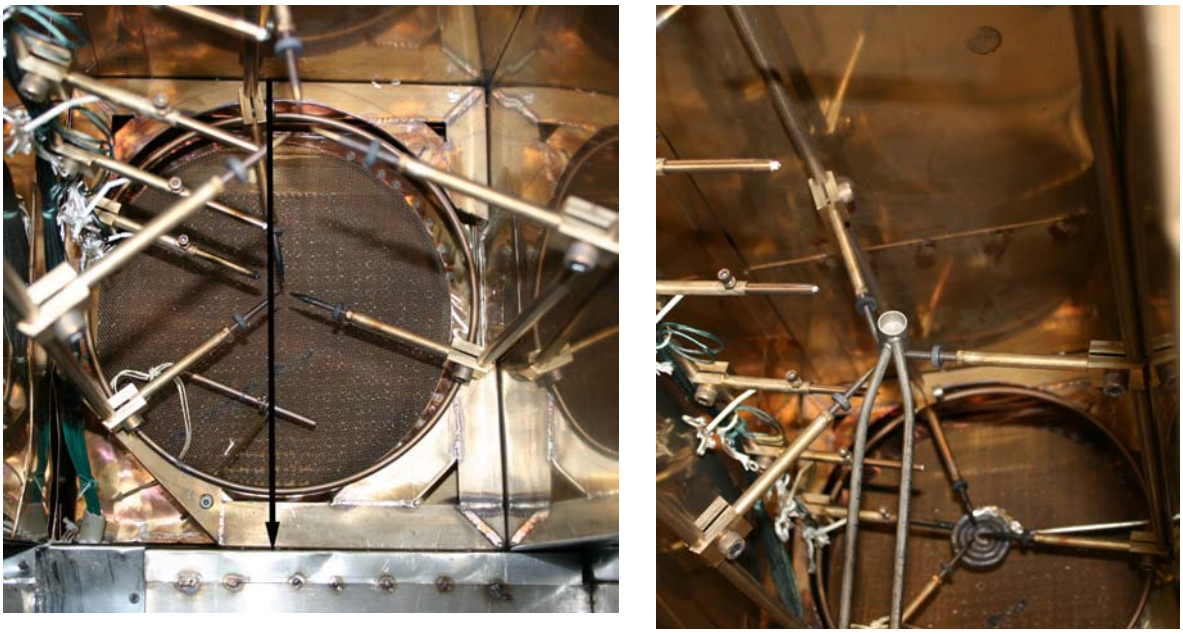

a) b)

Figure 12. a) bottom of the test channel, the black arrow shows the approximate path of velocity probe in velocity profile tests. b) bidirectional probe 370 mm above top of flow rectifier with burner 50 mm in diameter in place.

Flow velocity profiles are presented in Figure 13 to Figure 16. The origin corresponds to the centre of channel, negative x-axis denote direction towards rear wall and positive direction towards door.

Results from tests 120 mm above top of flow rectifier are presented in Figure 13 to Figure 15. This height represents conditions near the lowest part of the sample, some 20…30 mm above sample lower edge level. In Figure 13, results with the bidirectional probe are compared with results using the hot-wire anemometer, showing also here slightly higher flow rates with the bidirectional probe. Tests 6 and 7 with bidirectional probe show good repeatability. Lower flow velocities are measured at 30…90 mm from centre towards rear wall. This coincides with the location of the sample holder pin (Figure 12a) on the rear wall side, especially the knob 40 mm from centre of channel. A similar drop is noted 70 mm towards the door, where the shield of the heating controlling sensor forms an obstacle. The hot-wire anemometer does not react on the obstacle on the rear wall side, but the shield is noted as a slight velocity drop on the wall side. The reason is probably that the path of the hot wire anemometer was not directly above the sample holder pin, and did not react on the obstacle.

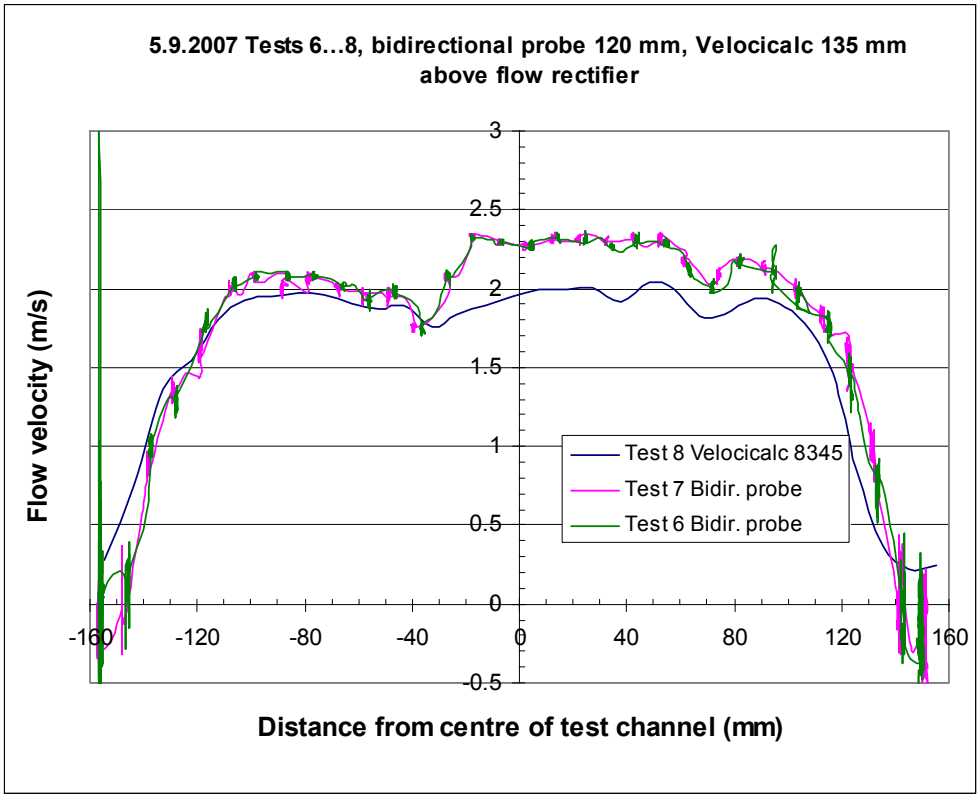

Figure 13. Flow velocity profile in test channel 120 mm above upper level of flow rectifier, without burner. Negative x-axis denote direction towards rear wall and positive direction towards door. Flow velocity before rectifier 2.6…2.7 m/s.

The effects of flow velocity on the profiles are shown in Figure 14. The influence of obstacles seems to be more pronounced at higher flow velocities as the three upmost curves are more irregular than the curves at 5 and 10 Hz. As the exact path of the probe above the sample holder pin is not known, small deviations in path between the tests can to some extent also explain the differences.

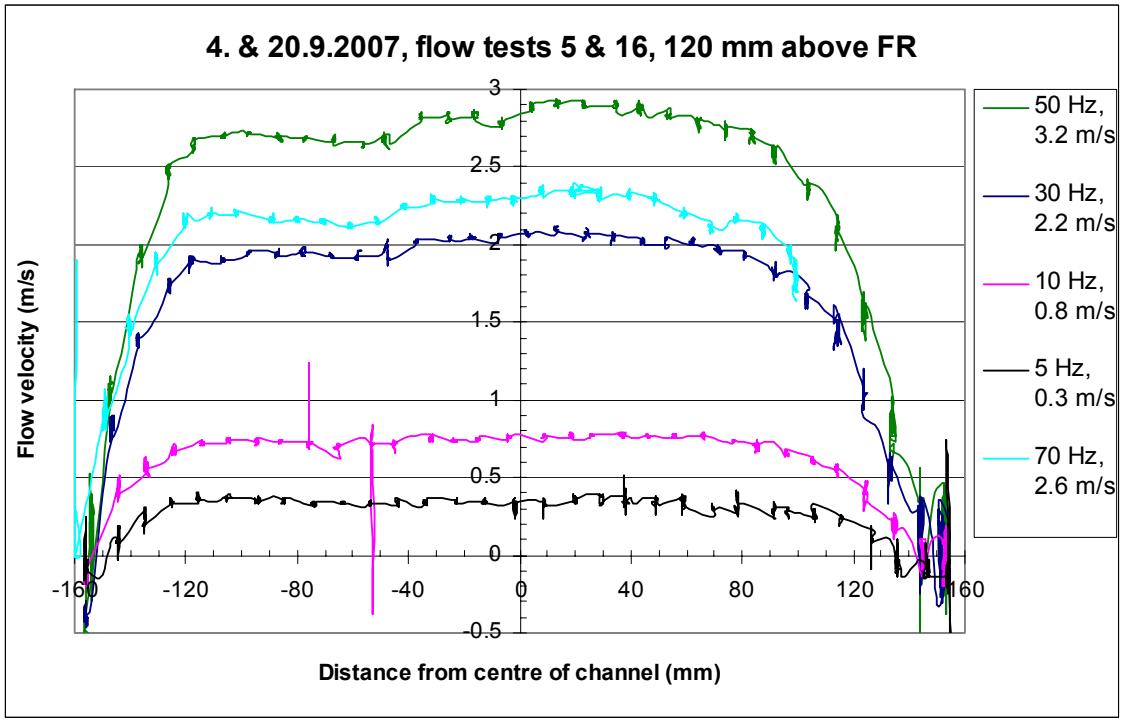

Figure 14. Air flow velocity profile in test channel 120 mm above FR at different frequency transformer settings, denoted in legend box together with flow velocity before honeycomb rectifier.

After these tests with different flow velocities in the test channel, the remaining flow tests 17…21 were carried out at flow 0.8 m/s as this was thought to be the actual flow during flame spread experiments. As presented later, a lower flow, 0.3 m/s (frequency transformer setting 5 Hz) was used. As shown by the similarity of 5 Hz and 10 Hz profiles in Figure 14, the difference in outcome is expected to be only flow rate level.

The influence of the unlit gas burner on the velocity profile is presented in Figure 15. The probe was 50 mm above the burner, which was 15 mm off centre of channel towards rear wall. A backward current is noted directly above the burner.

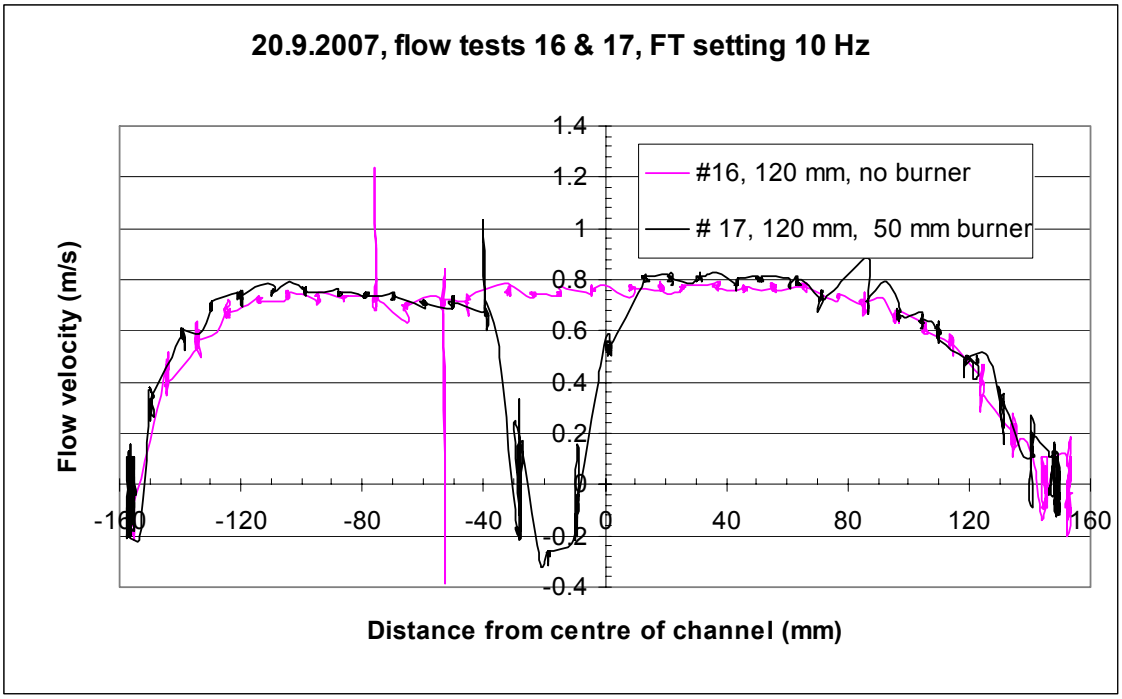

Figure 15. Influence of the 50 mm diameter gas burner on the flow velocity profile in test channel 120 mm above top of flow rectifier. Flow velocity before honeycomb rectifier 0.8 m/s.

Flow profiles at higher levels are presented in Figure 16 together with the result from test 17. There are no differences between the profiles 250 and 500 mm higher. No influence of roof hatch open/closed is seen. This is expected as the flow should be similar in the lower part of the channel because the only difference is that the same air is circulated in the device when the roof hatch is closed.

The sample holder was slightly rotated counter clockwise after test 18 to examine whether the different position of the support sticks could be noted. No significant difference was noticed.

When compared to the profile at 120 mm, the influence of the gas burner disappears at higher levels. The velocity near the rear wall is somewhat higher at 120 mm.

Overall, the flow velocity profile seems to be quite uniform up to 100 mm away from the centre of the channel. Due to symmetry, the same can be expected in other directions not studied here. The influence of the burner was noted only directly above. The hot-wire anemometer was not used in larger extent because it does not indicate the flow direction and has only manual reading of the display.

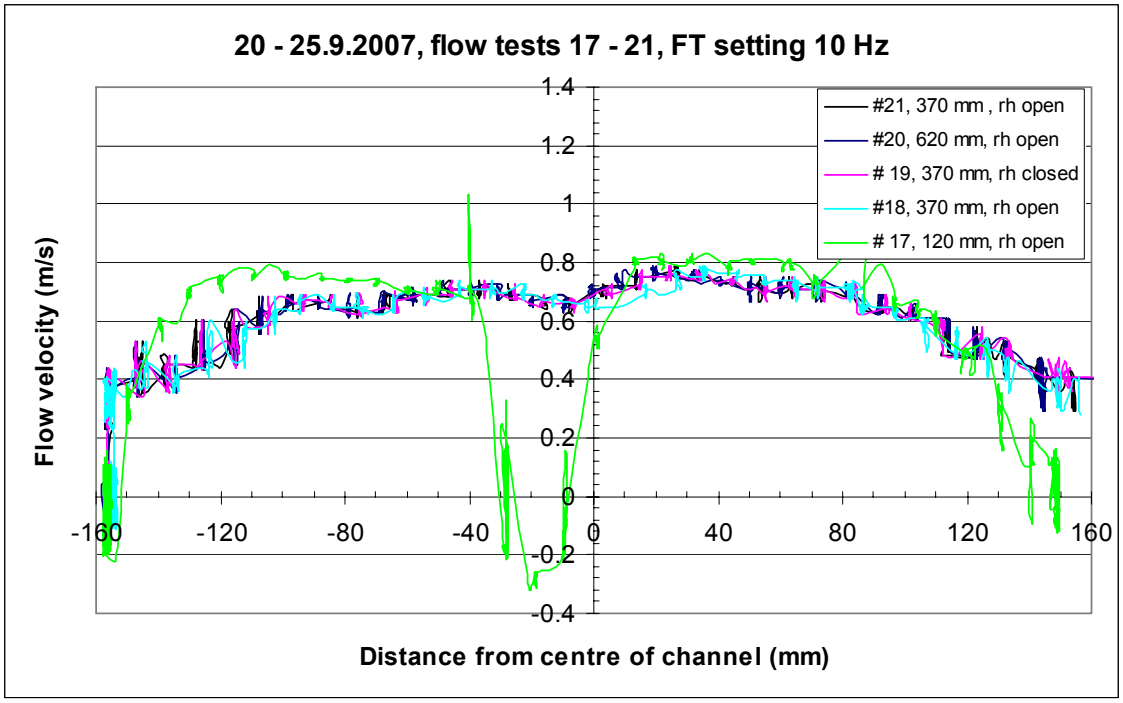

Figure 16. Air flow velocity profiles in test channel. Height above top of flow rectifier indicated in the legend box, rh = roof hatch. Flow velocity before honeycomb rectifier 0.8 m/s.

3.1.3 Eddy measurements near walls

The occurrence of eddies near the walls of the test channel was studied with a bidirectional probe. The probe was located in the lower rear/right wall corner (Figure 17a) at different positions about 10 mm above the sample holder support. The probe was then manually moved vertically upwards some 200…250 mm while the position was monitored with the displacement transducer. The time used for one elevation was 30…40 s. An example of the uniformity of vertical motion is presented in Figure 17b.

The co-ordinates for positions of the elevations are presented in Figure 18 together with flow velocities as a function of vertical displacement.

a)

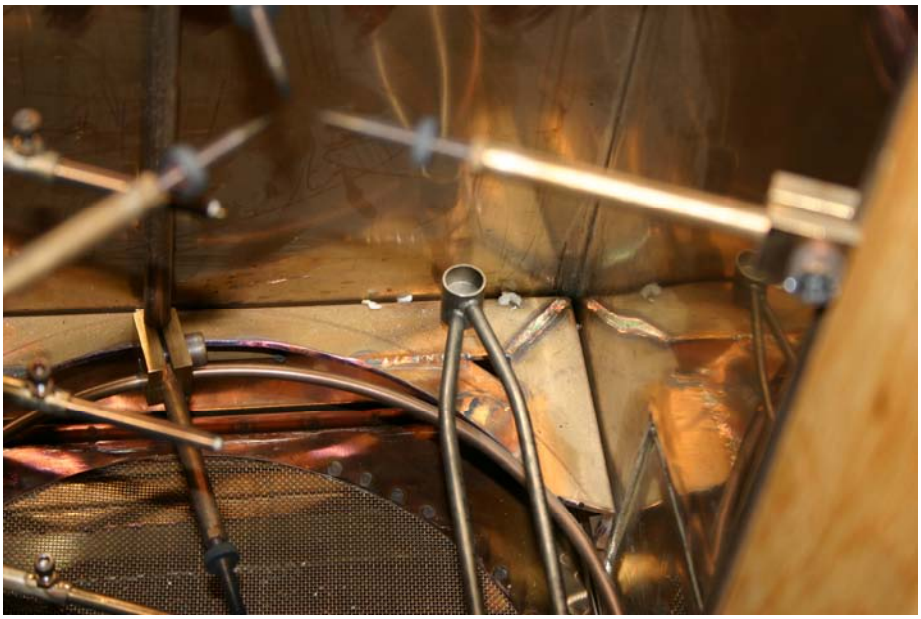

b)

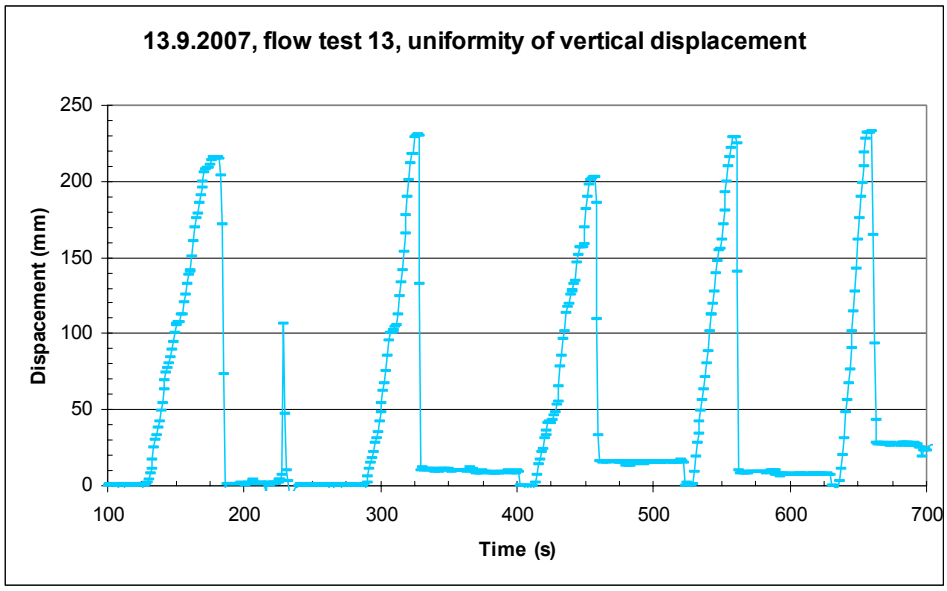

Figure 17. a) Lower rear/right wall corner in test channel where attempts to measure eddies with a bidirectional probe were carried out, b) vertical displacement of bidirectional probe as a function of time.

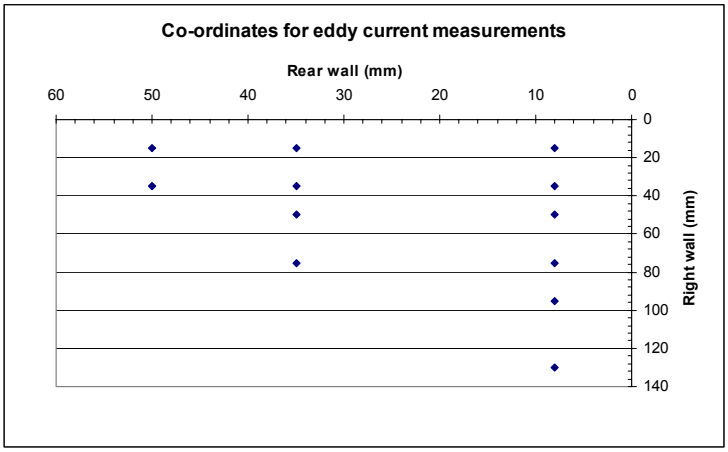

a)

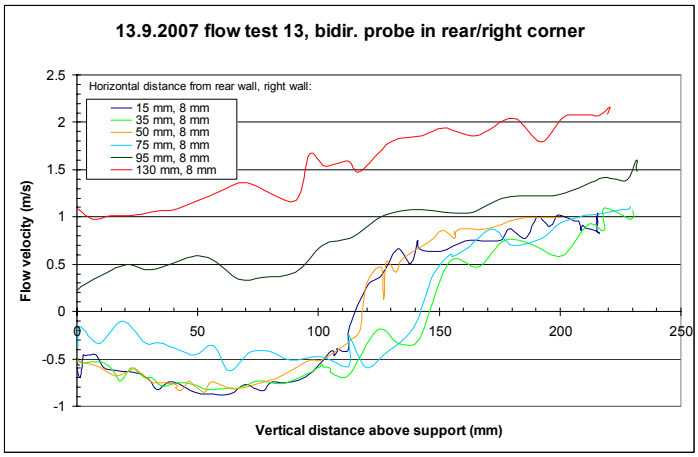

b)

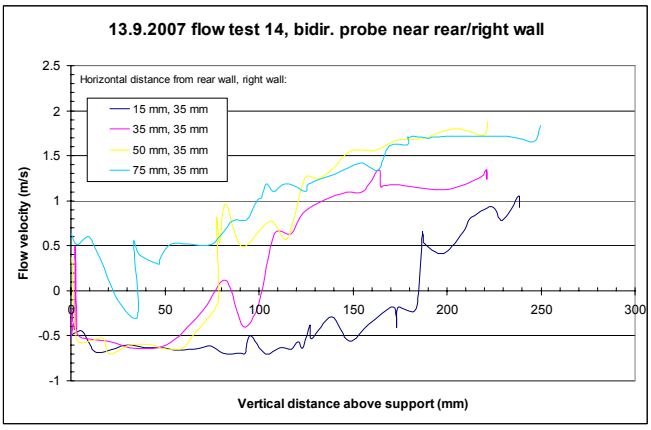

c)

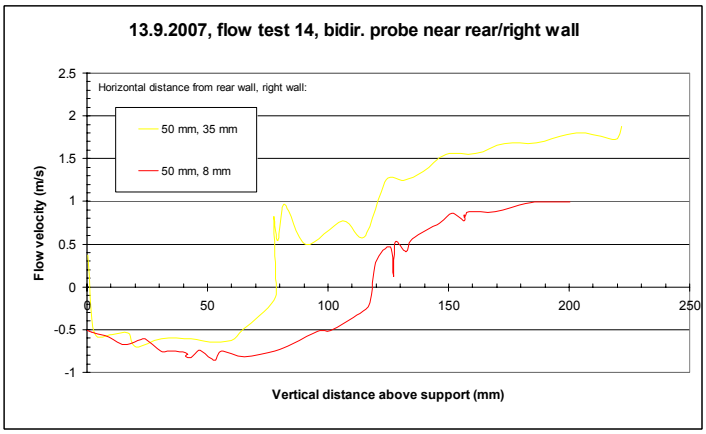

d)

Figure 18. a) horizontal co-ordinates for eddy measurements, b) to d) flow velocities in the lower part of the test channel; horizontal coordinates are given in the legend box. Flow velocity before honeycomb rectifier 3.2 m/s.

Reverse flow near the walls in the lower part of the test channel was observed as shown in Figure 18. The eddy subject was not continued as the bidirectional probe might be too crude to reveal small eddies. In addition, the experimental arrangements needed improvement from the manual control used.

3.2 Heating tests

A series of heating tests were carried out to check and improve times to reach desired temperature, reduce leaks, and improve insulation and uniformity of temperature in the test channel. A summary of the heating tests is presented in Table 2.

Table 2. Heating tests with 2 m apparatus. TC = thermocouple.

Test no	Frequency transformer setting (Hz)	Desired temperature (^{o}C)	Time to reach desired temperature (min:s)	Measure after experiment, remark
HT 1				Instrumentation check
HT 2	40	200	23:30	Extra Kaowool insulation on roof hatch
HT 3	40	200	24:10	TC wire feed-through insulation improved
HT 4	20	200	23:11	Upper and lower edge of door sealed with Kaowool
HT 5	50	200	24:40	Door sealed with ceramic sealing tape 3 mm x 20 mm and Kaowool at lower edge
HT 6	50	200	24:20	Door sealing improved with ceramic tape, extra Kaowool insulation on top of heating channel
HT 7	50	200	23:40	Flow rectifier and burner feed-through boxes sealed with ceramic tape
HT 8	50	300	45:00	
HT 9	50	300	45:40	Test performed without extra insulation on roof hatch Heating effects on birch rod checked
HT10	50	110	11	Check of radial TCs
HT11	50, 10	110	9	Check of radial TCs Test performed without extra insulation on roof hatch

3.2.1 Temporal behaviour

Examples of temperature-time curves are presented in Figure 19 showing times to reach desired temperature 110, 200 and 300 ^{o}C, i.e. setting of the temperature controller.

a)

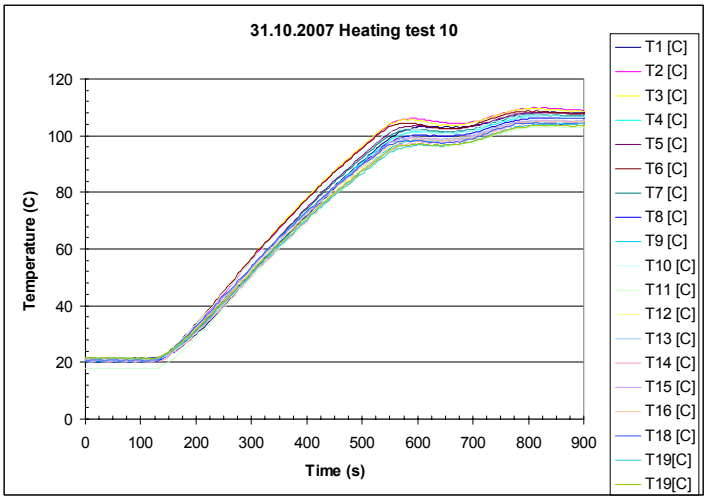

b)

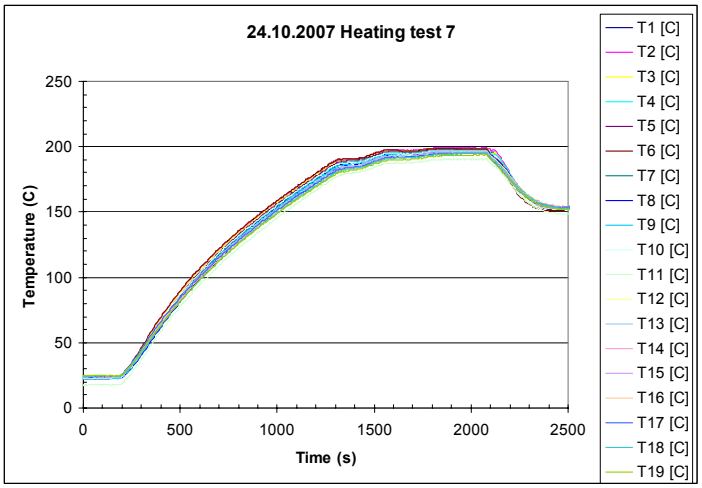

c)

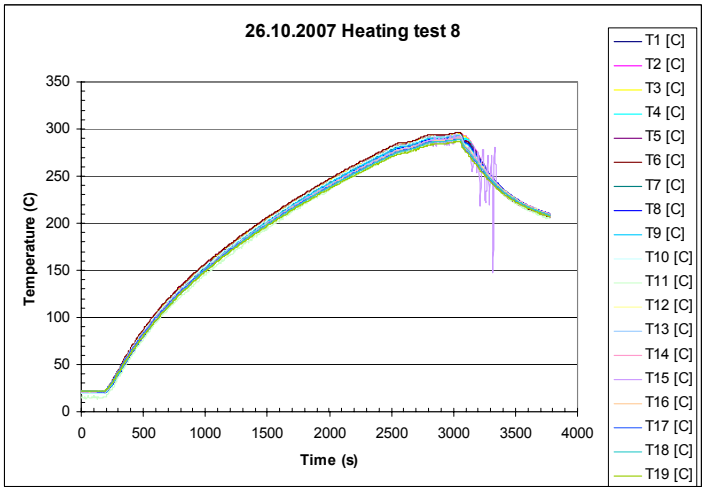

Figure 19. Temperature as a function of time, desired temperature a) 110 °C, b) 200 °C and c) 300 °C. Roof hatch opened at 2115 s (HT7) and 3100 s (HT8).

Air was circulated at highest speed, 2.8 m/s in test channel (frequency transformer setting 50 Hz), during the heating phase. Flow was lowered to 0.8 m/s in heating tests 7

and 8 after the desired temperature was reached, and the roof hatch was opened with heating still on. Temperatures in the test channel descended immediately.

3.2.2 Spatial behaviour

The uniformity of the vertical temperature distribution was increased as the sealing of the doors, roof hatch and feed-throughs was improved. Temperatures as a function of height are shown in Figure 20. Differences between lowest and highest temperature in the channel were at most 11 °C after desired temperature was reached in heating test 8. At 2883 s the difference was 10 °C, and maximum deviation from average temperature 289 °C was 2 %. Two minutes after opening of the roof hatch the maximum difference had increased to 23 °C.

The construction of the roof hatch was troublesome as a tight design lead to jamming of the hatch because of thermal expansion. This resulted in a hatch moving without jamming but leaking heat at the edges. The hatch was therefore sealed by adding Kaowool insulation and a weight upon the hatch. Differences between lowest and highest temperatures presented in Figure 21 show the improvement.

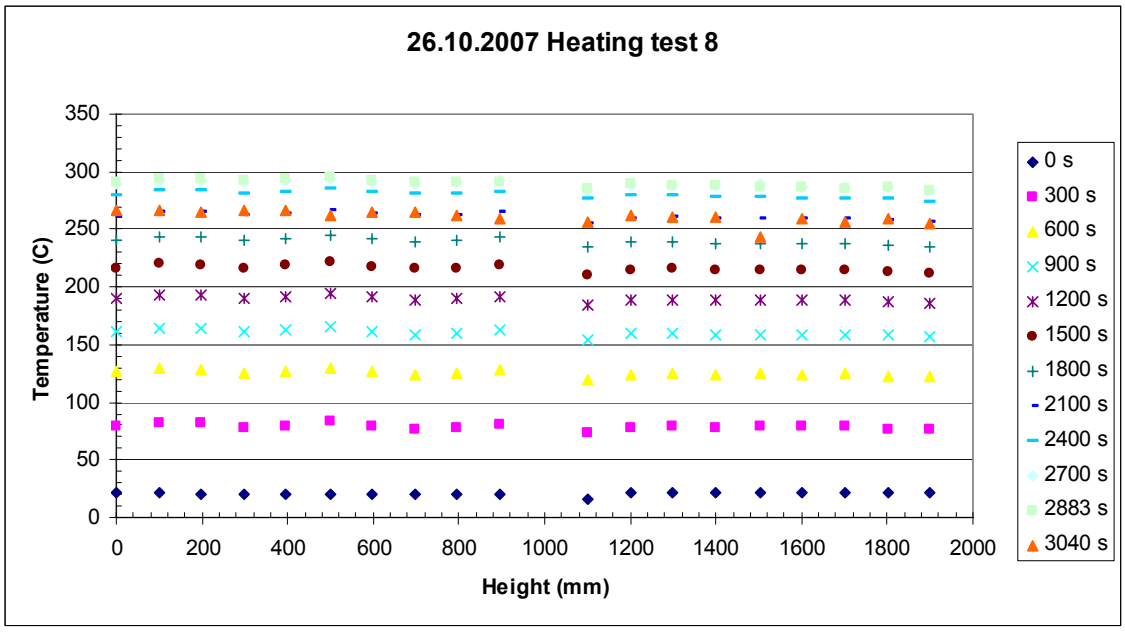

Figure 20. Temperatures in test channel as a function of height, zero corresponds to position of T1. Times in legend box are from start of heating. Time 3040 s corresponds to 2 min after opening of roof hatch.

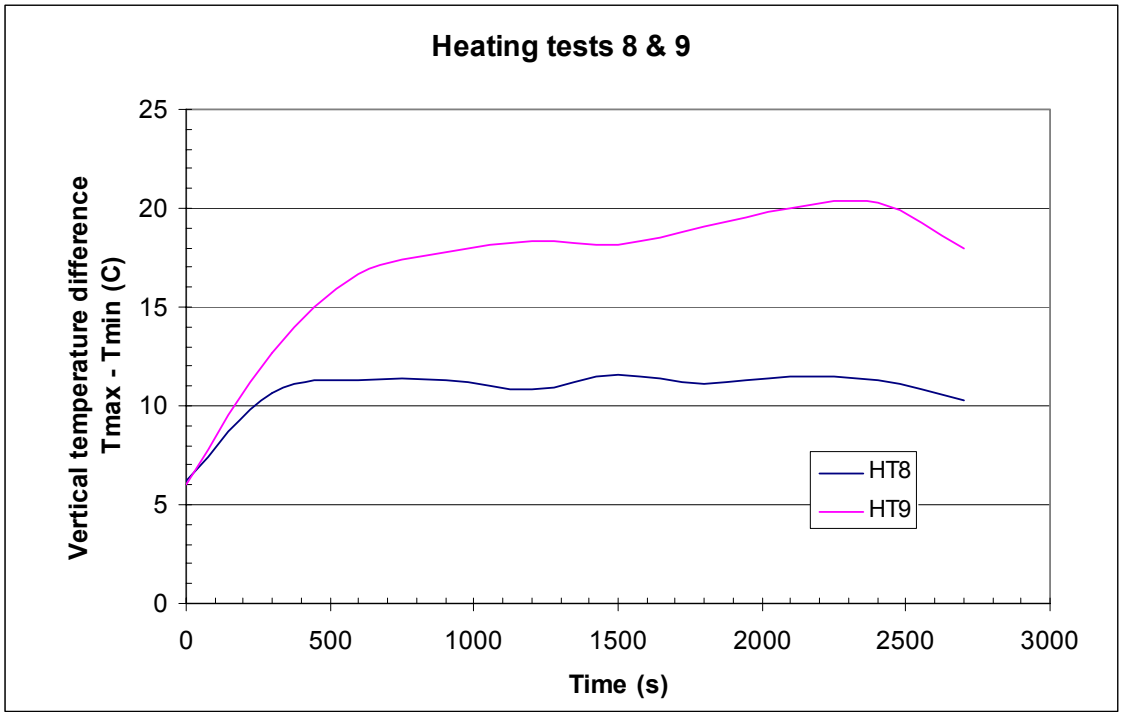

Figure 21. Improving uniformity of vertical temperature distribution: effect of additional roof hatch insulation (HT8) compared with no additional insulation (HT9).

The uniformity of temperature in a horizontal cross-section 830 mm above T1 was checked with an array of 12 thermocouples, symmetrically grouped at three distances from the centre, as shown on graph paper in Figure 22a. The scatter of temperatures at 2950 s in heating test 8 is shown as a function of radial distance from centre of test channel in Figure 22b and temperature-time curves in Figure 22c and d.

Temperatures decrease towards the walls, with a maximum deviation from the temperature at the centre of the test channel of 5 %. Average temperatures (distance from the centre) were 291 ^{o}C (30…34 mm), 287 ^{o}C (67...80 mm) and 282 ^{o}C (113…119 mm) Maximum deviations within each group were 1…2 % at these average temperatures.

The time-temperature curves during the heating phase show that the order between the temperatures measured at different positions does not change with time, indicating a steady flow. Temperature differences even out after lowering the flow velocity and opening of the roof hatch, indicating mixing of the flow.

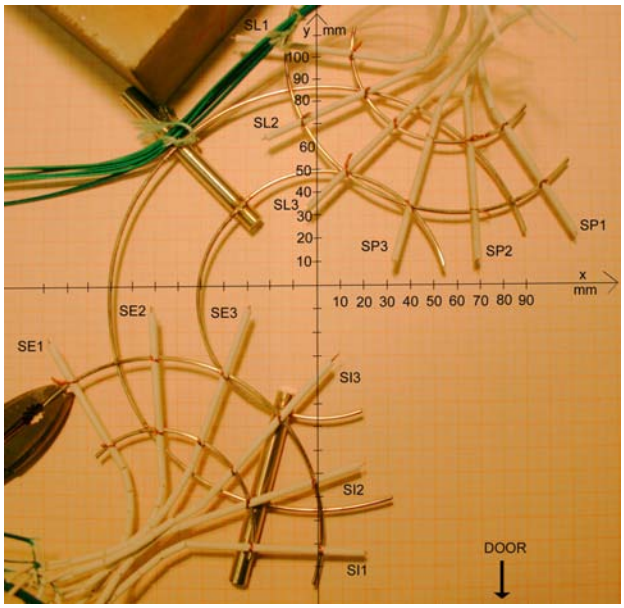

a)

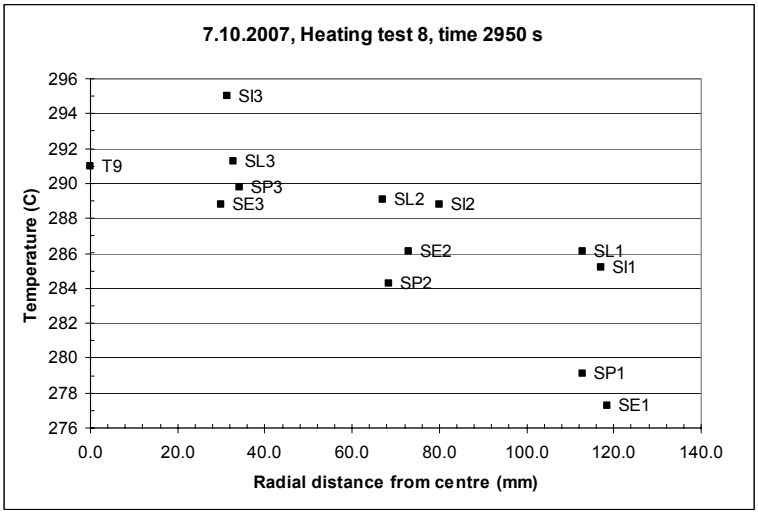

b)

c)

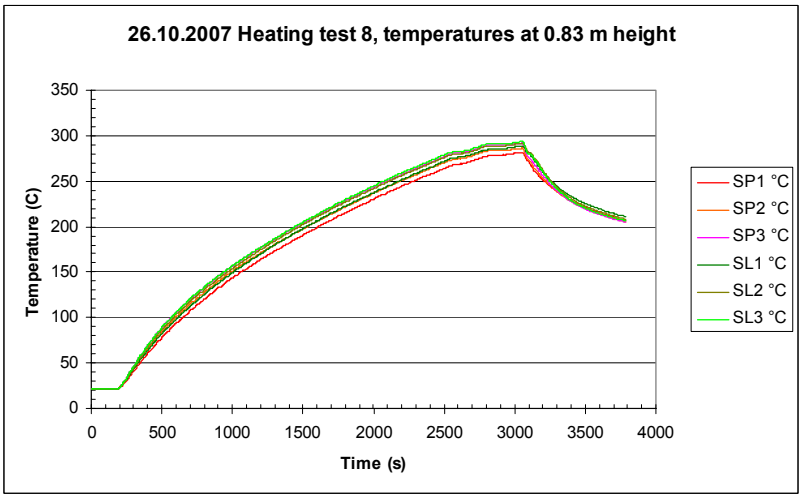

d)

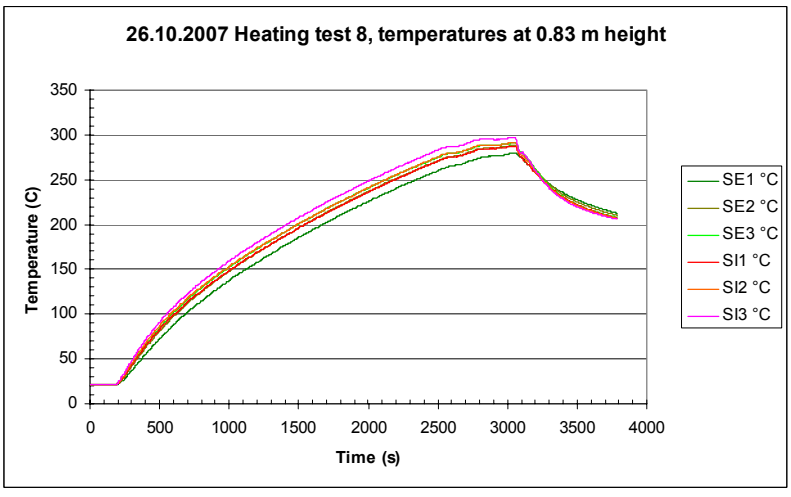

Figure 22. Uniformity of temperature cross-section 830 mm above T1. a) Co-ordinates of the thermo-couples with respect to centre of test channel, door side is indicated with an arrow b) temperatures as a function of radial distance from centre of test channel, T9 at the centre of the channel is shown as a reference, c) and d) temperature-time curves.

3.2.3 Volatilization of wood in heating test 9

The mass change of a 2.0 m long cylindrical birch wood rod 8 mm in diameter was checked in heating test 9. The rod of mass 62.32 g was mounted in the sample holder and heated up to 300 ^{o}C during 47 min until opening of the roof hatch. 17 min after opening of the roof hatch the mass loss of the rod was 12.6 g (20.2 %). The moisture determined in a sample taken from the same original rod was 6.8 weight %. Thus 13.4 % of the wood mass had volatilized during 64 min in the heated channel. The rod had blackened on the surface and throughout (Figure 23).

Figure 23. Blackening of upper, lower and centre part of birch wood sample in heating test HT 9.

4. Flame spread experiments on cylindrical birch wood samples

Commercially available cylindrical samples of birch wood were used for flame spread tests, continuing previous work. Samples of 2100 mm length were attached to the support and ignited from below as described in section 2.3. Photographs of a wood sample S are presented in Figure 24.

A list of the experiments and sample properties is presented in Table 3. Experimental features and results are tabulated in Table 4 and Table 5 and explained in detail in the following sections. Data were collected with a DaisyLab-Instrunet data acquisition system at 1 Hz frequency.

The samples were heated with air circulating at highest possible speed, frequency transformer setting 50 Hz, corresponding to 2.6 m/s air flow at room temperature in the test channel. Transition from heating phase to flame spread experiment consisted of the following sequence:

1. reaching desired temperature, heating was temporarily turned off
2. frequency transformer setting was lowered to 5 Hz, corresponding to 0.3 m/s air flow at room temperature (volumetric flow rate 30 dm^3/s)
3. heating was turned on
4. the heating of glow wire turned on
5. the propane gas line opened
6. burner ignition and sample in flame contact
7. the roof hatch opened

In experiments FS1 to FS5 the roof hatch was opened before the propane line was opened. To reduce cooling of the system before ignition, the order was reversed starting from FS6.

The propane burner was on until the thermocouples showed that the wood sample had ignited and flame spread was established. Burner flame durations were 1 to 1.5 min (Table 5) except FS2 where the burner was on for the whole experiment. Propane burner power was 0.2 kW in the birch wood experiments.

Experiment FS1 was a check of the system performance with a short sample and door open for visual observations, and flame spread was not determined.

A 175 mm long reference wood sample (R in Figure 24) was added starting from experiment FS5. The purpose of the reference sample was to measure temperature inside the sample and to estimate mass loss of an unburned piece during the heating. The sample was located 0.9 m above T1 level and at 100 mm horizontal distance from the sample. A 0.25 mm K-type thermocouple was inserted into a hole drilled 2.5 mm in diameter and 4 mm in depth to measure temperature inside the sample. The hole was plugged with a cylindrical wooden stick.

Table 3. Sample properties in flame spread experiments with cylindrical birch wood samples.

Exp.	Diameter (mm)	Mass before experiment (g)	Density (kg/m^3)	Moisture before heating (mass-%)	Estimated moisture at ignition (mass %)
FS1	Check of data collection system with door open, 765 mm long sample in middle of channel				
FS2	7.8	67.0	670 [a)]	5.6	5.6
FS3	7.8	62.09	610 [a)]	6.0	6.0
FS4	7.9	59.3	580 [a)]	4.5	2.6
FS5	7.9	59.91	580 [a)]	5.3	2.4
FS6	7.8	61.45	610 [a)]	5.4	2.3
FS7	8.0	64.81	580 [b)]	6.3	dry
FS8	7.7	57.4	550 [b)]	5.8	dry
FS9	8.0	not weighed	680 [b)]	5.1	dry
FS10	7.8	60.45	560 [b)]	6.3	dry
FS11	7.9	70.26	640 [b)]	6.1	dry

[a)] calculated from mass before experiment, including moisture
[b)] calculated from dry mass

Figure 24. Birch wood sample S and reference wood sample R in test channel before experiment FS6.

4.1 Moisture conditions

Experiments FS1…FS6 were carried out with samples stored in ordinary indoor conditions and were in equilibrium moisture when assembled into the test channel. The moisture of each sample was determined by drying a similar piece of wood in an oven at 105 °C.

Drying of a wood piece in the oven as a function of time was determined (Figure 25). Combined with original moisture of the flame spread experiment sample and known heating time, the moisture at time of ignition was estimated in experiments FS4…FS6.

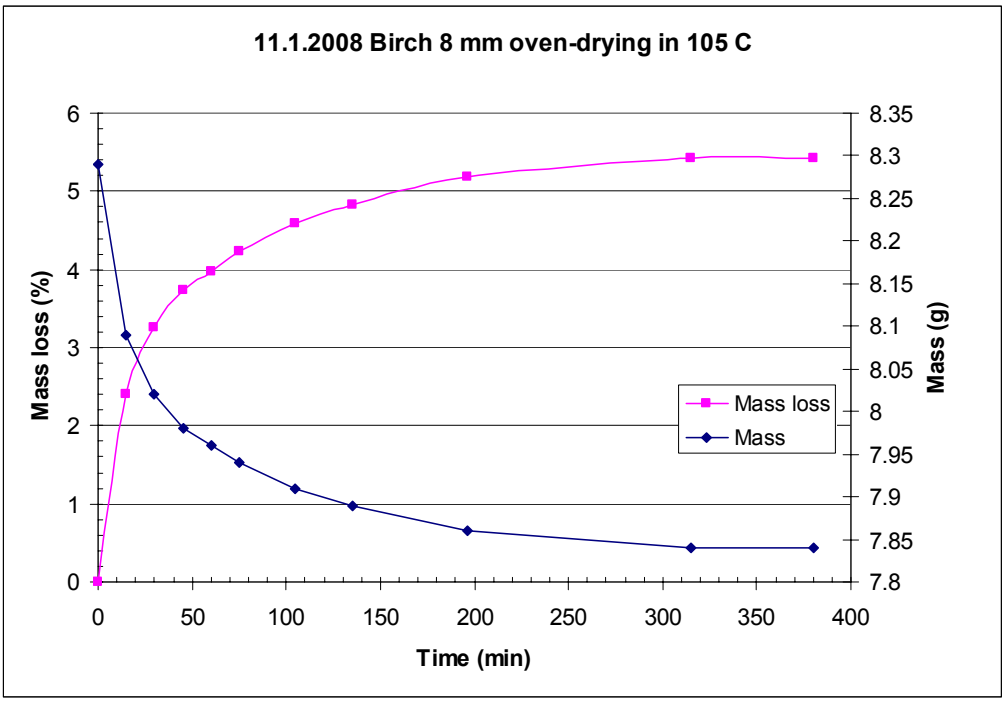

Figure 25. Drying of a cylindrical birch rod 8 mm in diameter in an oven at 105 °C.

It was estimated from Figure 25 that drying the sample approximately four hours would be sufficient to remove practically all moisture from a birch rod 8 mm in diameter. Experiment FS7 was carried out drying the birch wood sample for 4 h 13 min at a temperature of 110…115 °C, after which the sample was cooled to room temperature (21…28 °C) with roof hatch open and frequency transformer setting 50 Hz (highest flow rate) for 19 min. The flow rate was lowered to 5 Hz setting, glow wire turned on, and propane gas line opened. Temperatures in the test channel rose however to an average temperature of 32 °C because of heat transfer from the hot walls and to some extent from the glow wire, as the burner did not ignite until 5 min after turning glow on.

In experiments FS8 to FS11 the sample was dried at 105 °C for some hours after which the system was heated to desired temperature. Drying and heating times are presented in Table 5.

4.2 Temperature conditions

Vertical temperature-time curves are presented in Appendix A. Maximum gas temperatures (T_{max}) in the test channel were measured immediately before turning heating temporarily off and lowering flow rate. After this the temperatures decreased somewhat until ignition of the sample (T_{ign}) as seen from the temperature – time curves. The magnitude of the cooling appears from the vertical temperatures at different heights at time for T_{max} and T_{ign} presented in Appendix A. The gas temperature ranges at these moments are given in Table 4. The cooling as a single number is given as the difference between average T_{max}- and T_{ign}-temperatures. This average cooling was 7…17 ^{o}C and the transition sequence lasted 79…139 s (Table 4 and Table 5). An estimate of the uniformity of vertical temperature distribution in the test channel is obtained from the deviation of highest and lowest temperatures from average temperature, which was 2...7 % in both T_{max} and T_{ign} ranges.

The temperature of the flame spread experiment is denoted T_{ave} and calculated as the average temperature of thermocouples T2…T19 immediately before turning the burner on (Table 5). T1 is omitted because of the influence from the glow wire as presented in section 2.3.

Temperatures T_{ref} inside the reference sample are presented in Appendix A together with gas temperature T10 at the same height. Inside temperature at time of ignition is given in Table 4. Temperatures inside reference sample were at most 5…6 ^{o}C lower than corresponding gas temperature T10. In FS7, where the 2 m sample had been dried in the test channel and then cooled to room temperature, the reference sample temperature is higher than T10.

Mass loss of reference sample is presented in Table 5 and colour changes in the reference samples in Figure 26.

Horizontal temperatures in FS2 to FS9 are presented as 3-D figures in Appendix A. The radial temperature measurement system showed to be prone to short-cuts and radial temperatures are not presented from experiment FS10 onwards.

4. Flame spread experiments on cylindrical birch wood samples

Table 4. Experimental features in flame spread experiments with cylindrical birch wood samples, temperature conditions. Abbreviations are explained in the text.

Exp.	T_{max} range (^{o}C)	T_{ign} range and average (^{o}C)	Average temperature drop (^{o}C)	T_{ref} and T10 at ignition (^{o}C)
FS2	No heating	19…23 22	-	-
FS3	No heating	24…28 26	-	-
FS4	104…112	92…101 97	11	-
FS5	154…169	137…151 142	17	ref: 132 T10: 138
FS6	183…198	175…190 181	8	ref: 172 T10:177
FS7	-	27…35 32	-	ref: 34 T10: 28
FS8	169…177	161…166 162	10	ref: 157 T10: 157
FS9	197…219	190…205 197	7	ref: 188 T10: 192
FS10	236…257	228…245 233	9	ref: 226 T10: 229
FS11	277…300	264…283 271	17	ref: 270 T10. 266

Table 5. Experimental features in flame spread experiments with cylindrical birch wood samples. Heating time to ignition counts from start of experiment in experiments without heating, otherwise from end of drying. Abbreviations are explained in the text.

Exp.	T_{ave} at ignition (C)	Drying time at 115 °C (h:min)	Heating time to ignition (min :s)	Duration of transition sequence (s)	Burner flame duration (s)	Mass loss of reference sample (g (mass-%))	Rate of flame spread (mm/s)
FS2	22	-	0	-	540	-	6.4
FS3	26	-	0	-	95	-	6.5
FS4	97	-	13:21	116	75	-	8.4
FS5	142	-	20:55	115	90	0.28 (5.2 %)	13.5
FS6	181	-	25:50	79	55	0.32 (5.8 %)	25.5
FS7	32	4:13	-	-	54	0.31 (6.4 %)	10.6
FS8	162	3:46	16	139	59	0.24 (6.0 %)	21.7
FS9	197	3:48	22	57	97	0.40 (7.3 %)	25.5
FS10	233	3:39	27	50	54	0.65 (14.6 %)	48.2
FS11	271	3:00	31:22	82	58	1.69 (32.8 %)	61.5

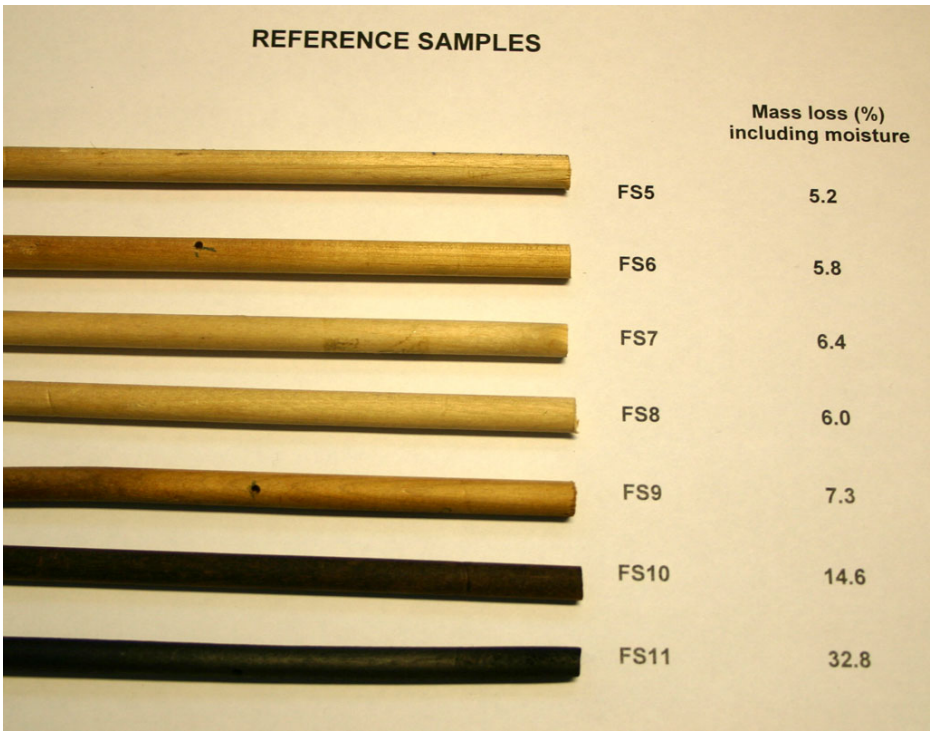

Figure 26. Reference wood samples after experiments, colour changes due to hot air. Mass loss during experiment is shown to the right.

4.3 Rate of flame spread

Rate of flame spread in the 2 m apparatus is deduced from temperature measurements, which requires some ignition criterion related to the temperature curves measured with thermocouples T1…T19. Visual inspection of the temperature-time curves indicates that around 300 ^{o}C the temperature rise is steepest for most of the curves. Time of ignition of the sample at a certain height was thus determined as the moment when the corresponding thermocouple indicated temperature rise above 300 ^{o}C.

Flame front (ignition at a certain height) as a function of time are presented in Appendix A. The curves indicate that after some 0.4 m of burning, the flame front approaches constant velocity. A straight line was fitted to this part of the curve, giving rate of flame spread as the slope of the line (Table 5). Higher temperatures introduce some scatter from the straight line, especially near the upper end of the sample. A straight line still fits the data from the middle part of the sample. Rate of flame spread as a function of ambient temperature is presented in Figure 27 for both oven-dry and indoor moisture samples. Temperature dependence seems to be roughly exponential.

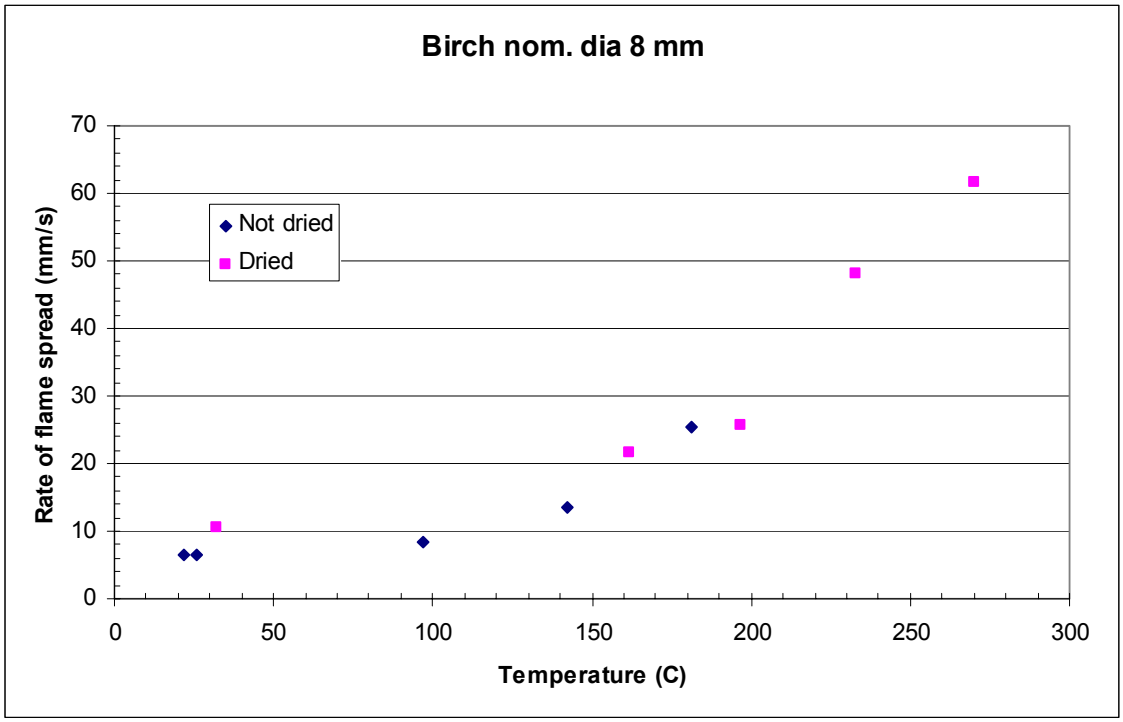

Figure 27. Rate of flame spread as a function of ambient temperature for cylindrical birch samples 8 mm in nominal diameter.

One critical question concerning the measurement of flame spread with the vertical thermocouple rake relates to the symmetry of the flame front on the cylindrical sample. An oscillatory behaviour could be possible e.g. due to anisotropy of the sample, as noted in experiments W16 and W17 in Keski-Rahkonen and Mangs (2005a, 2006).

Visual observation of the flame is possible only from above through the smoke outlet, and some visual observations were made together with photographs during the experiments. Because of the angle of view, definite conclusions about the occurrence of oscillations were not possible. The samples seemed yet to be completely surrounded by flames, as shown in Figure 28.

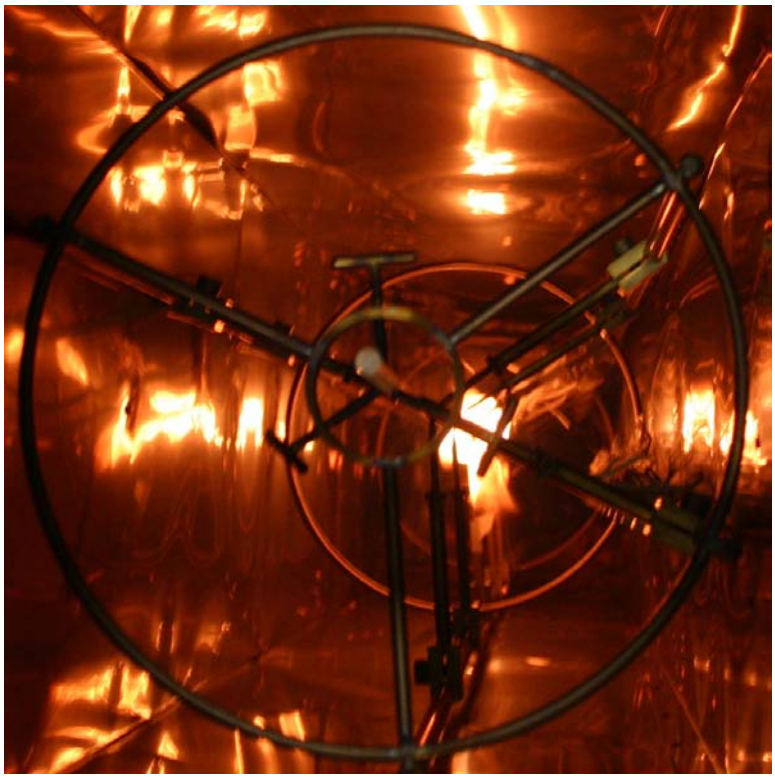

Figure 28. Flame spread on a birch wood sample in experiment FS4, photograph from above through the smoke outlet.

5. Flame spread experiments on PVC cables

A series of flame spread experiments was carried out on cables of type MMJ 4 x 1.5 mm^2 with PVC sheath and PVC insulation. The structure of the cable is presented in Figure 29 and mass relations determined from a piece of cable are given in Table 6. The outer diameter of the cable was 9.5 mm.

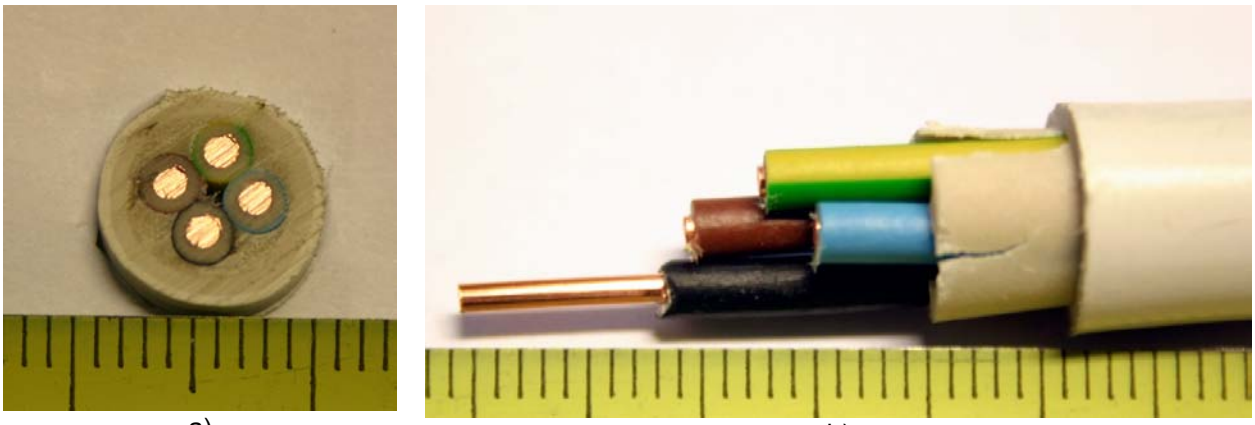

a) b)

Figure 29. a) cross-section, b) structure of MMJ 4 x 1.5 mm^2 cable. Scale in mm.

Table 6. Mass relations of MMJ 4 x 1.5 mm^2 cable sample.

Structural part	Linear mass	
	g/m	%
Total	137.7	100
Sheath	46.3	34
Filler	17.8	13
Insulation	23.7	17
Copper	50.1	36

The samples were 2.0 m long with initial masses in the range 275...280 g. The experiments were carried out with cable samples stored in ordinary indoor conditions. The

procedure was the same as with the birch samples except burner power output and duration. Cable materials melt at higher temperatures, and therefore short pieces of MMJ cable were heated to find out the highest temperature at which the sample remains stiff enough to carry out an experiment. A 0.8 m MMJ sample was solid enough to hold to the sample support at temperatures 209...191 ^{o}C measured with thermocouples T2...T8. An 80 mm long MMJ sample melted and dropped from the support in a test where T_{max} near the sample was 240 ^{o}C (Figure 30). Temperature 210 ^{o}C was considered to be an approximate upper temperature limit for the experiments.

Figure 30. Melted MMJ sample on Al-foil after a test where T_{max} near the sample was 240 ^{o}C.

As noted in section 2.3, cable samples do not ignite as easily as wood samples. A more powerful propane flame was used for a longer time in the MMJ cable experiments. Burner power output was 0.4...0.6 kW and burner flame duration 130...260 s (Table 7).

Three experiments were carried out, at room temperature, 130 ^{o}C and 187 ^{o}C. The cable sample ignited and was completely consumed in all three cases. Flame spread in experiment MMJ1 is illustrated in Figure 31 and the charred cable after experiment MMJ2 in Figure 32. Vertical temperatures as a function of time, maximum temperatures and temperatures at ignition as a function of height and flame front as a function of time with straight line fit are presented in Appendix B. Main results are presented in Table 7 and rate of flame spread as a function of ambient temperature in Figure 33.

The cable material melted after ignition and caused disturbances in the temperature measurements as seen in the temperature-time curves. Parts with extensive scattering were removed from the figures. Higher temperatures cause also here scatter from the straight line fitted to flame front data.

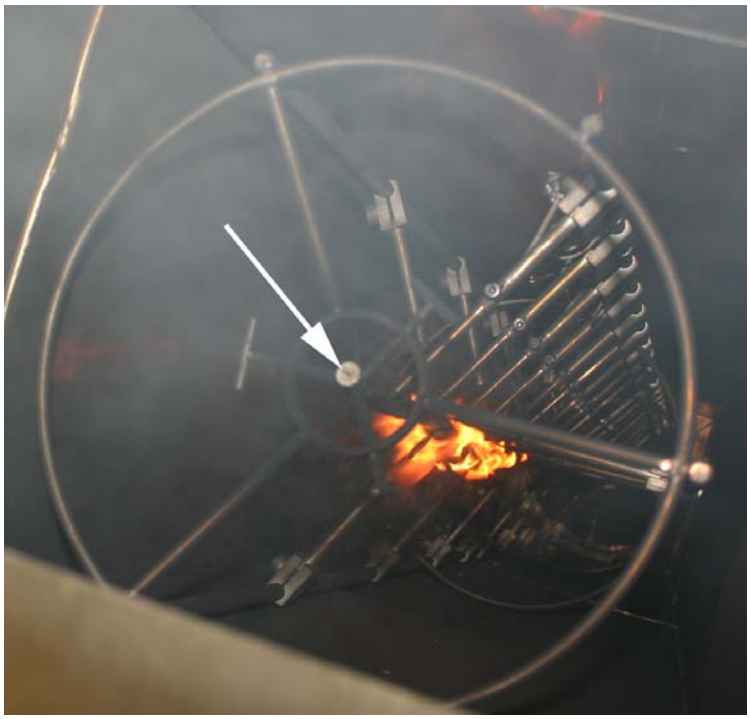

Figure 31. Flame spread on a MMJ cable sample in experiment MMJ1, photograph from above through the smoke outlet. The upper end of the sample is indicated with an arrow.

5. Flame spread experiments on PVC cables

Figure 32. Charred MMJ cable sample after experiment MMJ2. The white reference cable sample to the left is slightly deformed only at point of suspension.

Table 7. Experimental features in flame spread experiments with samples of PVC cable MMJ 4 x 1.5 mm^2.

Exp.	Heating time to ignition (min :s)	Duration of transition sequence (s)	T_{max} range (^{o}C)	T_{ign} range and average (^{o}C)	Average temperature drop (^{o}C)	Burner flame duration (s)	Rate of flame spread (mm/s)
MMJ 1	0	-	No heating	21...24 22	-	263	2.6
MMJ 2	17:00	122	133...158	125...143 130	11	302	6.1
MMJ 3	30:00	347	173...209	175...212 187	4	130	8.4

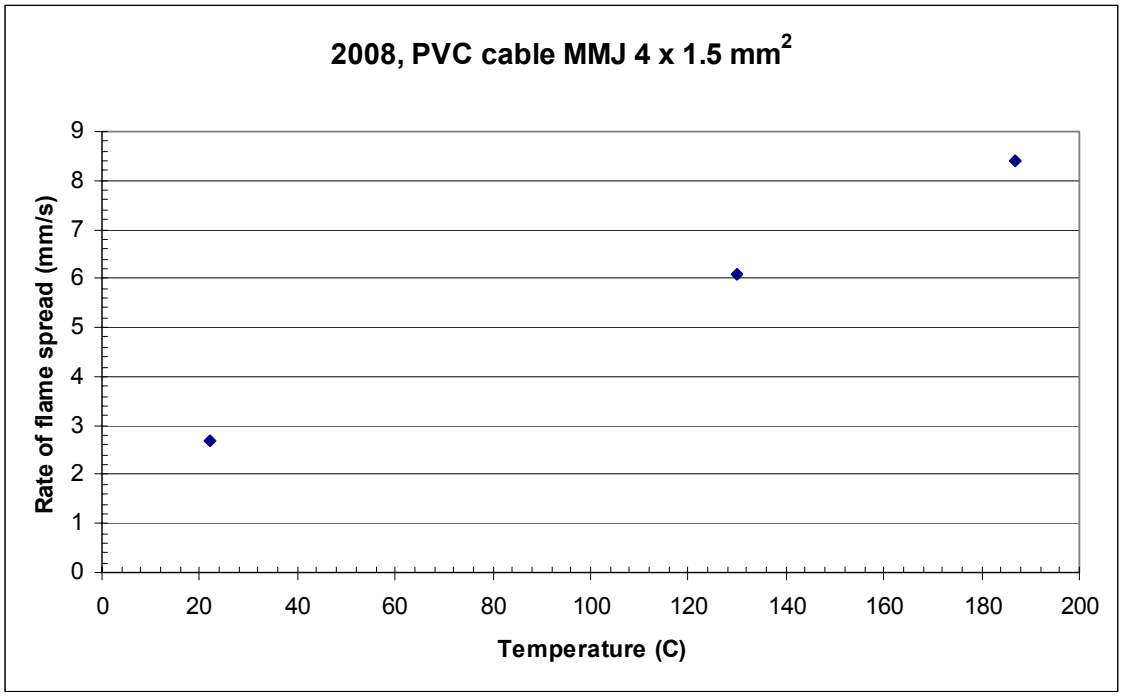

Figure 33. Rate of flame spread as a function of ambient temperature for MMJ cable samples.

6. Discussions and conclusions

The realization of a new test rig for flame spread measurements on pre-heated 2 m long samples is described, as well as start-up tests on the instrument testing its functionality, and rate of flame spread experiments on wood and PVC cable samples.

The air flow velocity range in the test channel was determined for different fan speeds. Flow profiles in the test channel at different heights and flow velocities are presented, showing that the flow profile is quite uniform in the centre of the test channel. The influence of the unlit propane burner on flow is notable only some 50 mm above the burner.

Heating tests were carried out to examine possible leaks and improve insulation, and to examine uniformity of temperature in the test channel. The system showed quite well uniformity, with maximum deviations from average vertical temperatures 2 %, and horizontal temperature deviation 1…3 % in a cross-section at 0.83 m above lowest thermocouple T1 level. These values were obtained at 289 ^{o}C average vertical temperature.

An estimate of the uniformity of vertical temperature distribution in the test channel in routine flame spread experiments gives slightly higher deviation of highest and lowest temperatures from average temperature, 2...7 %.

Flame spread velocities as a function of ambient temperature were measured in two series of experiments, on cylindrical birch wood samples and on PVC sheathed and insulated MMJ cable samples. Flame spread velocities in the range 6 ... 62 mm/s were determined in a temperature at ignition range 22...271 ^{o}C for wood samples and velocities 3...8 mm/s in a temperature at ignition range 22...187 ^{o}C for PVC cable samples.

The new apparatus seems to be appropriate for determining vertical flame spread as a function of temperature.

References

Hostikka, S. & Keski-Rahkonen, O. 2007. Simulation of vertical flame spread by FDS in DNS mode – Numerical excursions into flames for designing physical experiments and guiding engineering modelling. Research report VTT-R-00567-07, 56 p.

Keski-Rahkonen, O. & Mangs, J. 2005a. Assessing of flame spread on NPP cables. Zhou, Y. Yu, S. & Xu, Y. (eds.). Proceedings of the 18th International Conference on Structural Mechanics in Reactor Technology. SMiRT 18. Beijing, China, August 7–12, 2005. Atomic Energy Press. Beijing. Pp. 3972–3983. www.iasmirt.org

Keski-Rahkonen, O. & Mangs, J. 2005b. POTFIS project special report – Experiments and modelling on vertical flame spread. In: Räty, H. & Puska, E. K. (eds.). 2004. SAFIR, The Finnish Research Programme on Nuclear Power Plant Safety 2003–2006, Interim Report, VTT Research Notes 2272. VTT, Espoo. Pp. 257–265. ISBN 9513865150; ISSN 12350605. http://virtual.vtt.fi/inf/pdf/tiedotteet/2004/T2272.pdf.

Keski-Rahkonen, O. & Mangs, J. 2006. Flame spread on cables – Literature study, bench scale experiments and modelling, (internal unpublished report), 228 p.

Mangs J., Keski-Rahkonen, O. & Hostikka, S. 2006. Vertical flame spread. Developments of and experiments on calorimeters, vertical test rigs and their instrumentation, (internal unpublished report), 110 p.

Appendix A: Temperatures from experiments on 8 mm cylindrical birch wood samples

T_{ave} refers to average gas temperature at start of flame spread experiment.

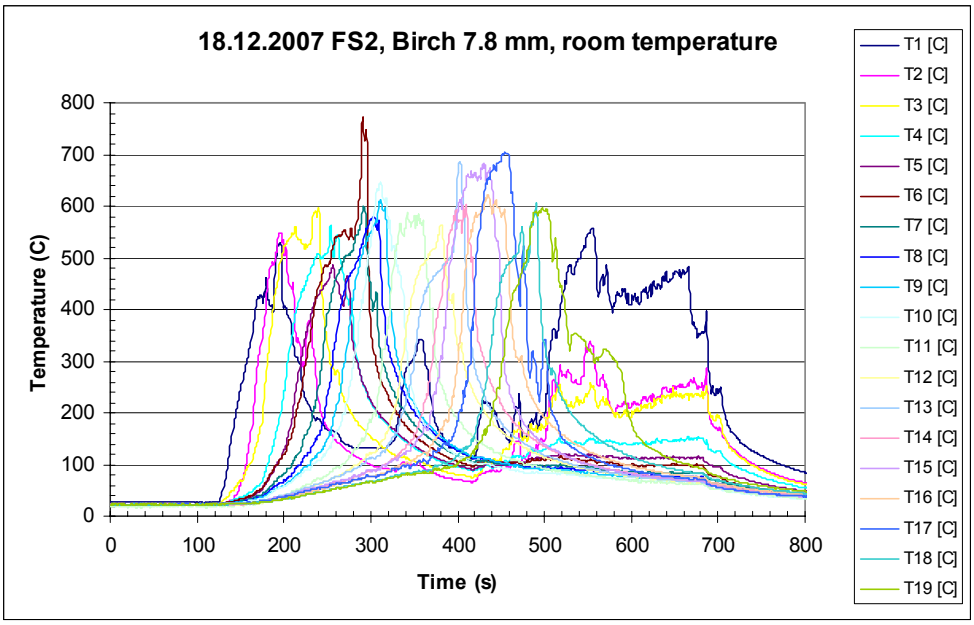

Figure A1. Vertical temperatures in flame spread experiment FS2.

Appendix A: Temperatures from experiments on 8 mm cylindrical birch wood samples

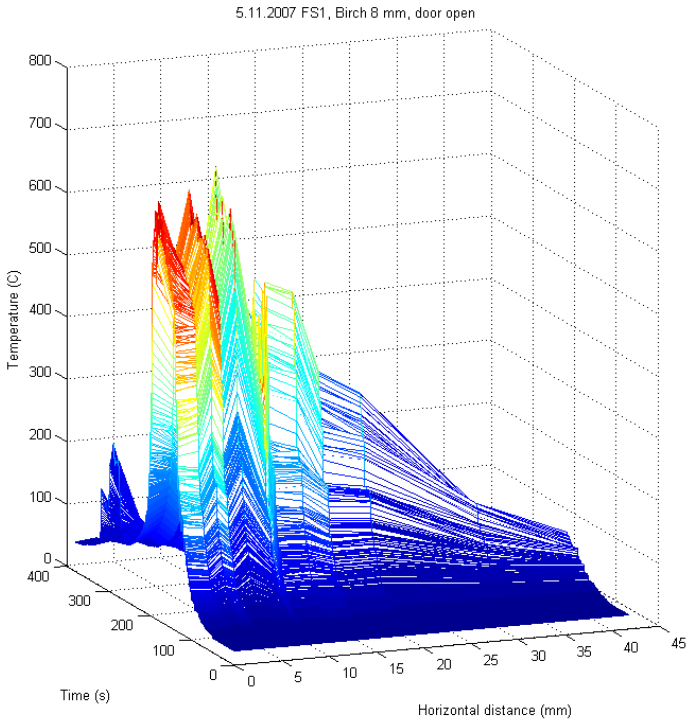

Figure A2. Horizontal temperatures in flame spread experiment FS2.

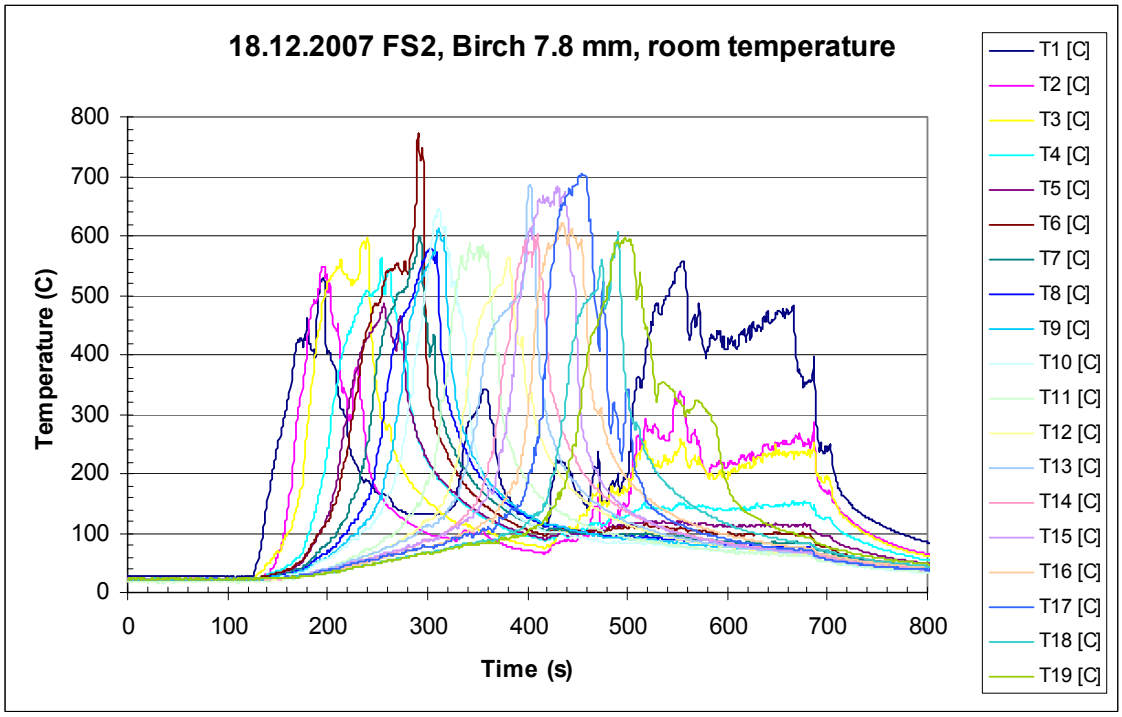

Figure A3. Vertical temperatures in flame spread experiment FS2.

Appendix A: Temperatures from experiments on 8 mm cylindrical birch wood samples

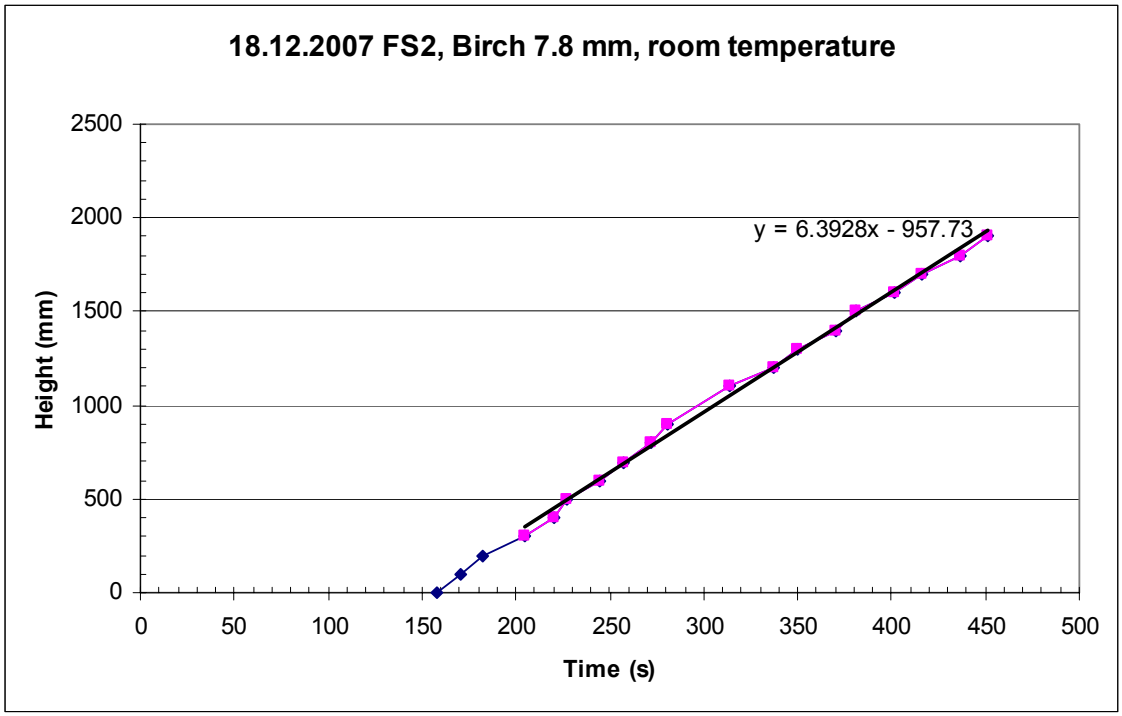

Figure A4. Flame front as a function of time in flame spread experiment FS2.

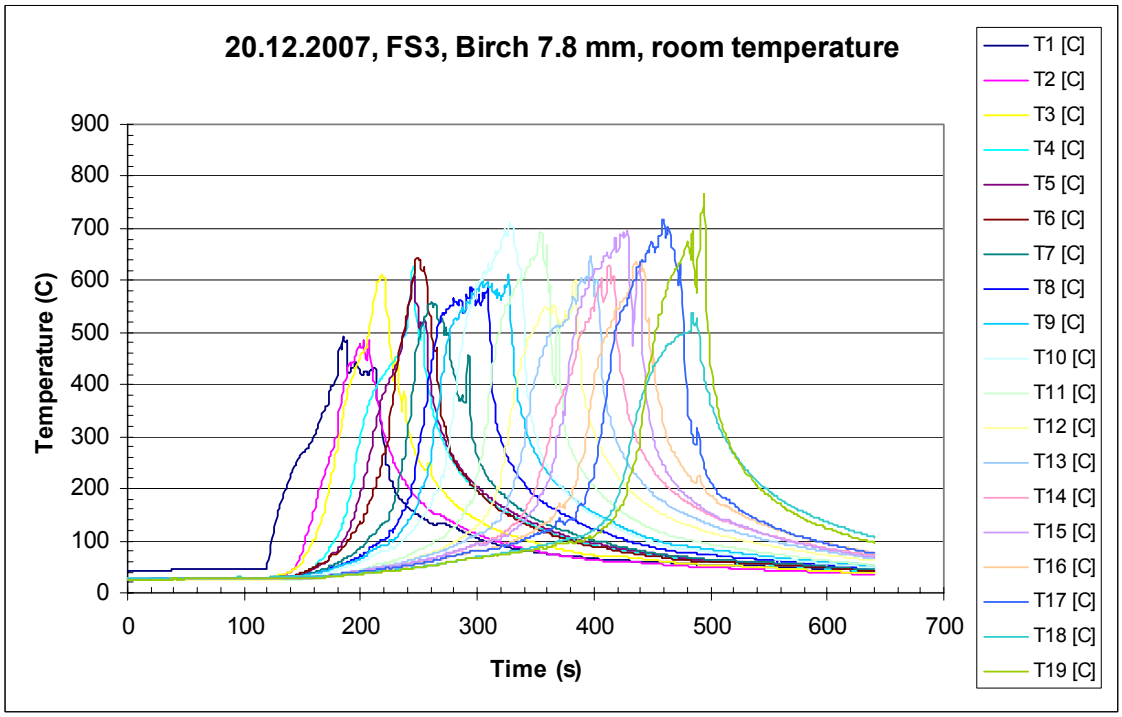

Figure A5. Vertical temperatures in flame spread experiment FS3.

Appendix A: Temperatures from experiments on 8 mm cylindrical birch wood samples

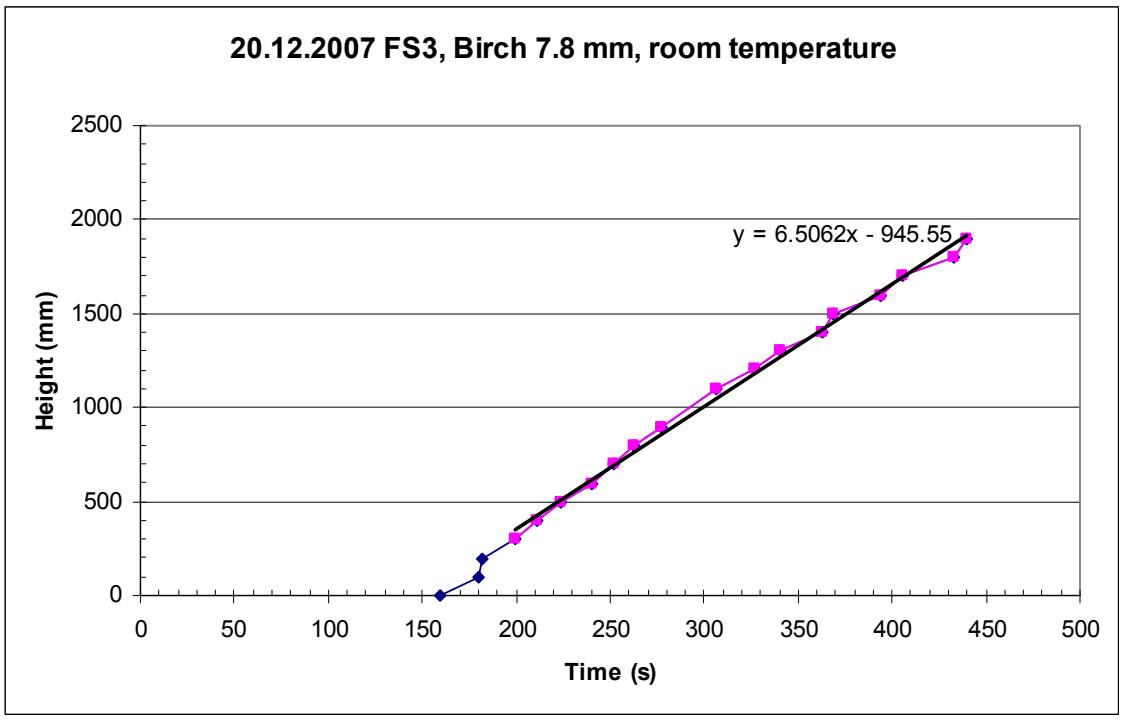

Figure A6. Flame front as a function of time in flame spread experiment FS3.

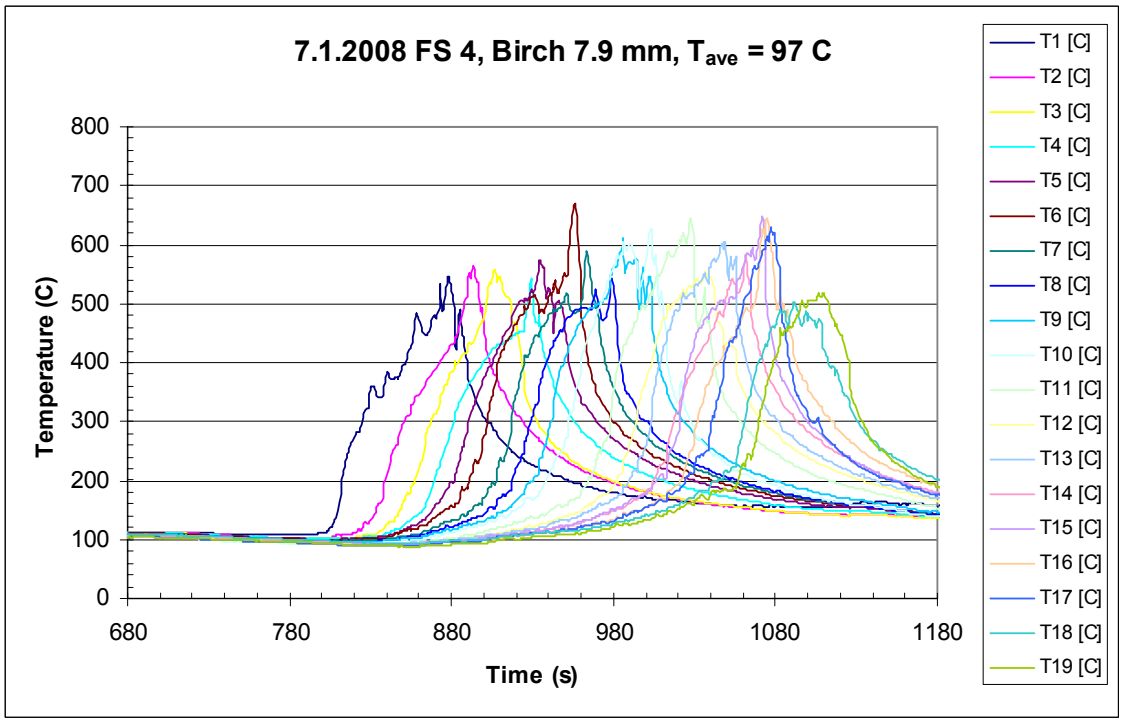

Figure A7. Vertical temperatures in flame spread experiment FS4.

Appendix A: Temperatures from experiments on 8 mm cylindrical birch wood samples

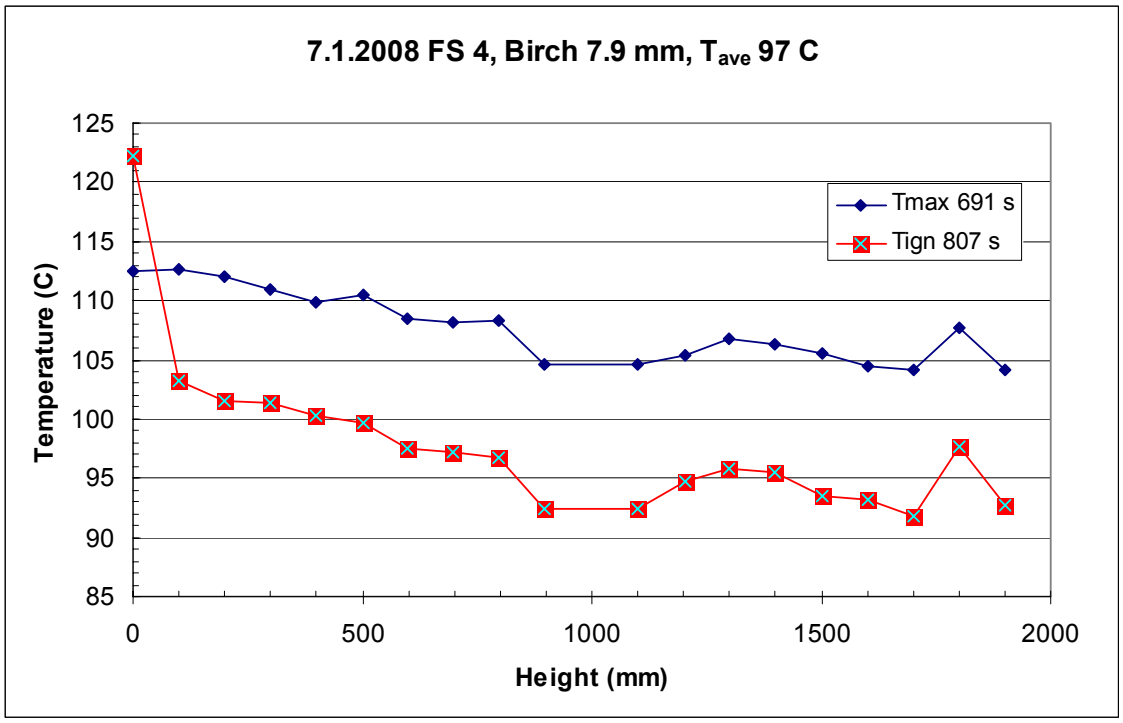

Figure A8. Vertical temperature distributions in flame spread experiment FS4, at maximum temperature and at ignition.

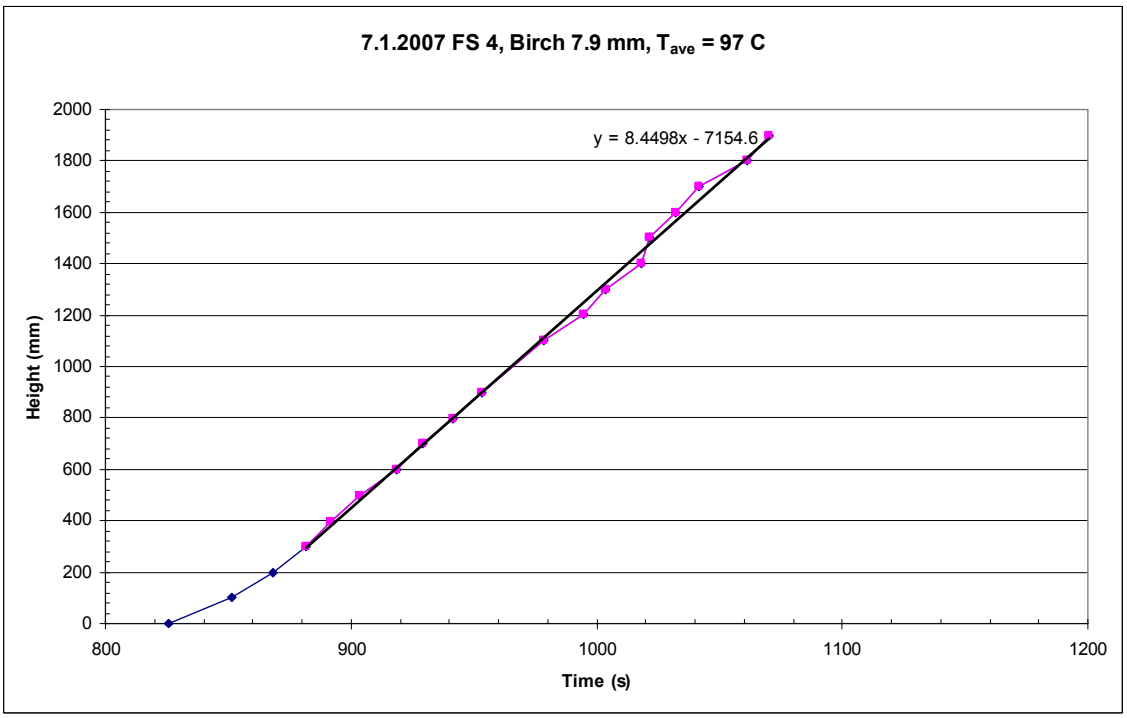

Figure A9. Flame front as a function of time in flame spread experiment FS4.

Appendix A: Temperatures from experiments on 8 mm cylindrical birch wood samples

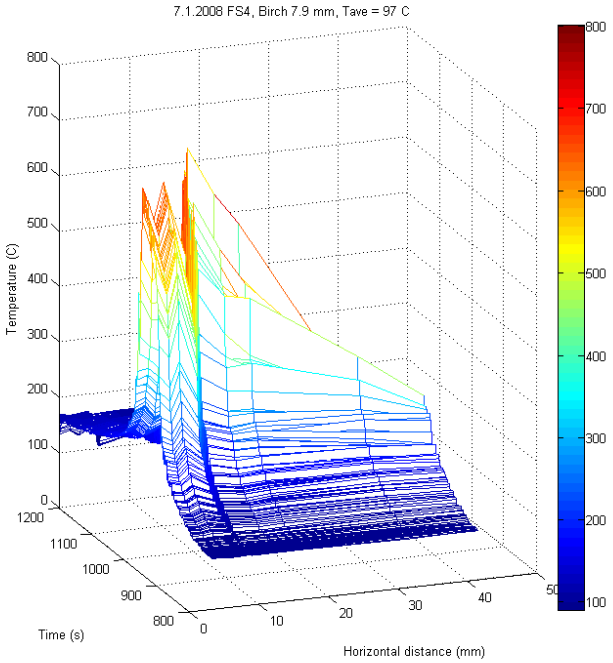

Figure A10. Horizontal temperatures in flame spread experiment FS4.

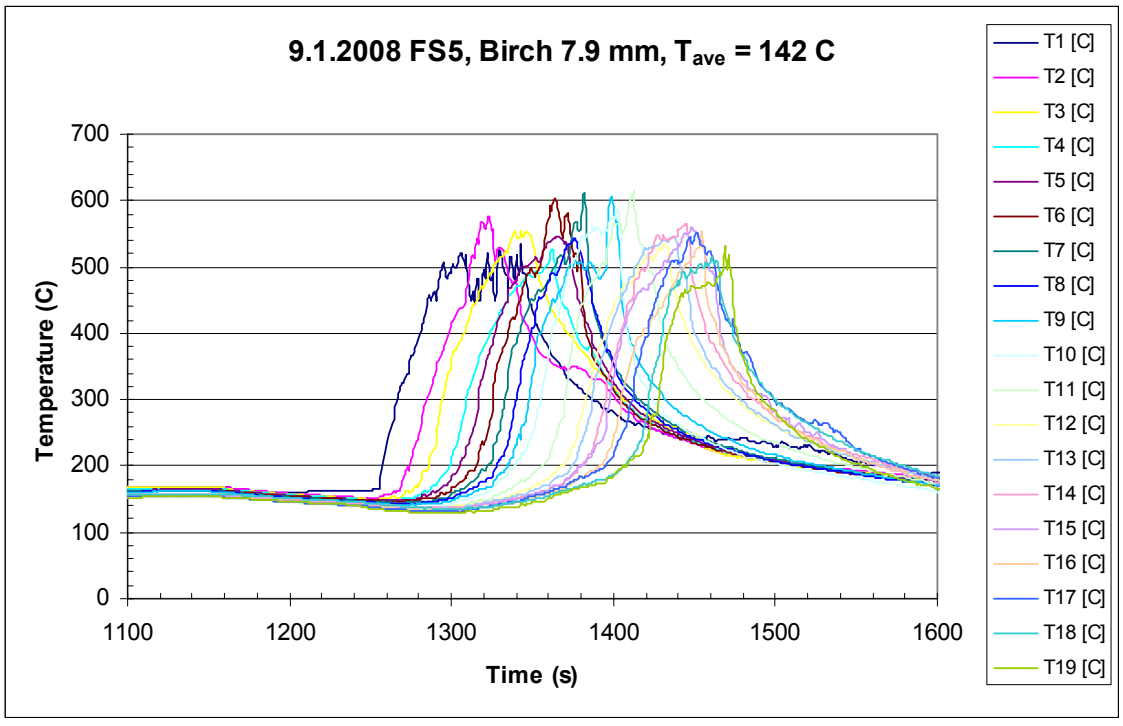

Figure A11. Vertical temperatures in flame spread experiment FS5.

Appendix A: Temperatures from experiments on 8 mm cylindrical birch wood samples

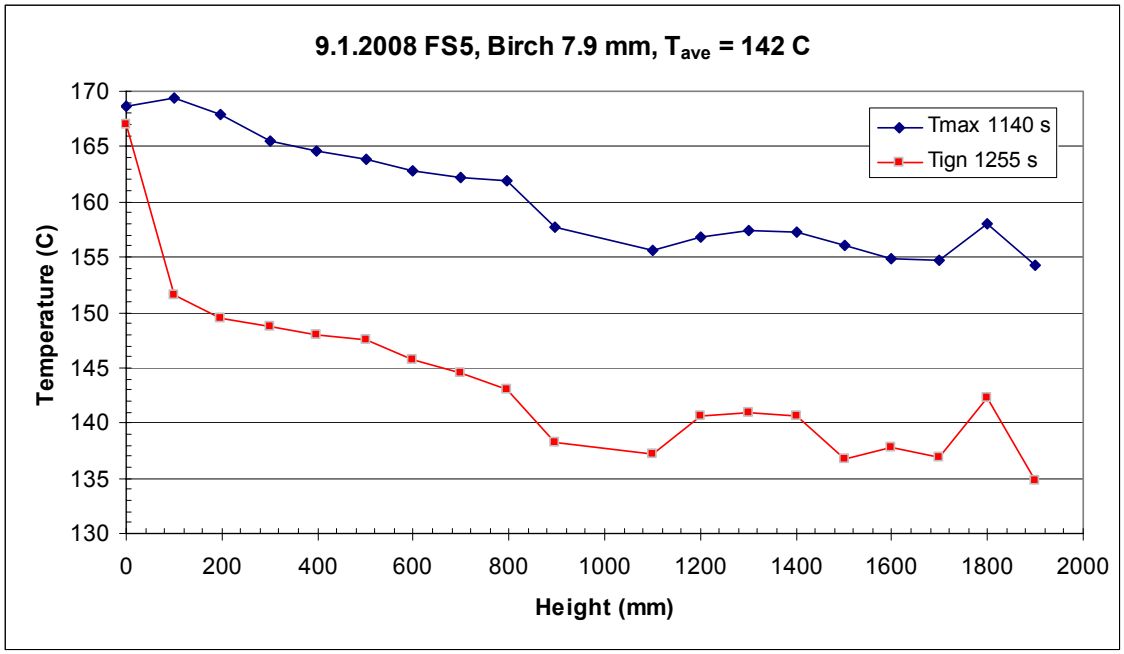

Figure A12. Vertical temperature distributions in flame spread experiment FS5, at maximum temperature and at ignition.

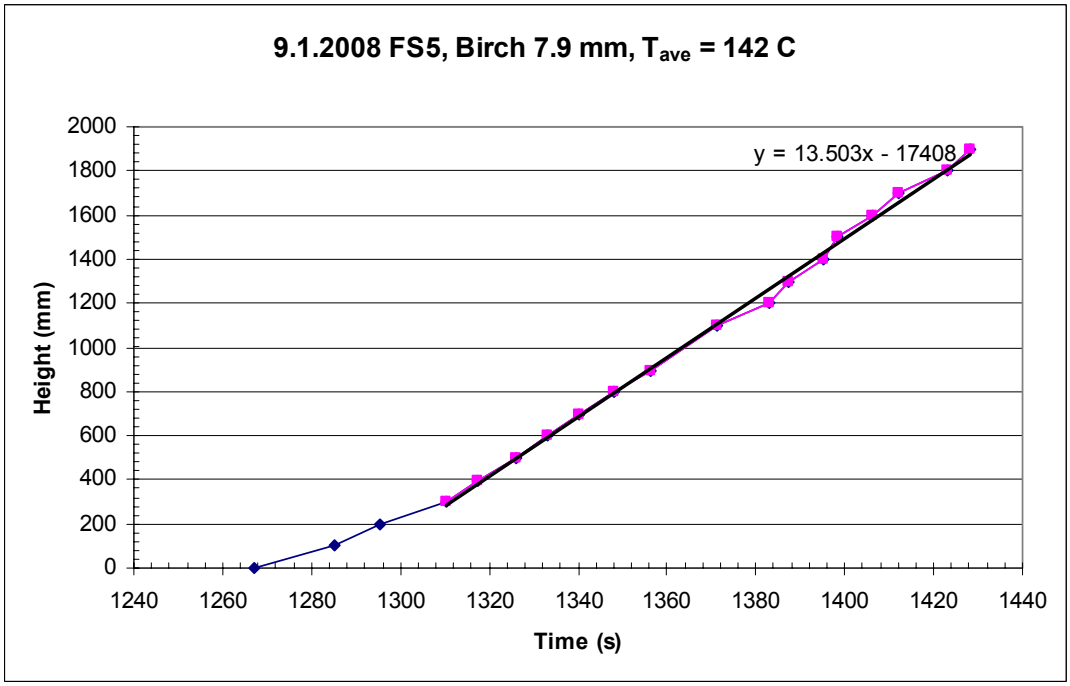

Figure A13. Flame front as a function of time in flame spread experiment FS5.

Appendix A: Temperatures from experiments on 8 mm cylindrical birch wood samples

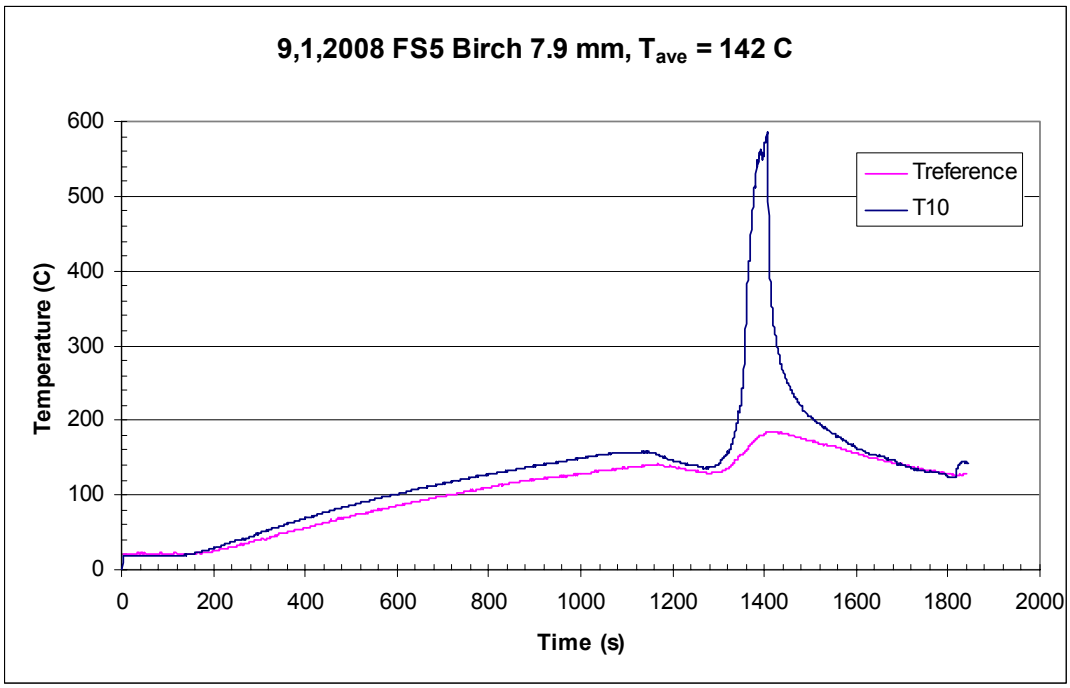

Figure A14. Temperature inside reference wood sample and gas temperature T10 in flame spread experiment FS5.

Appendix A: Temperatures from experiments on 8 mm cylindrical birch wood samples

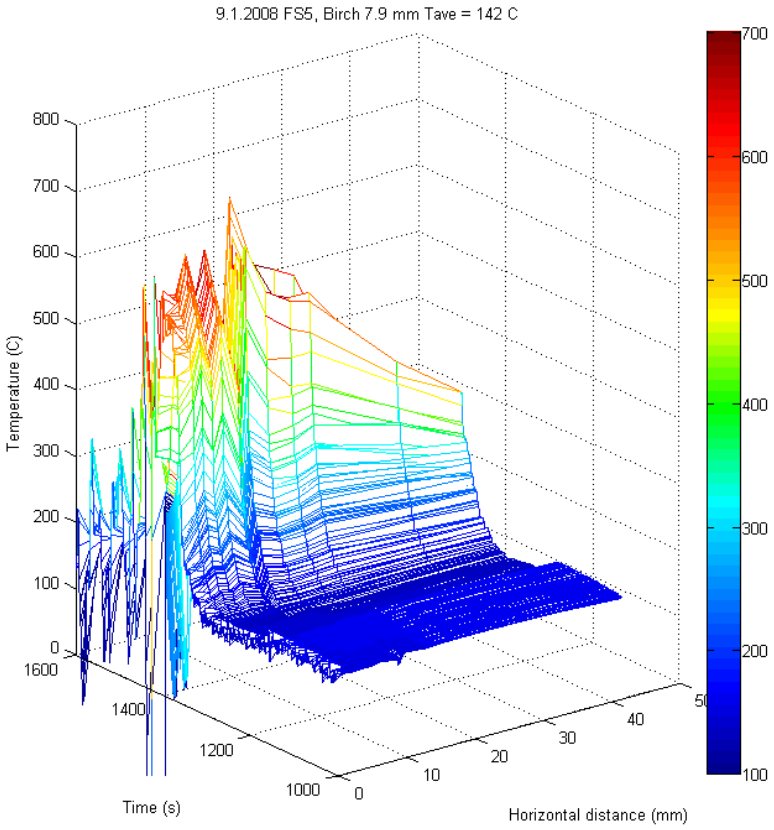

Figure A15. Horizontal temperatures in flame spread experiment FS5.

Appendix A: Temperatures from experiments on 8 mm cylindrical birch wood samples

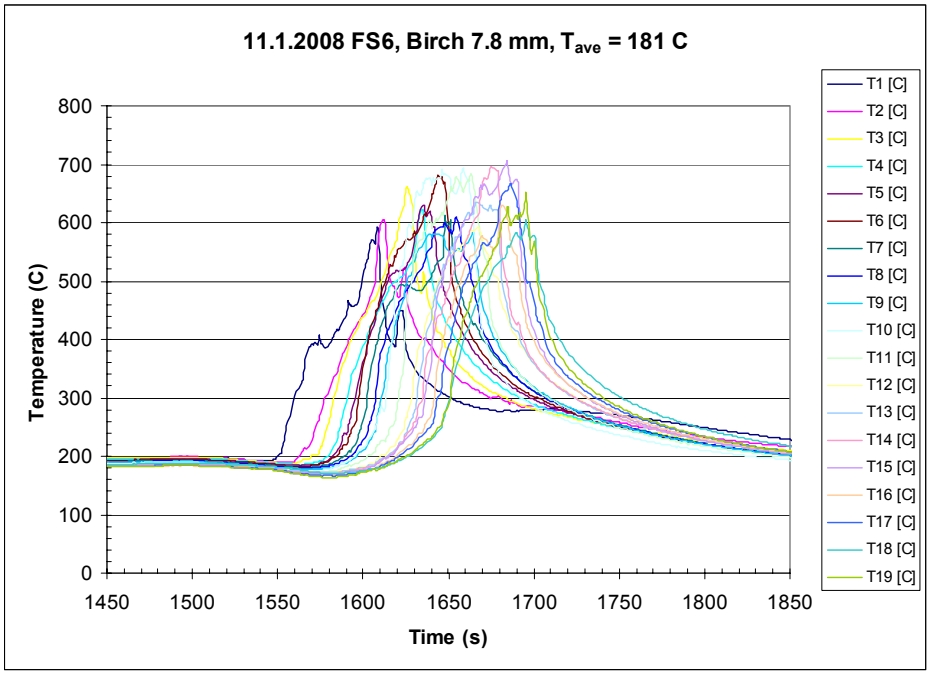

Figure A16. Vertical temperatures in flame spread experiment FS6.

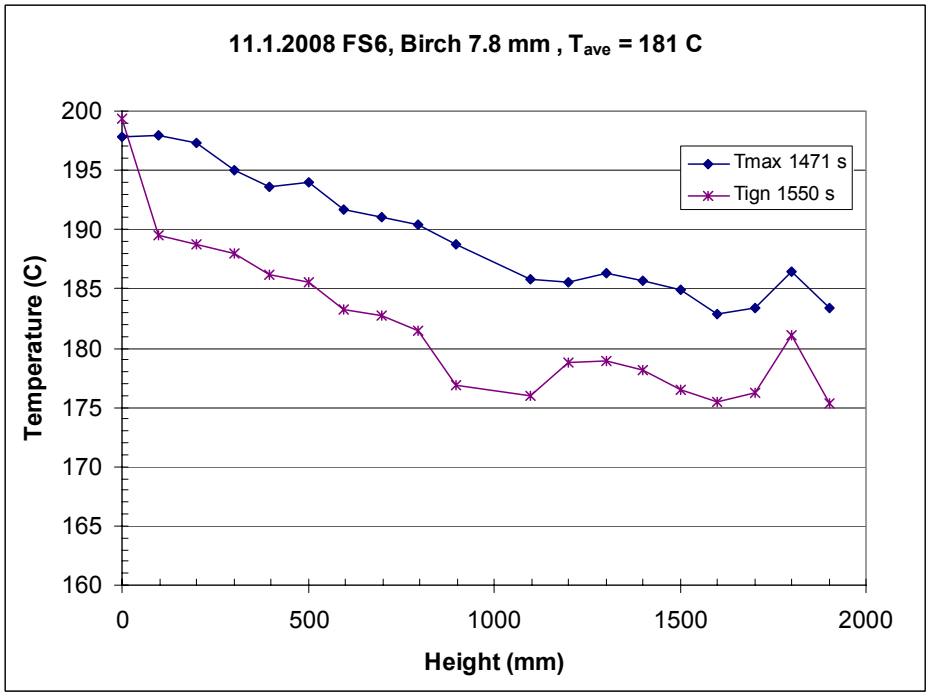

Figure A17. Vertical temperature distributions in flame spread experiment FS6, at maximum temperature and at ignition.

Appendix A: Temperatures from experiments on 8 mm cylindrical birch wood samples

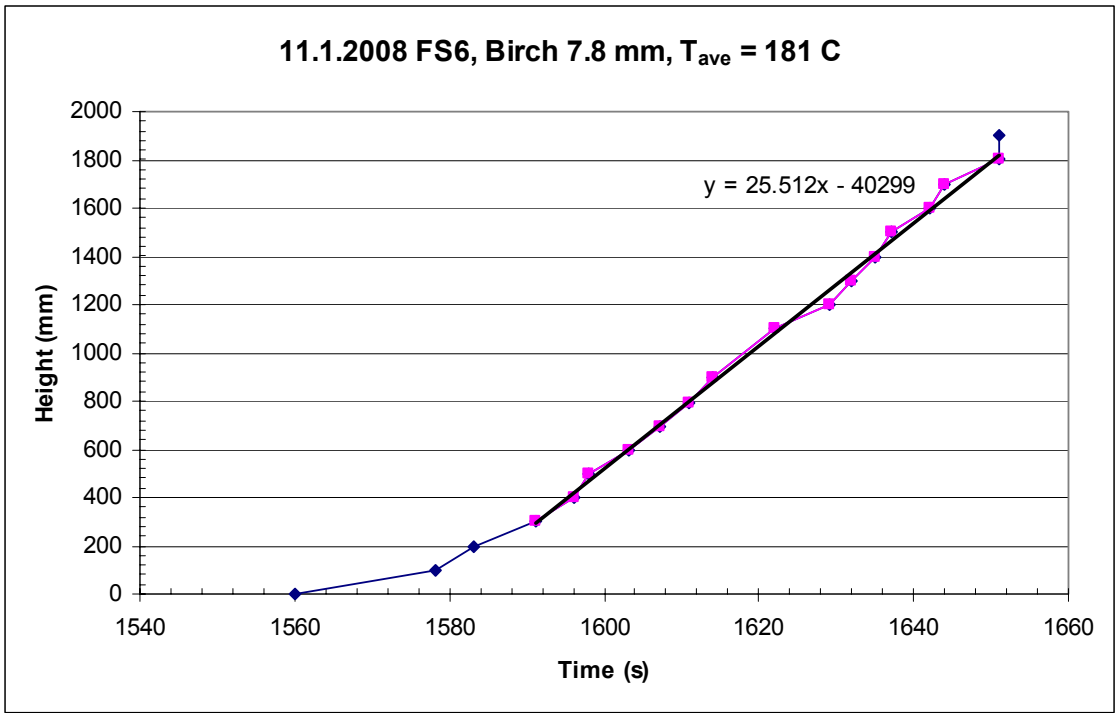

Figure A18. Flame front as a function of time in flame spread experiment FS6.

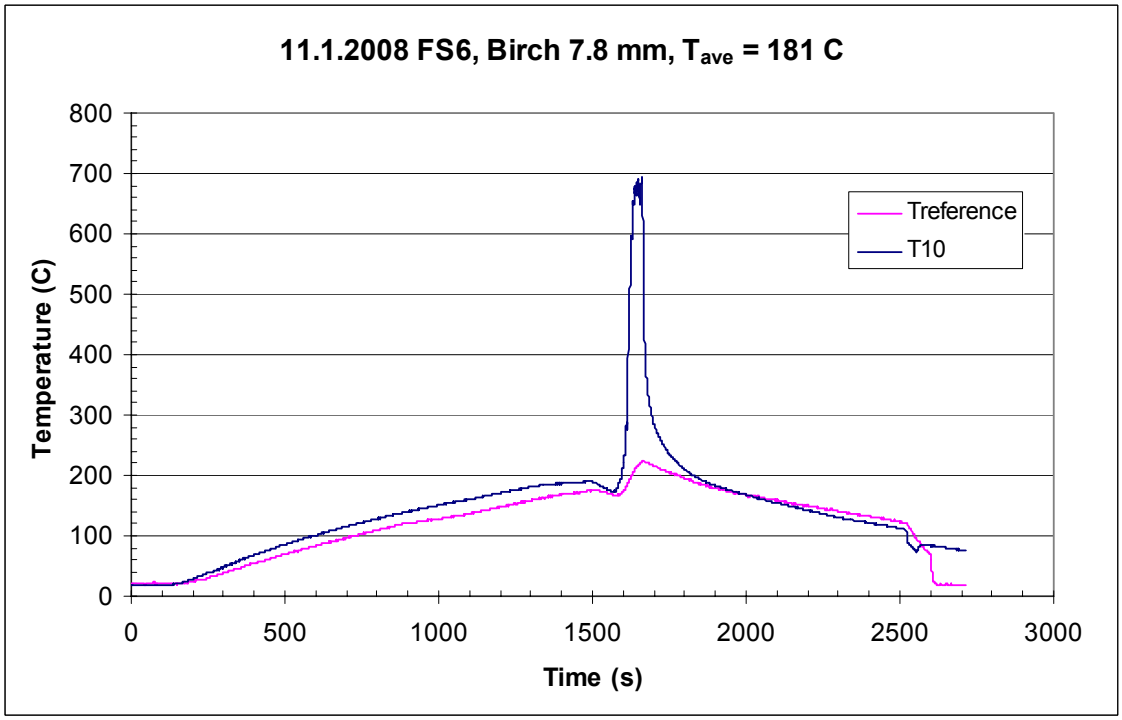

Figure A19. Temperature inside reference wood sample and gas temperature T10 in flame spread experiment FS6.

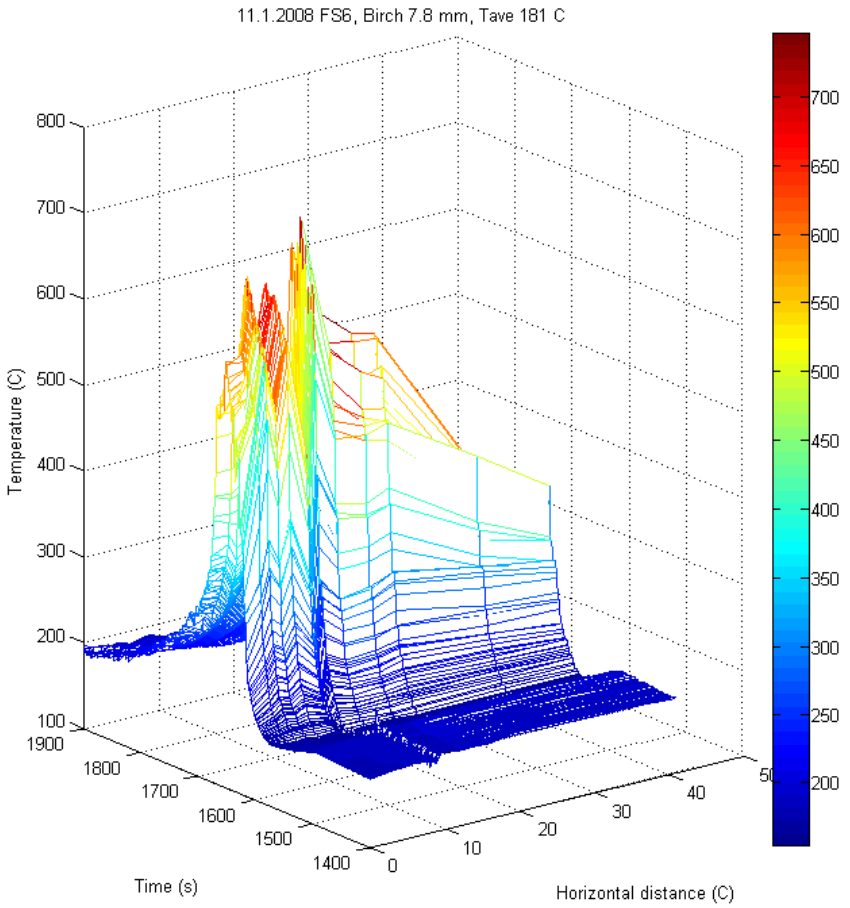

Figure A20. Horizontal temperatures in flame spread experiment FS6.

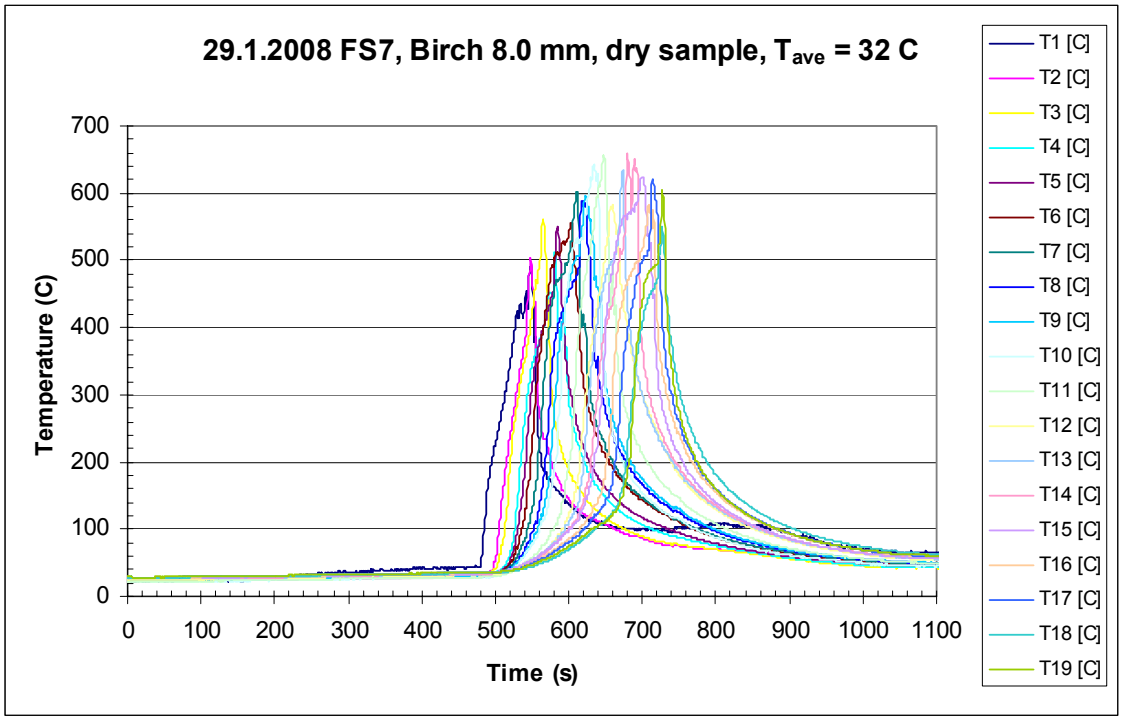

Figure A21. Vertical temperatures in flame spread experiment FS7.

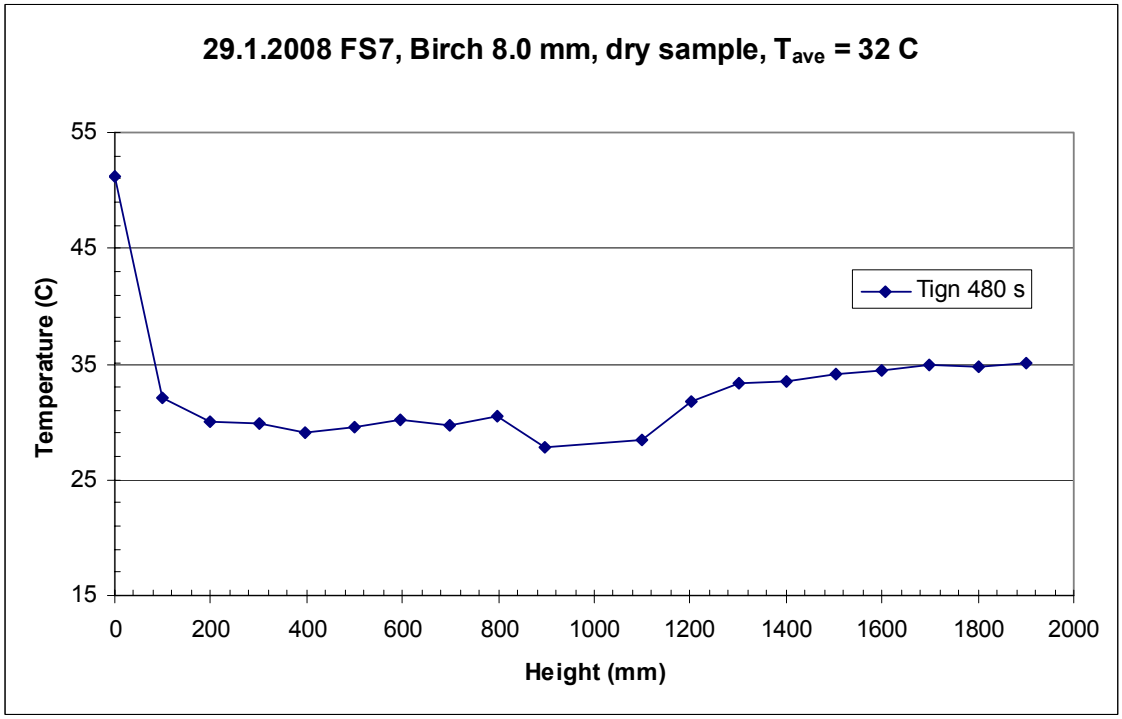

Figure A22. Vertical temperature distribution in flame spread experiment FS7, at ignition.

Appendix A: Temperatures from experiments on 8 mm cylindrical birch wood samples

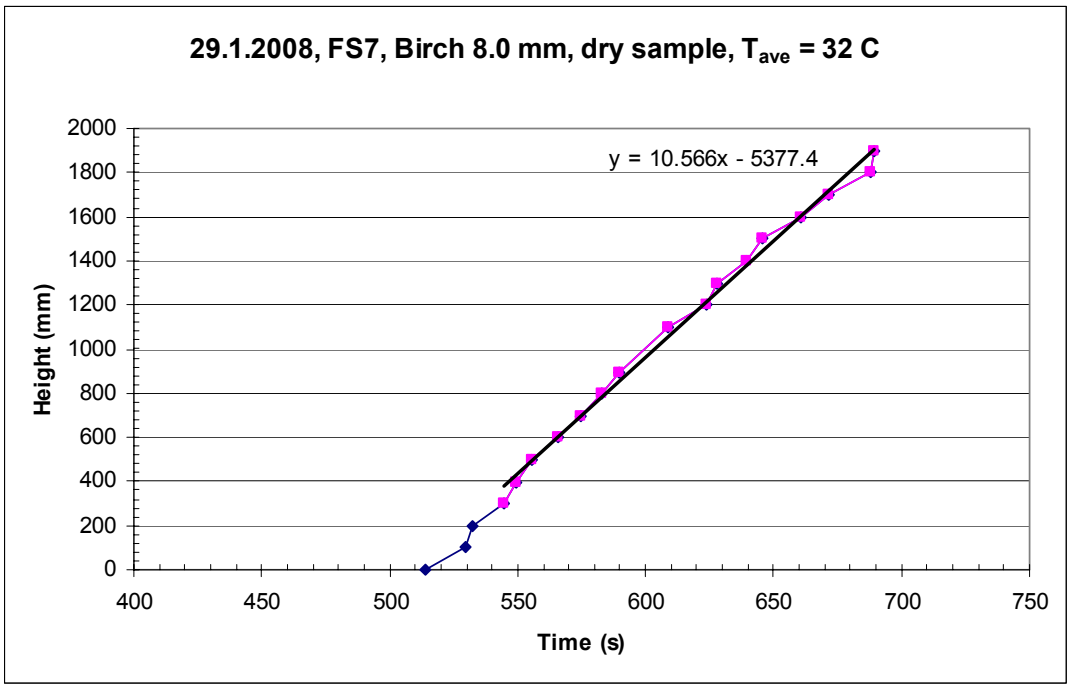

Figure A23. Flame front as a function of time in flame spread experiment FS7.

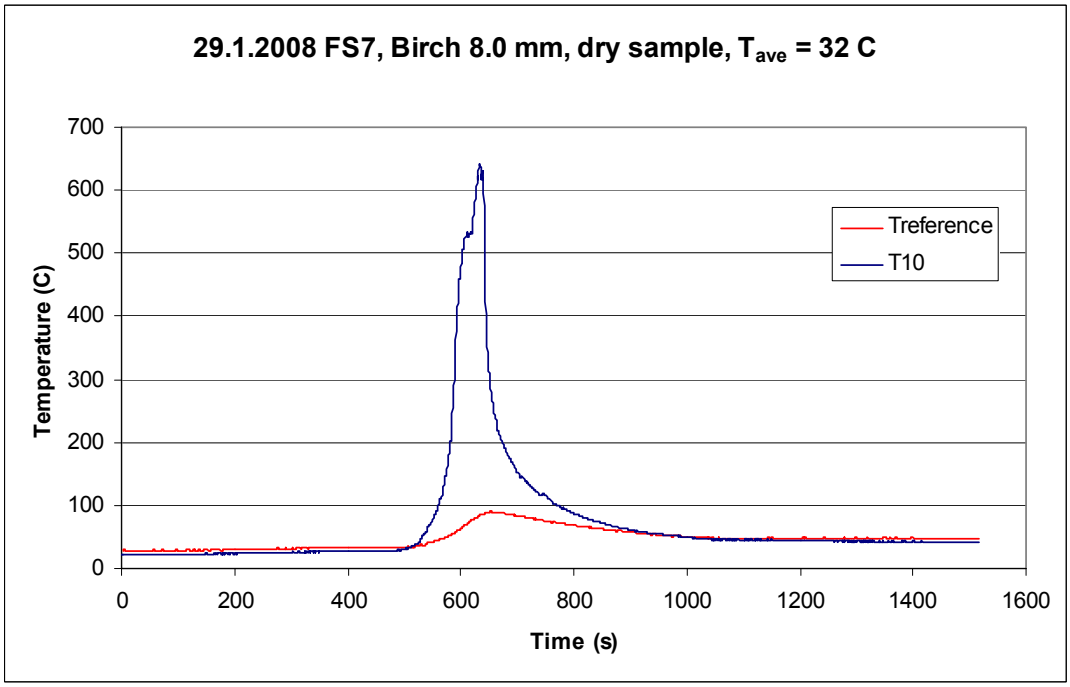

Figure A24. Temperature inside reference wood sample and gas temperature T10 in flame spread experiment FS7.

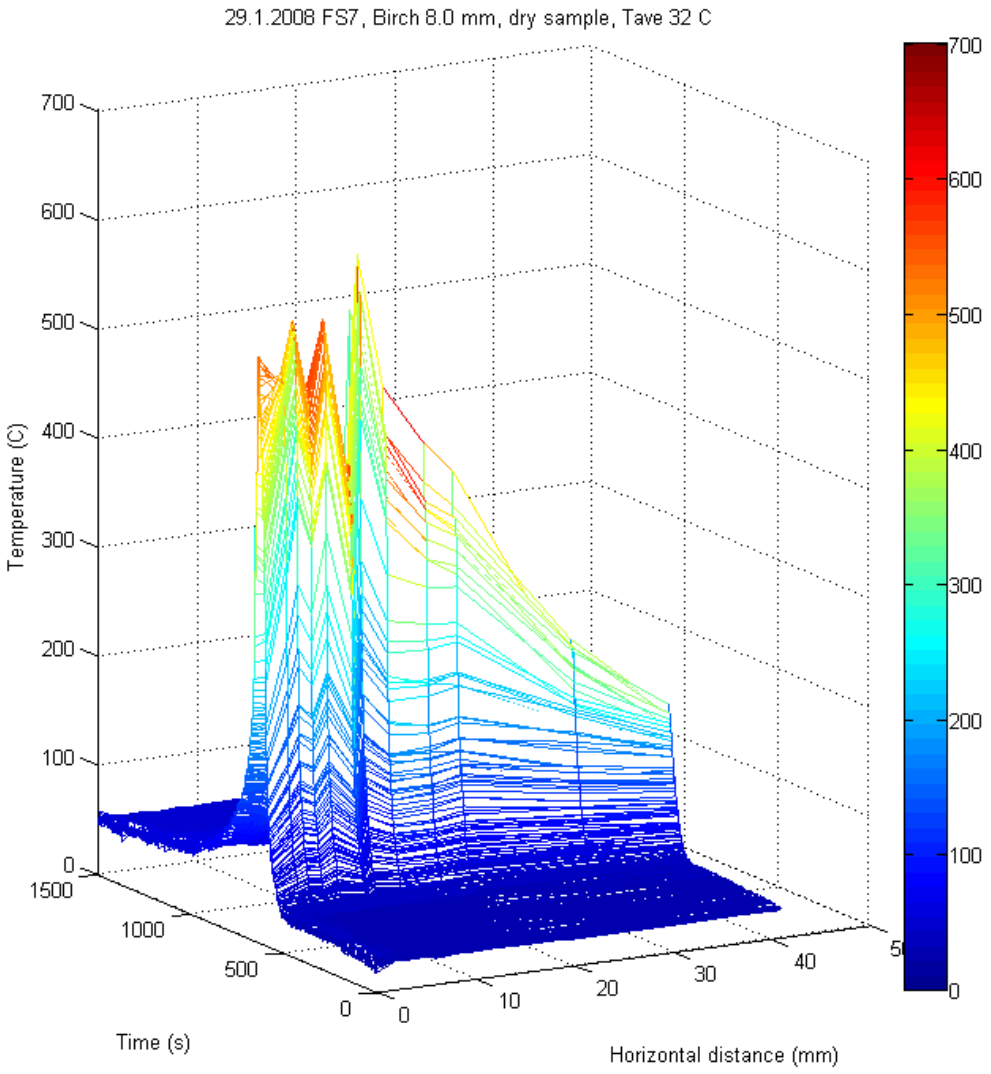

Figure A25. Horizontal temperatures in flame spread experiment FS7.

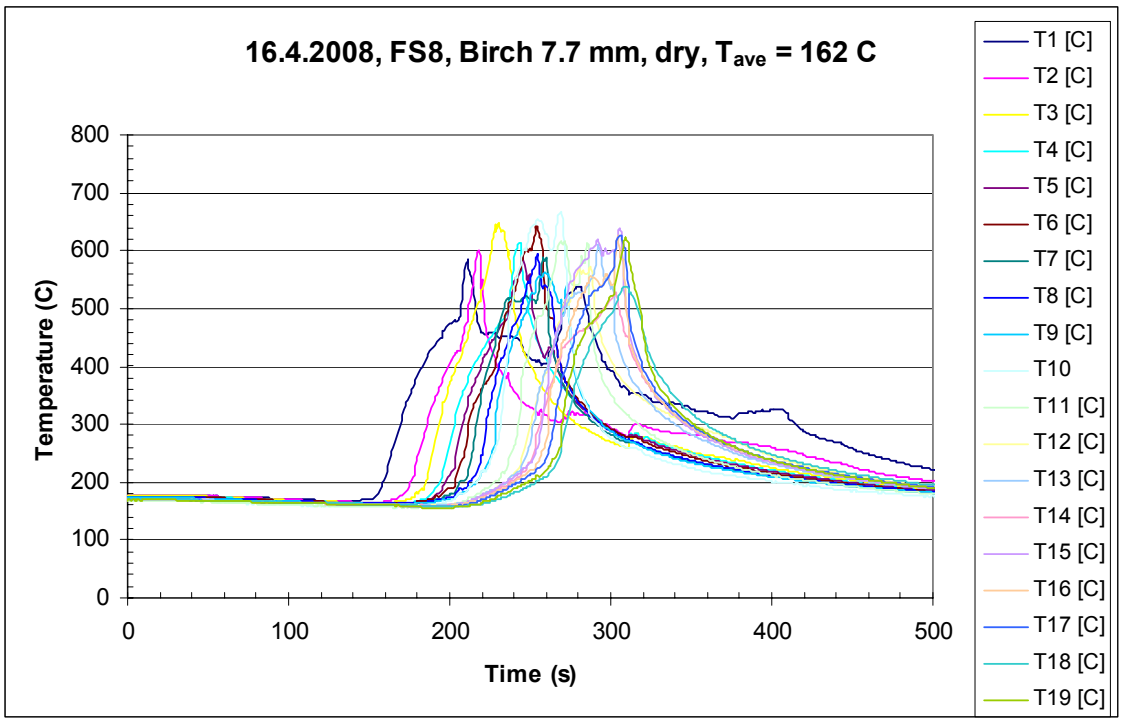

Figure A26. Vertical temperatures in flame spread experiment FS8.

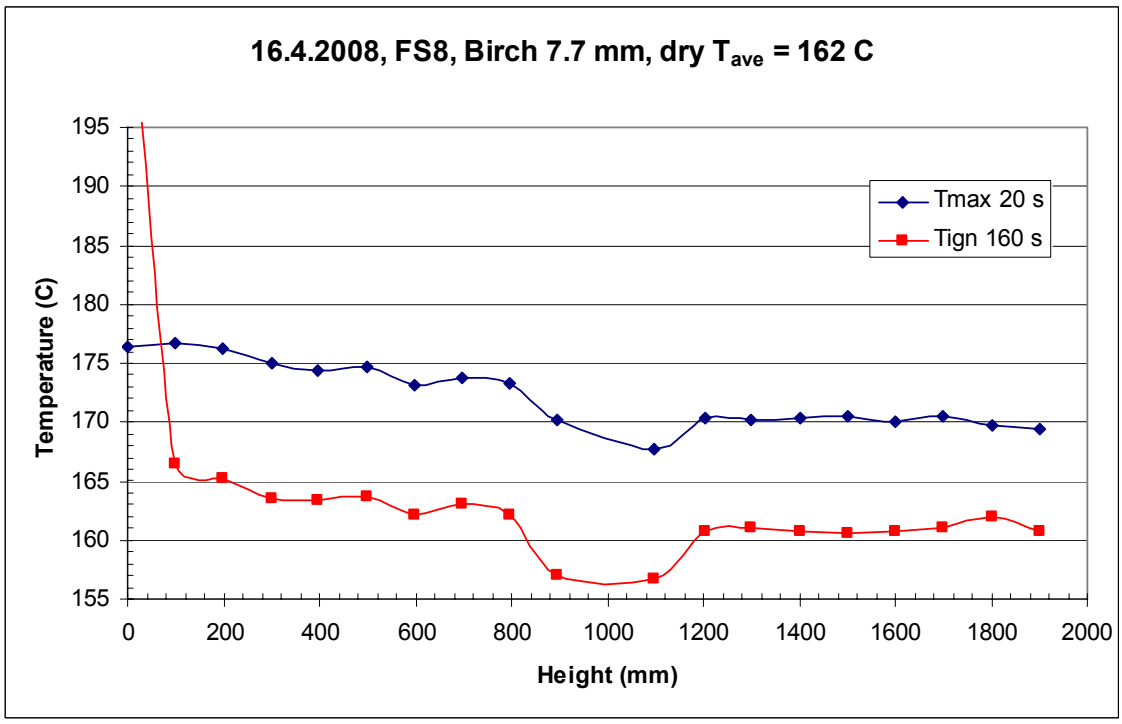

Figure A27. Vertical temperature distributions in flame spread experiment FS8, at maximum temperature and at ignition.

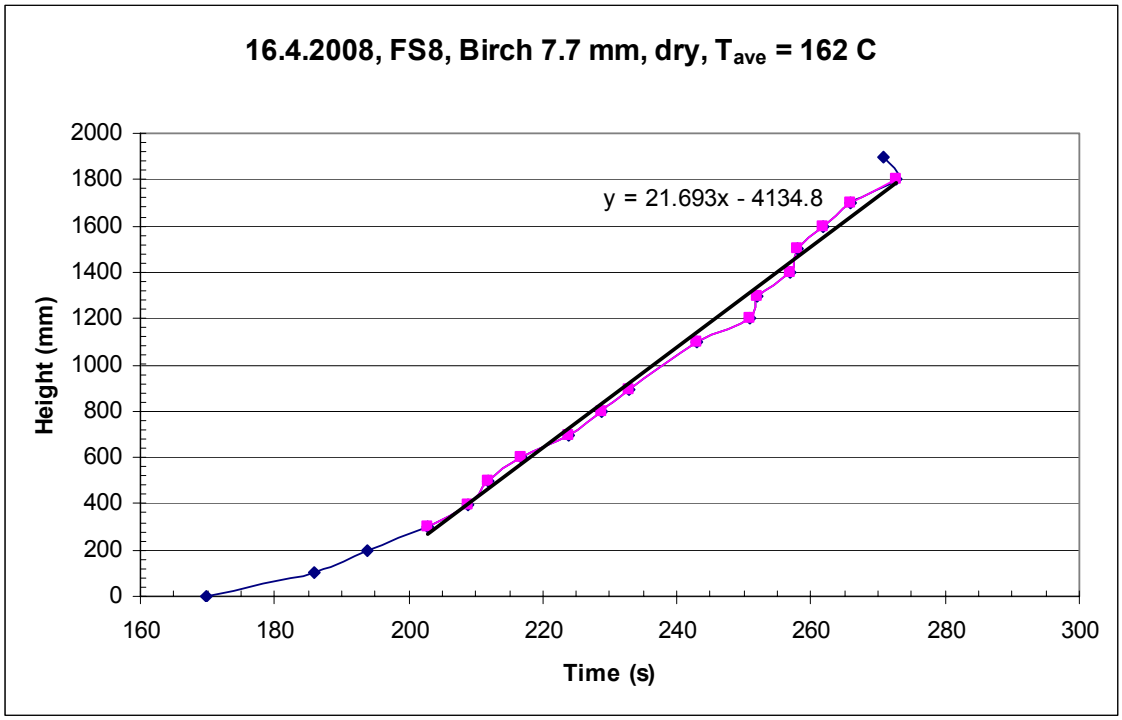

Figure A28. Flame front as a function of time in flame spread experiment FS8.

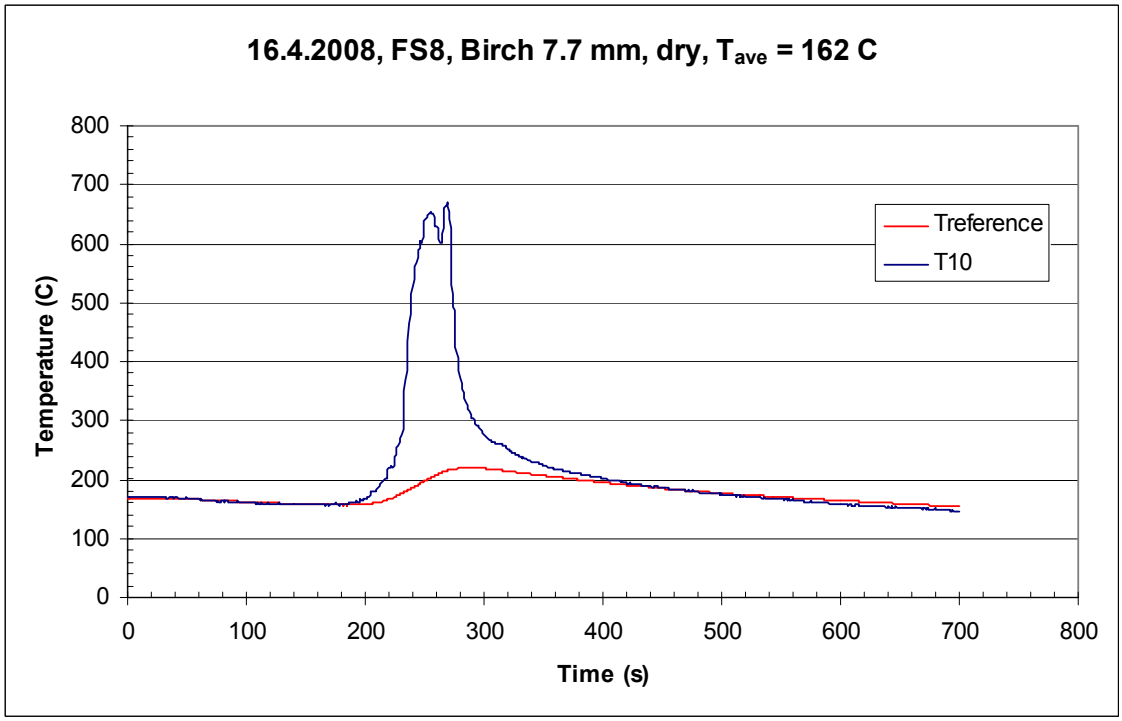

Figure A29. Temperature inside reference wood sample and gas temperature T10 in flame spread experiment FS8.

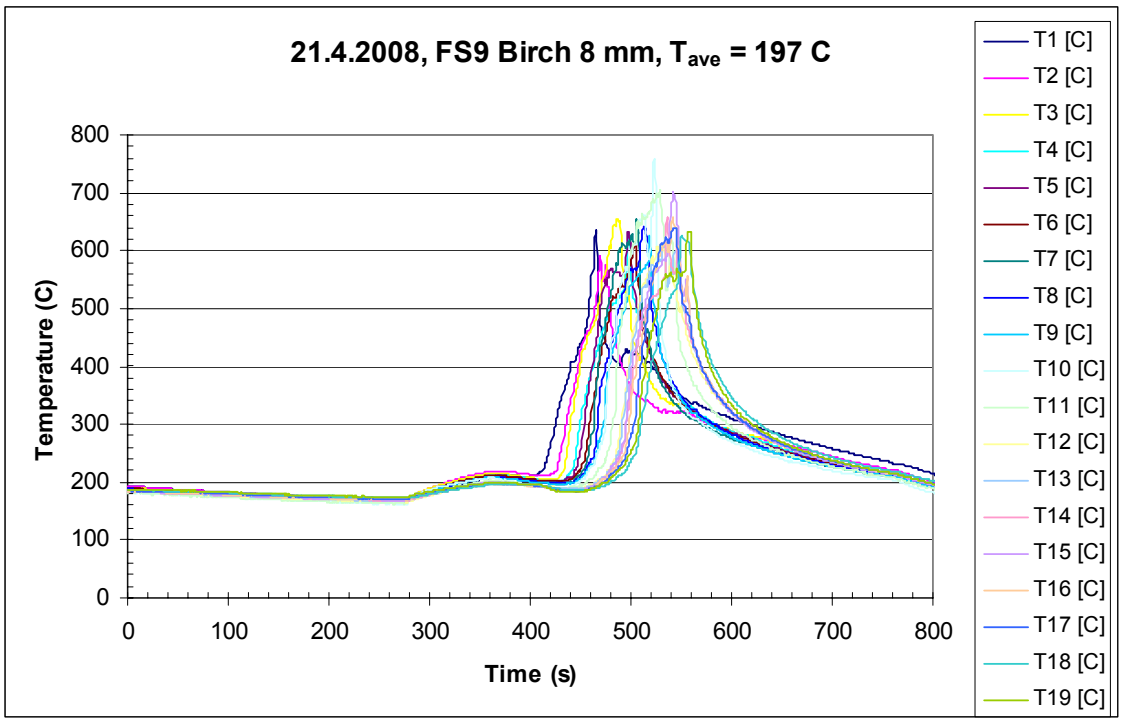

Figure A30. Vertical temperatures in flame spread experiment FS9.

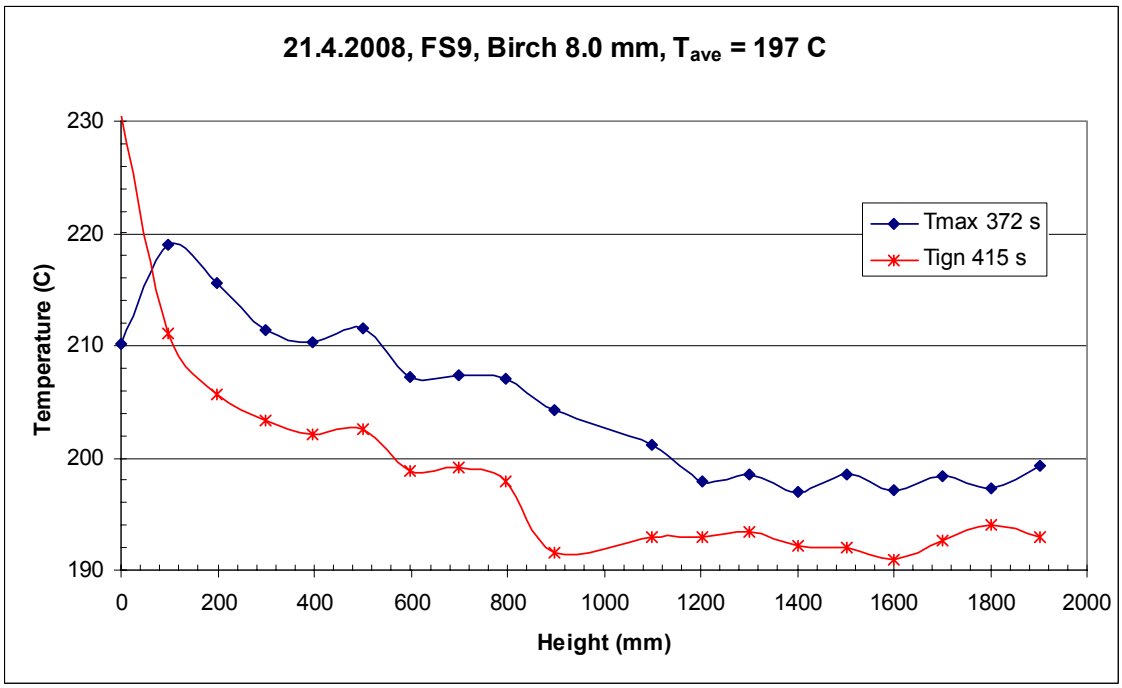

Figure A31. Vertical temperature distribution in flame spread experiment FS9, at maximum temperature and at ignition.

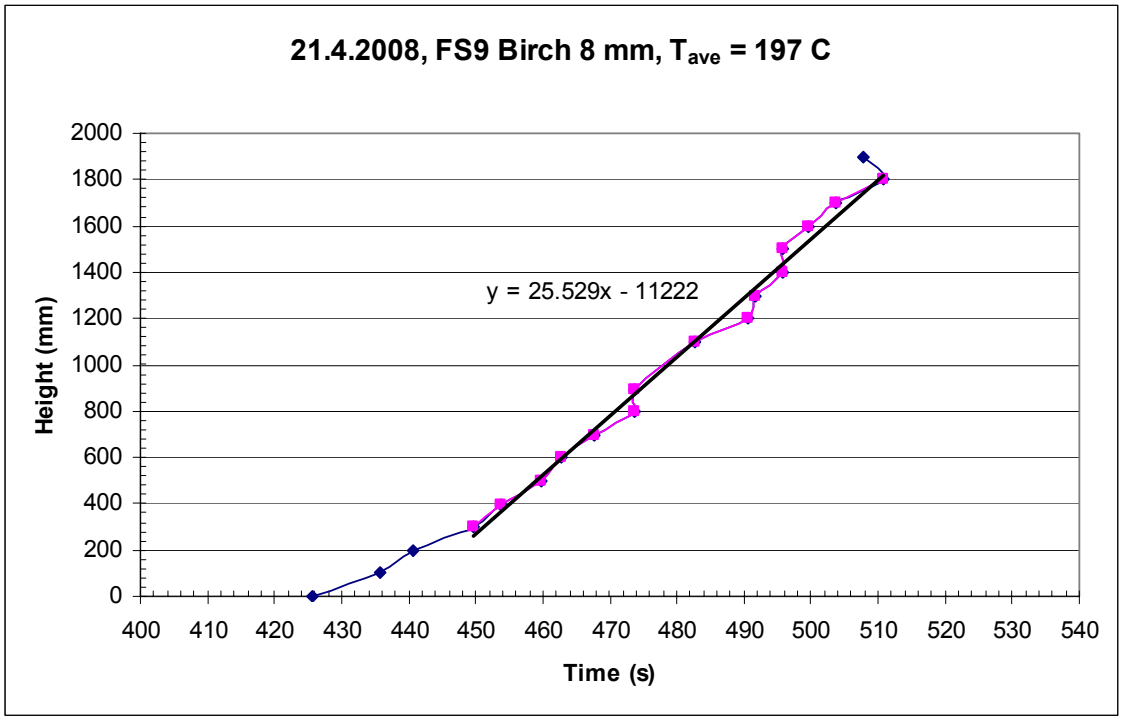

Figure A32. Flame front as a function of time in flame spread experiment FS9.

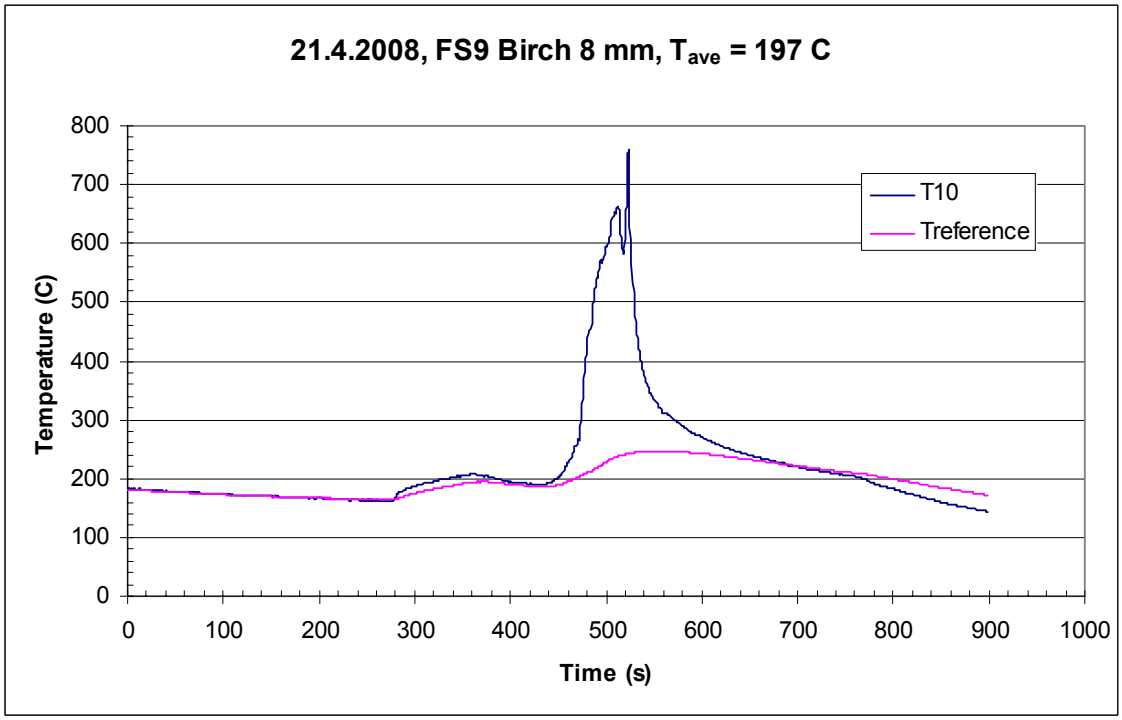

Figure A33. Temperature inside reference wood sample and gas temperature T10 in flame spread experiment FS9.

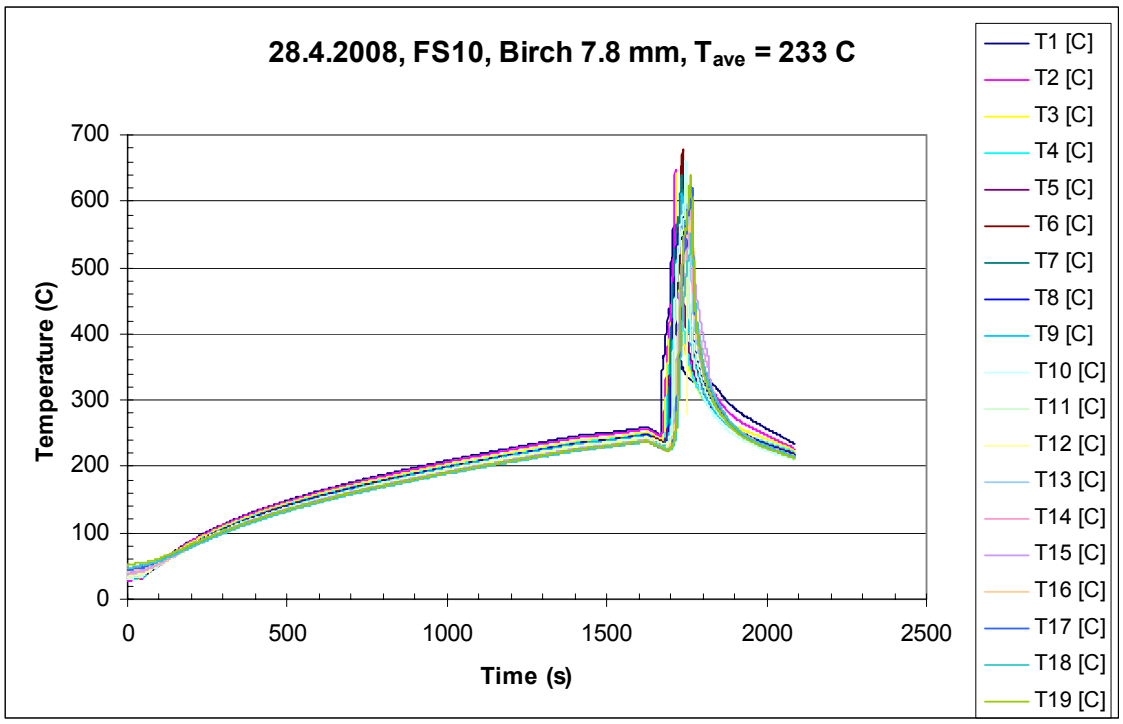

Figure A34. Vertical temperatures in flame spread experiment FS10.

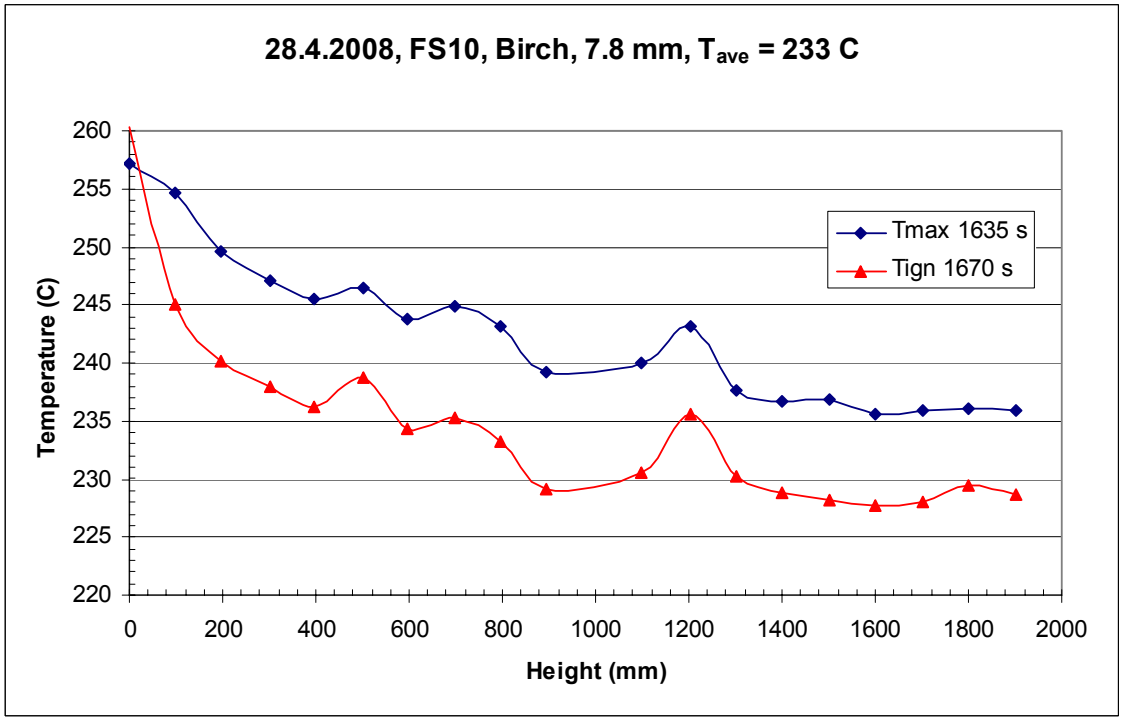

Figure A35. Vertical temperature distributions in flame spread experiment FS10, at maximum temperature and at ignition.

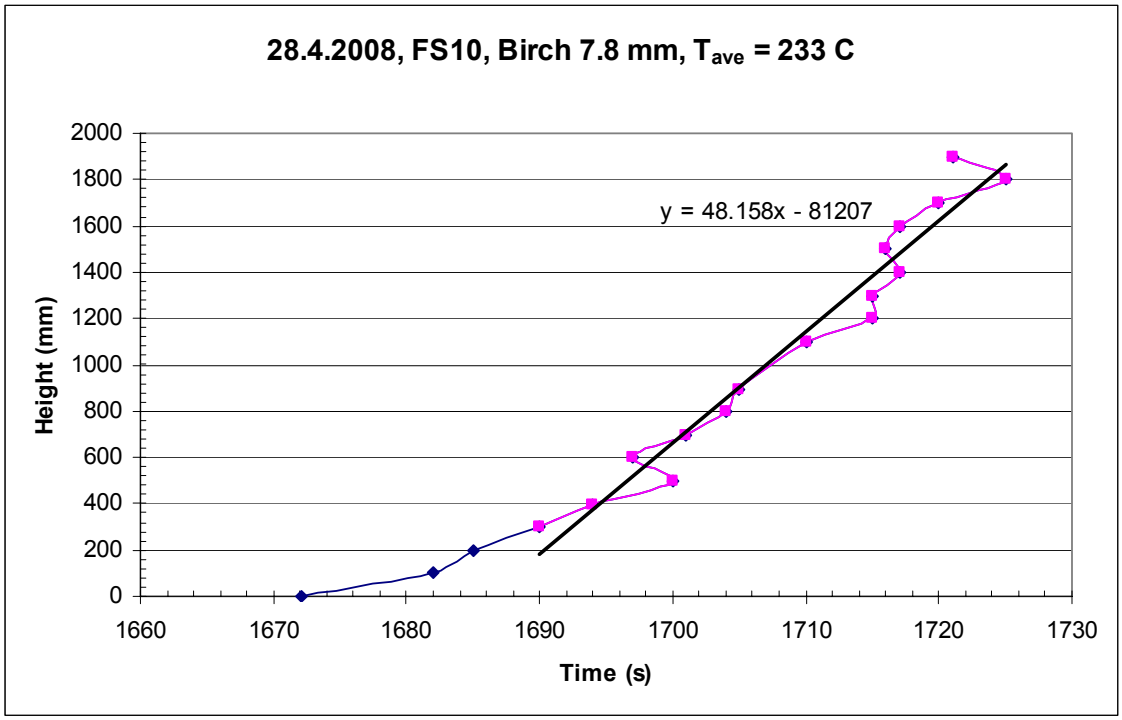

Figure A36. Flame front as a function of time in flame spread experiment FS10.

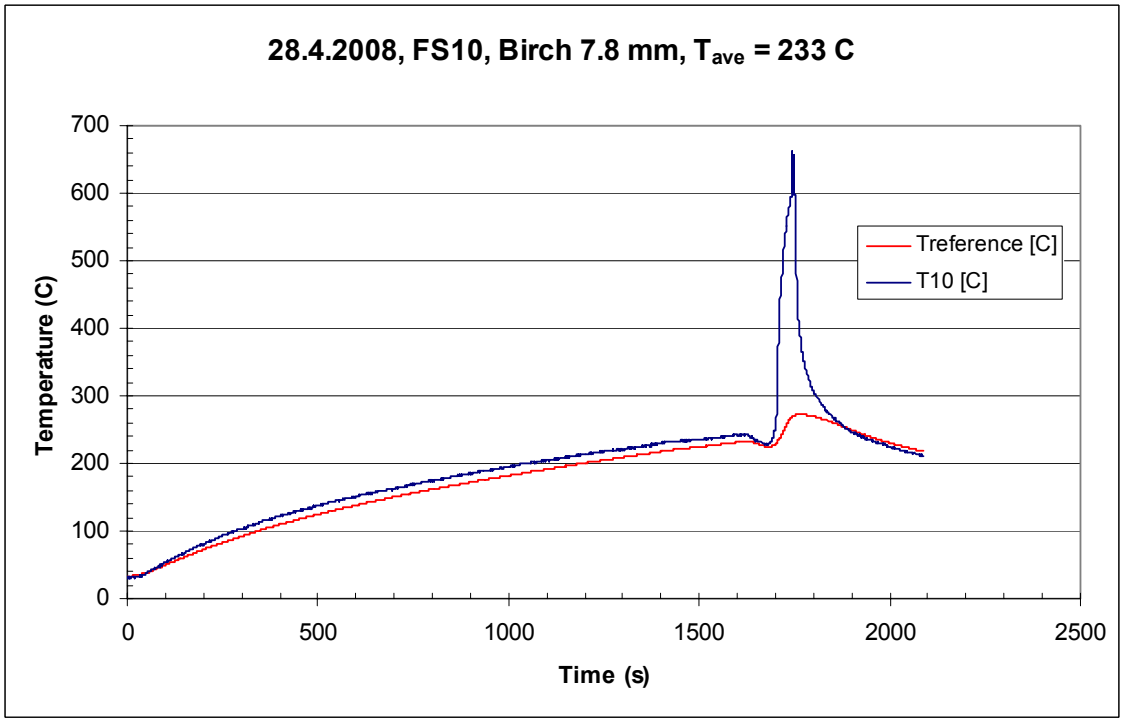

Figure A37. Temperature inside reference wood sample and gas temperature T10 in flame spread experiment FS10.

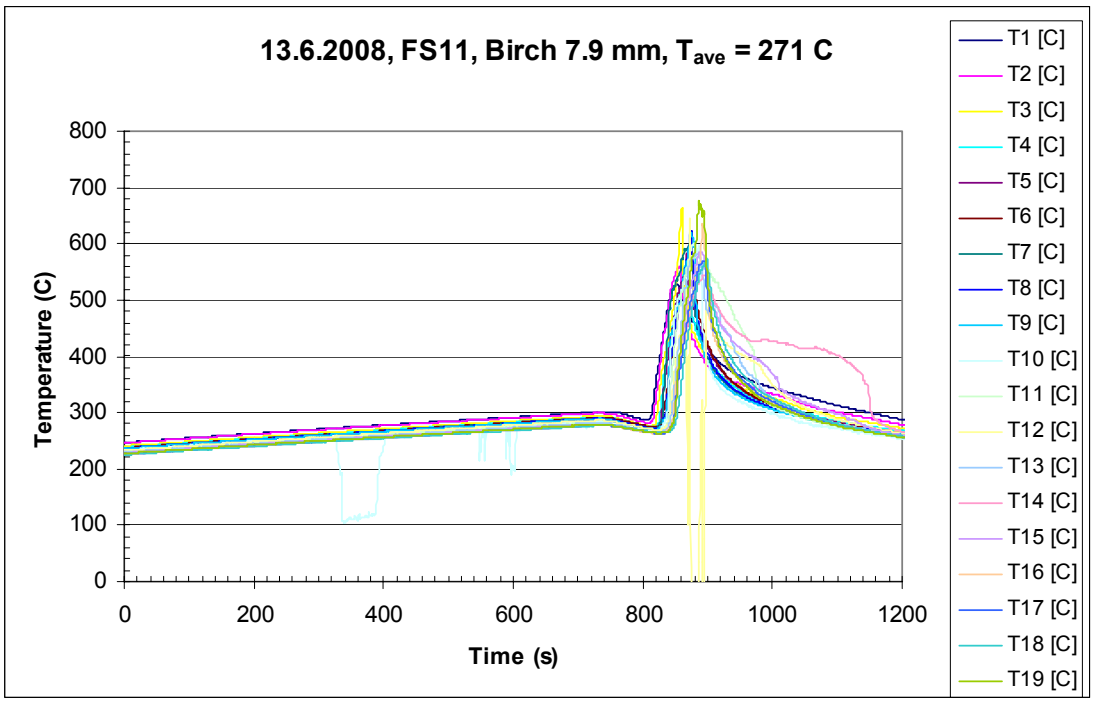

Figure A38. Vertical temperatures in flame spread experiment FS11.

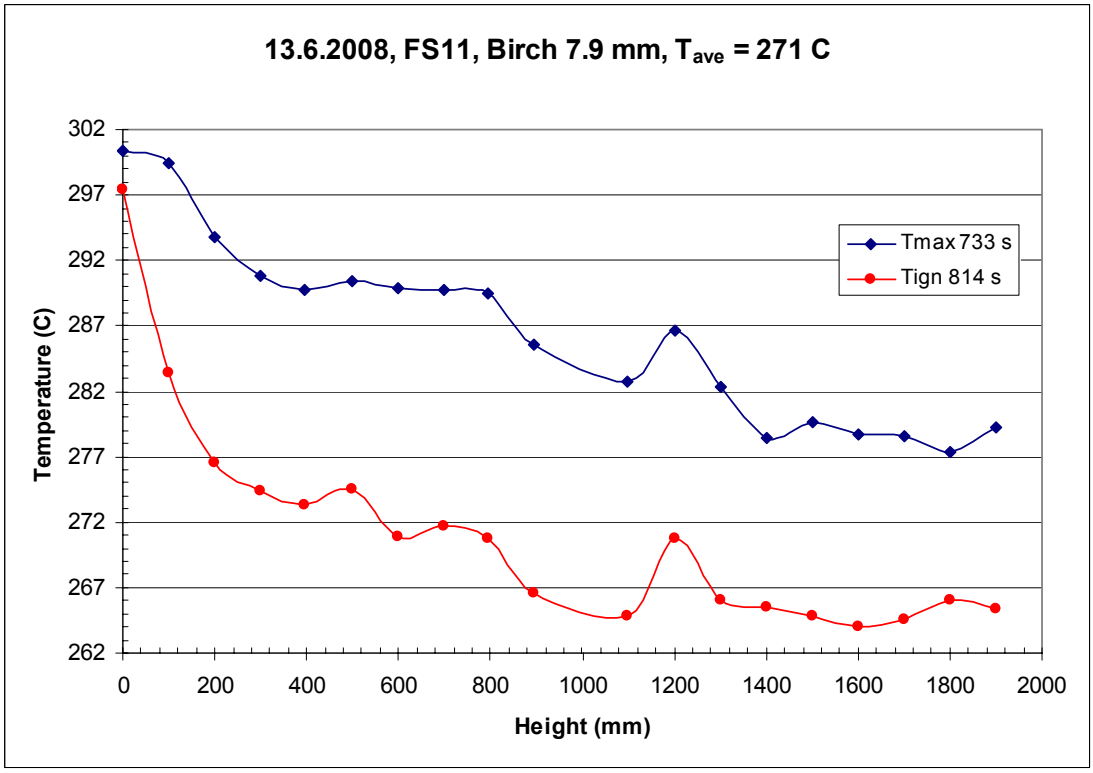

Figure A39. Vertical temperature distributions in flame spread experiment FS11, at maximum temperature and at ignition.

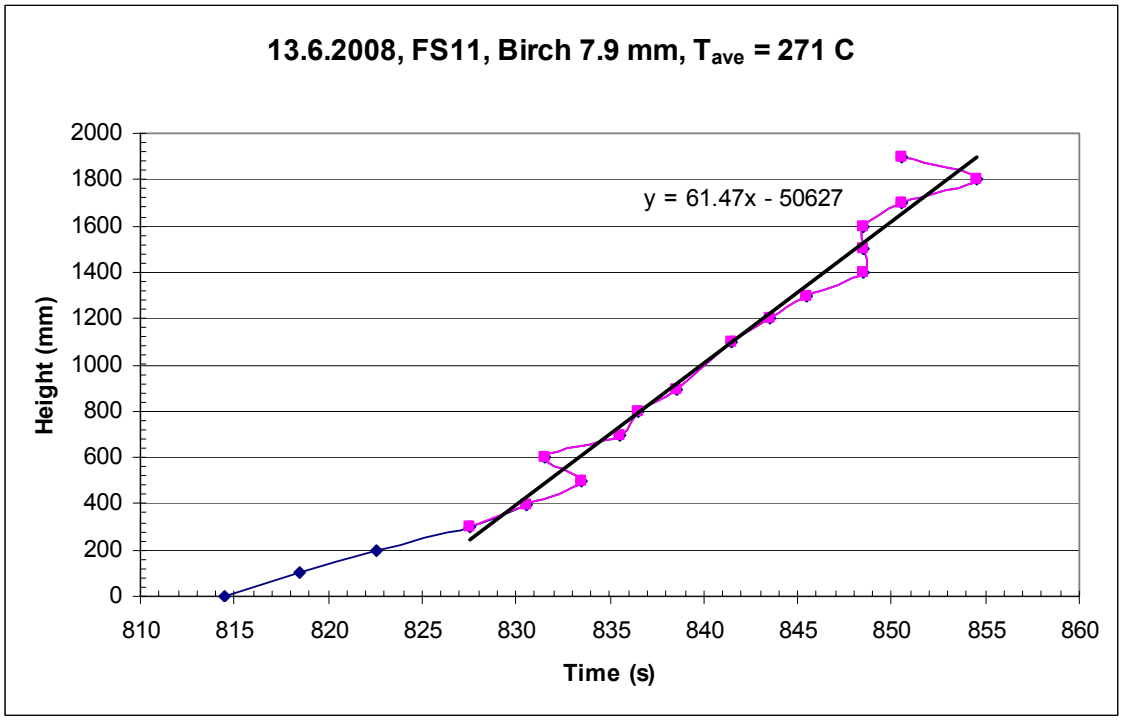

Figure A40. Flame front as a function of time in flame spread experiment FS11.

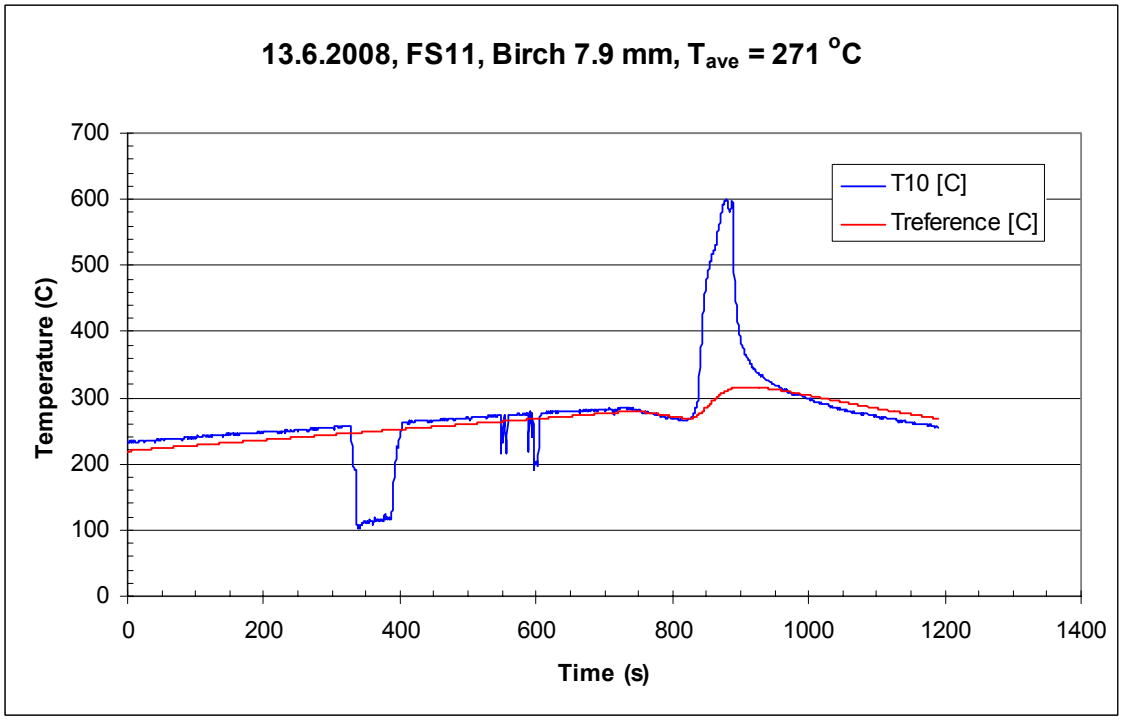

Figure A41. Temperature inside reference wood sample and gas temperature T10 in flame spread experiment FS11.

Appendix B: Temperatures from experiments on MMJ 4 x 1.5 mm^2 PVC cable samples

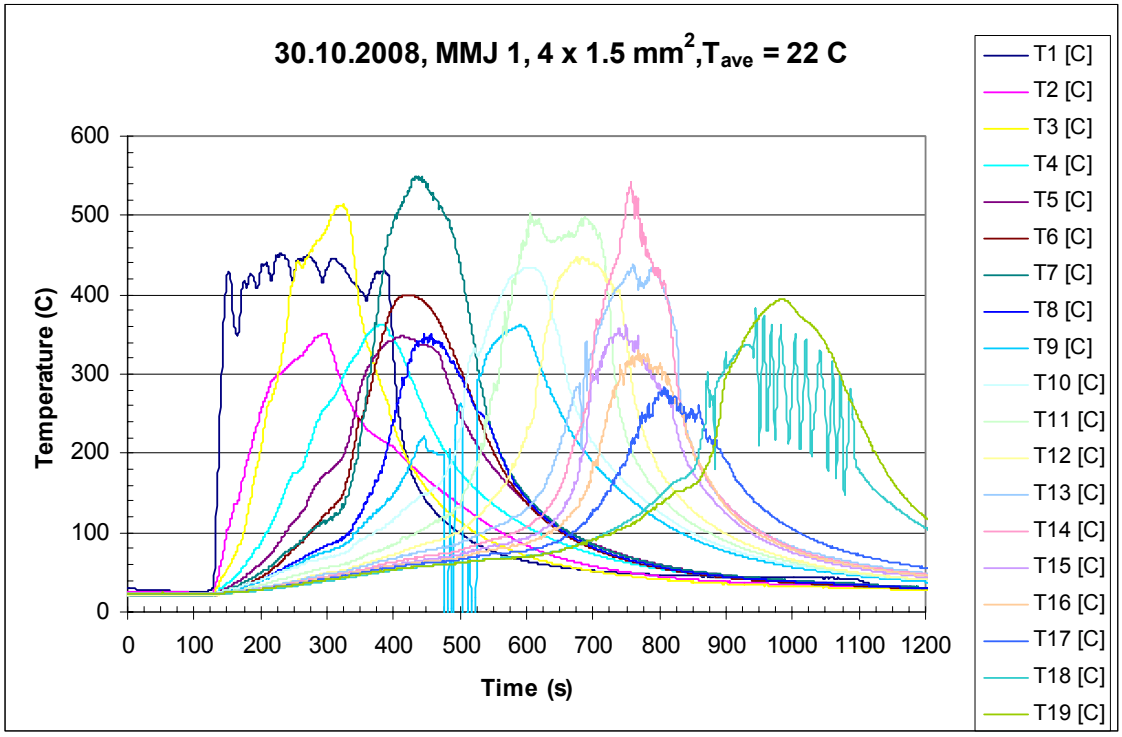

Figure B1. Vertical temperatures in flame spread experiment MMJ 1.

Appendix B: Temperatures from experiments on MMJ 4 x 1.5 mm2 PVC cable samples

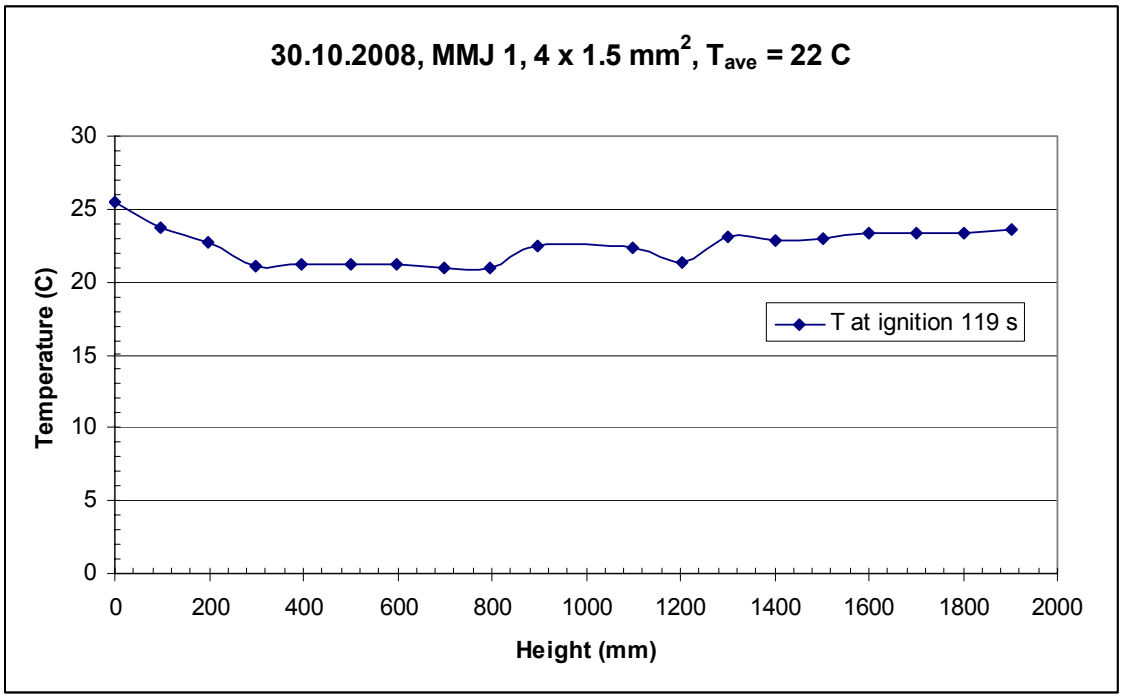

Figure B2. Vertical temperature distributions in flame spread experiment MMJ 1 at ignition.

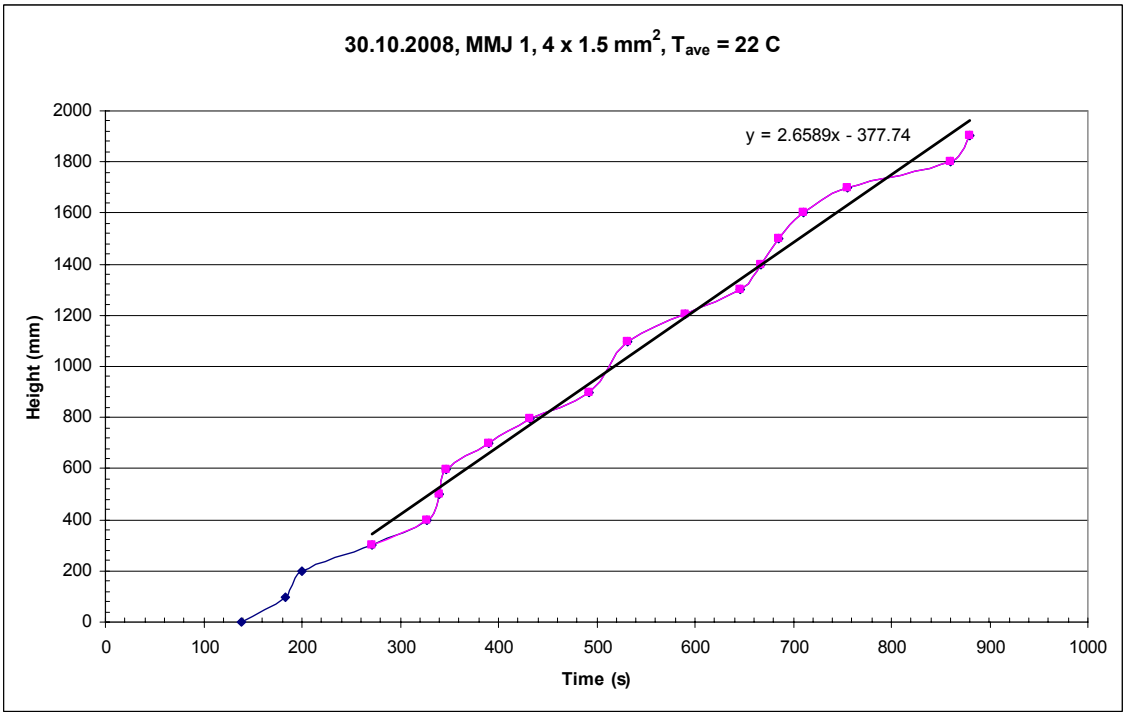

Figure B3. Flame front as a function of time in flame spread experiment MMJ 1.

Appendix B: Temperatures from experiments on MMJ 4 x 1.5 mm2 PVC cable samples

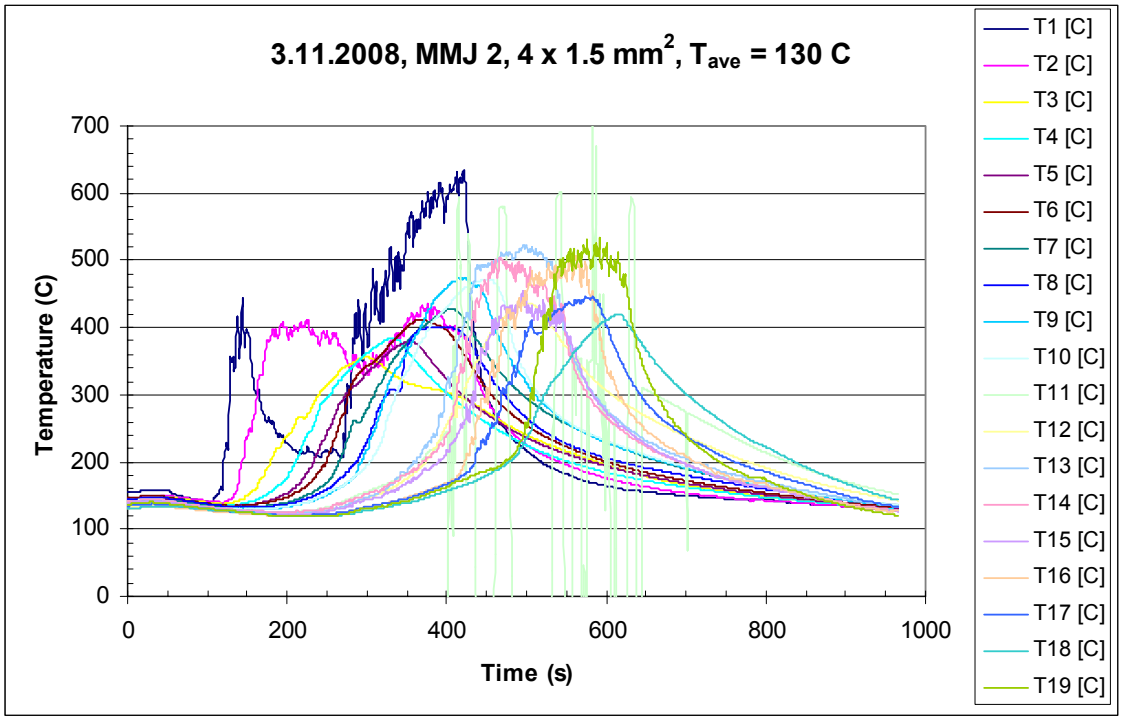

Figure B4. Vertical temperatures in flame spread experiment MMJ 2.

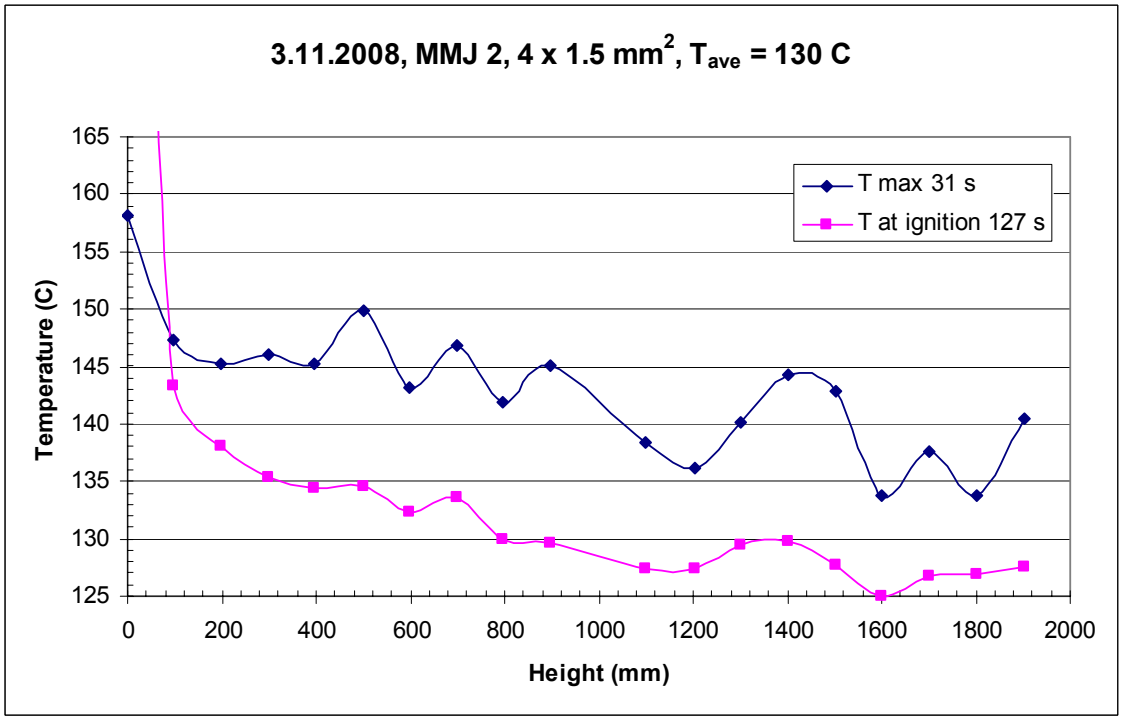

Figure B5. Vertical temperature distributions in flame spread experiment MMJ 2, at maximum temperature and at ignition.

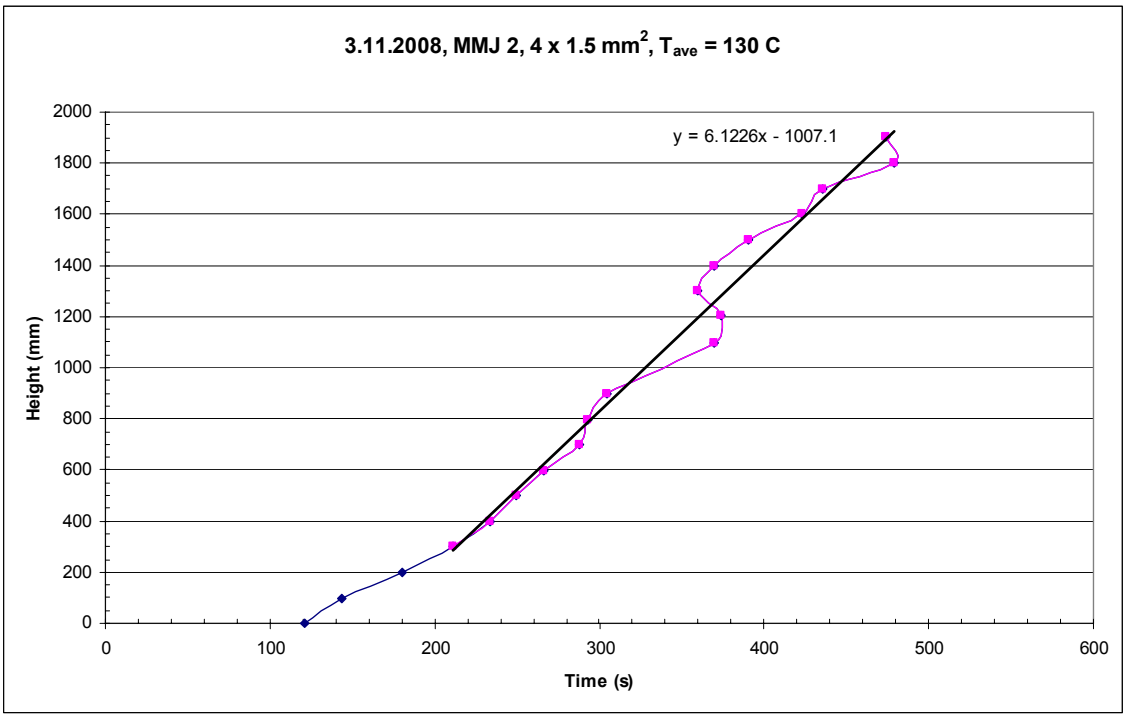

Figure B6. Flame front as a function of time in flame spread experiment MMJ 2.

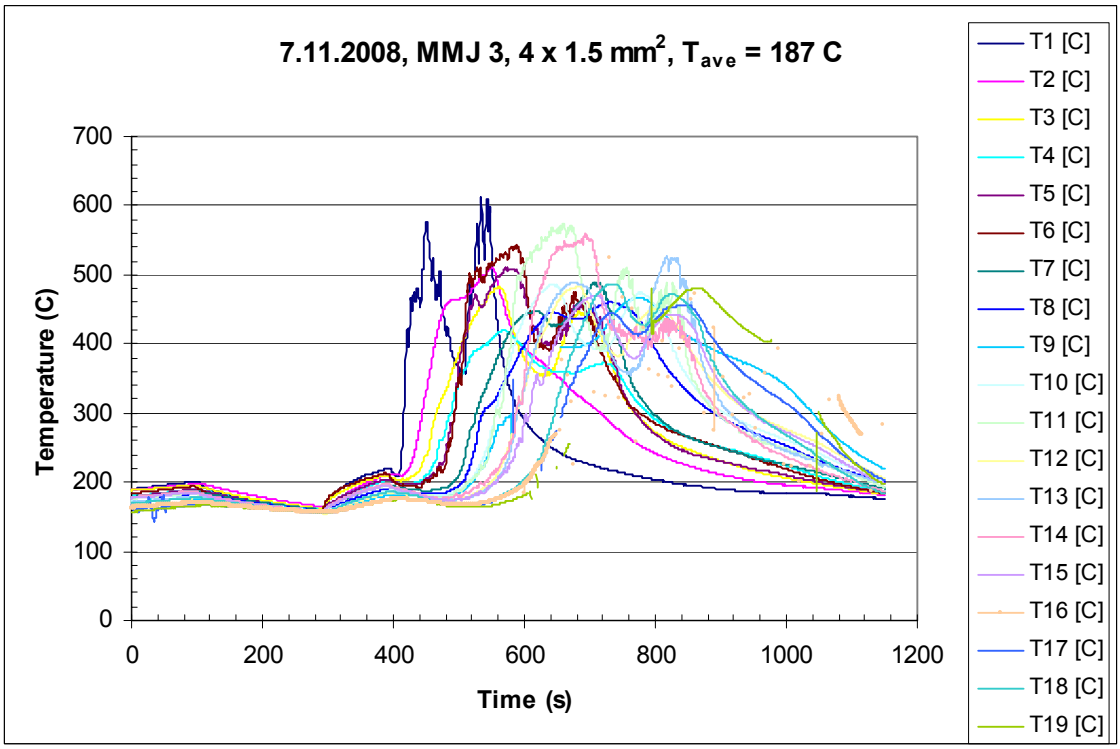

Figure B7. Vertical temperatures in flame spread experiment MMJ 3.

Appendix B: Temperatures from experiments on MMJ 4 x 1.5 mm2 PVC cable samples

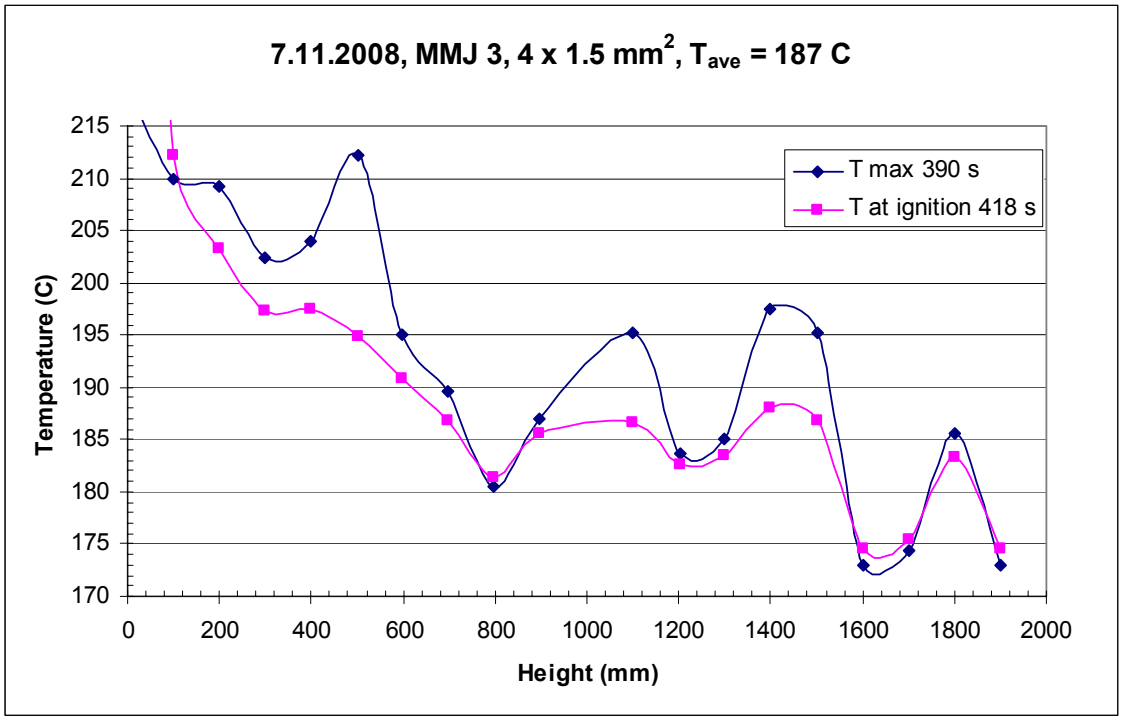

Figure B8. Vertical temperature distributions in flame spread experiment MMJ 3, at maximum temperature and at ignition.

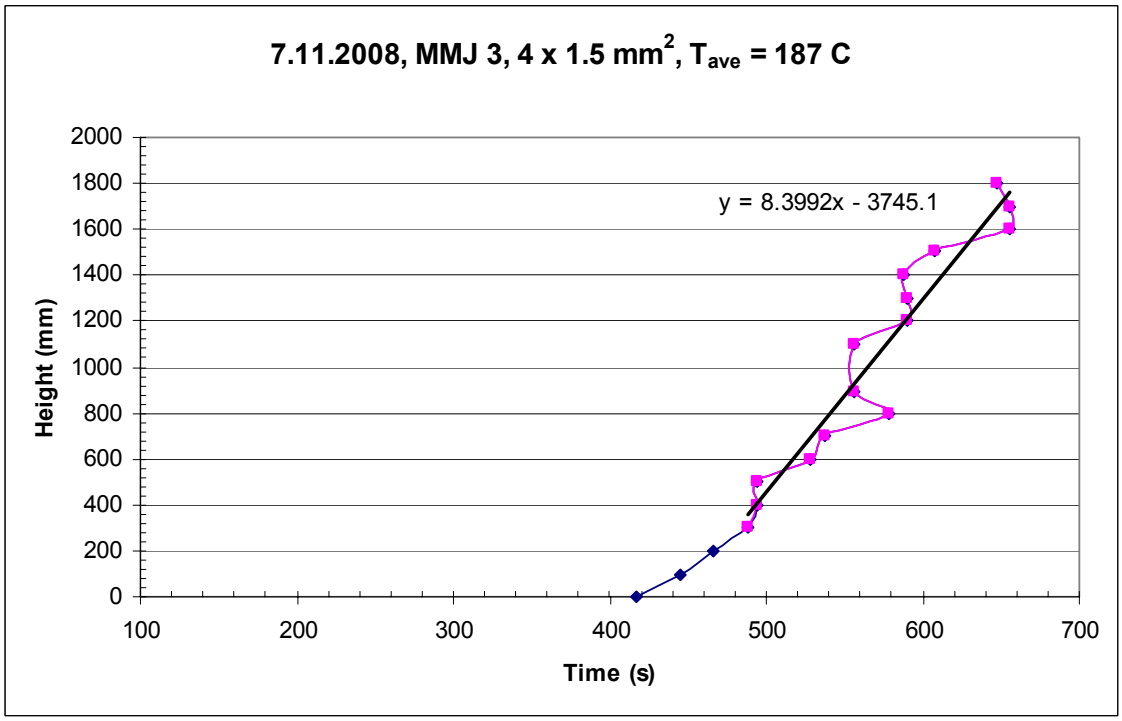

Figure B9. Flame front as a function of time in flame spread experiment MMJ 3.

VTT Working Papers

101 Stephen Fox, Patrick Ehlen, Matthew Purver, Elizabeth Bratt, Matthew Frampton, Ichiro Kobayashi, Bevan Jones, Rob Monroe & Stanley Peters. Applying computational semantics to the real-time communication of skill knowledge. 2008. 85 p.

102 Stephen Fox. Ontological uncertainty and semantic uncertainty in global network organizations. 2008. 122 p.

103 Kati Tillander, Helena Järnström, Tuula Hakkarainen, Juha Laitinen, Mauri Mäkelä & Panu Oksa. Palokohteiden savu-, noki- ja kemikaalijäämät ja niiden vaikutukset työturvallisuuteen. Polttokokeet ja altistumisen arviointi. 2008. 67 s.

104 Eija Kupi, Sanna-Kaisa Ilomäki, Virpi Sillanpää, Heli Talja & Antti Lönnqvist. Aineettoman pääoman riskienhallinta. Riskit ja riskienhallinnan käytännöt yrityksissä. 2008. 44 s.

105 Teemu Mutanen, Joni Niemi, Sami Nousiainen, Lauri Seitsonen & Teppo Veijonen. Cultural Event Recommendations. A Case Study. 2008. 17 p.

106 Hannele Holttinen. Tuulivoiman tuotantotilastot. Vuosiraportti 2007. 2008. 44 s. + liitt. 8 s.

107 Kari Keinänen, Jarkko Leino & Jani Suomalainen. Developing Keyboard Service for NoTA. 2008. 17 p. + app. 2 p.

108 Hannele Antikainen, Asta Bäck & Pirjo Näkki. Sosiaalisen median hyödyntäminen paikallisissa mediapalveluissa. 2008. 64 s.

109 Raine Hautala, Pekka Leviäkangas, Jukka Räsänen, Risto Öörni, Sanna Sonninen, Pasi Vahanne, Martti Hekkanen, Mikael Ohlström, Bengt Tammelin, Seppo Saku & Ari Venäläinen. Benefits of meteorological services in South Eastern Europe. An assessment of potential benefits in Albania, Bosnia-Herzegovina, FYR Macedonia, Moldova and Montenegro. 2008. 63 p. + app. 35 p.

110 Jaana Leikas. Ikääntyvät, teknologia ja etiikka. Näkökulmia ihmisen ja teknologian vuorovaikutustutkimukseen ja -suunnitteluun. 2008. 155 s.

111 Tomi J. Lindroos. Sectoral Approaches in the Case of the Iron and Steel Industry. 2008. 58 p. + app. 11 p.

112 Johan Mangs. A new apparatus for flame spread experiments. 2009. 51 p. + app. 28 p.

ISBN 978-951-38-7173-4 (URL: http://www.vtt.fi/publications/index.jsp)
ISSN 1459-7683 (URL: http://www.vtt.fi/publications/index.jsp)